

Structural transitions and the rheology of soft sphere suspensions

Citation for published version (APA):

Kaldasch, J. (1996). *Structural transitions and the rheology of soft sphere suspensions*. [Phd Thesis 1 (Research TU/e / Graduation TU/e), Chemical Engineering and Chemistry]. Technische Universiteit Eindhoven.
<https://doi.org/10.6100/IR460312>

DOI:

[10.6100/IR460312](https://doi.org/10.6100/IR460312)

Document status and date:

Published: 01/01/1996

Document Version:

Publisher's PDF, also known as Version of Record (includes final page, issue and volume numbers)

Please check the document version of this publication:

- A submitted manuscript is the version of the article upon submission and before peer-review. There can be important differences between the submitted version and the official published version of record. People interested in the research are advised to contact the author for the final version of the publication, or visit the DOI to the publisher's website.
- The final author version and the galley proof are versions of the publication after peer review.
- The final published version features the final layout of the paper including the volume, issue and page numbers.

[Link to publication](#)

General rights

Copyright and moral rights for the publications made accessible in the public portal are retained by the authors and/or other copyright owners and it is a condition of accessing publications that users recognise and abide by the legal requirements associated with these rights.

- Users may download and print one copy of any publication from the public portal for the purpose of private study or research.
- You may not further distribute the material or use it for any profit-making activity or commercial gain
- You may freely distribute the URL identifying the publication in the public portal.

If the publication is distributed under the terms of Article 25fa of the Dutch Copyright Act, indicated by the "Taverne" license above, please follow below link for the End User Agreement:

www.tue.nl/taverne

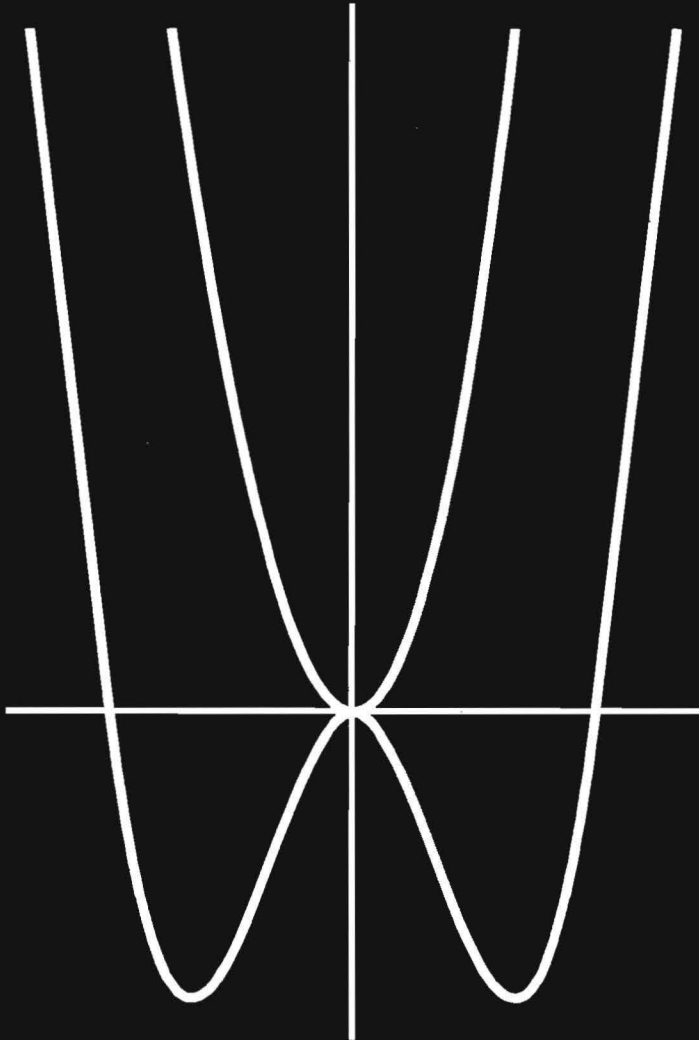
Take down policy

If you believe that this document breaches copyright please contact us at:

openaccess@tue.nl

providing details and we will investigate your claim.

**STRUCTURAL TRANSITIONS
AND THE RHEOLOGY OF SOFT
SPHERE SUSPENSIONS**



JOACHIM KALDASCH

Structural Transitions and the Rheology of Soft Sphere Suspensions

PROEFSCHRIFT

ter verkrijging van de graad van doctor aan
de Technische Universiteit Eindhoven, op
gezag van de Rector Magnificus, prof.dr.
J.H. van Lint, voor een commissie
aangewezen door het College van Dekanen
in het openbaar te verdedigen op donderdag
2 mei 1996 om 16.00 uur

door

JOACHIM KALDASCH

geboren te Nauen

Dit proefschrift is goedgekeurd door de promotoren:

prof.dr. H.N. Stein

en

prof.dr. D. Bedeaux

en de copromotor dr. J. Laven

Aan mijn moeder

CONTENTS

Chapter I. GENERAL CONSIDERATIONS AND OVERVIEW	1
1. Introduction	1
Literature	16
Chapter II. THEORY	24
2. Theoretical Background on Structural Transitions	24
2.1 Introduction	24
2.2 General Considerations on Structural Transitions and the Landau Theory	26
Appendix A	34
Literature	38
3. The Equilibrium Phase Diagram of Suspensions of Electrically Stabilised Colloidal Particles	39
3.1 Introduction	39
3.2 Theory	41
3.3 Numerical Procedure	49
3.4 Results and Discussion	49
3.5 Conclusions	54
Literature	57
4. The Rheology of Equilibrium Colloidal Suspensions Close to Structural Transitions	61
4.1 Introduction	61
4.2 Theory	63
4.3 Discussion	76
4.4 Conclusions	86
Appendix C	87
Appendix D	90
Literature	97
5. A Theory for the Melting of Colloidal Crystals Induced by Static Shear	100
5.1 Introduction	100
5.2 Theory	101
5.3 Discussion	111
5.4 Conclusions	113
Literature	114

Contents

6. Shear Thickening as a Consequence of an Acoustic Resonance in Sheared Colloidal Crystals	117
6.1 Introduction	117
6.2 Theory	118
6.3 Discussion	135
6.4 Conclusions	139
Appendix E	140
Literature	142
Chapter III. EXPERIMENT	145
7. Rheology and Rheo-optics of Concentrated Colloidal Suspensions	145
7.1 Introduction	145
7.2. Experimental	146
7.4. Results	150
7.5. Discussion	164
7.6. Conclusions	168
Literature	170
Chapter IV. CONCLUSIONS	172
SUMMARY	175
SAMENVATTING	177
SYMBOLS	179
CURRICULUM VITAE	183
DANKWOORD	184

CHAPTER I.

GENERAL CONSIDERATIONS AND OVERVIEW

1. Introduction

This thesis deals with structural transitions of colloidal suspensions and the related rheological phenomena. We will focus our interest on concentrated colloidal suspensions. These systems are highly viscoelastic materials showing a number of flow phenomena not yet clearly understood.

This study originated as a followup of previous work by Boersma [1], that was focused on shear thickening and flow blockage of concentrated colloidal dispersions. The theoretical and experimental results of that work indicate an intimate connection between the dispersion microstructure and the macroscopic transport properties.

While the rheology of low volume fraction suspensions can be understood analytically by the hydrodynamics of a small number of particles it is a hopeless task to apply these techniques to very concentrated dispersions. A more appropriate approach is to focus on the global structures formed by the colloidal particles and to study their long time scale behaviour. In particular, transitions between structures are accompanied by a dramatic change in the transport properties.

With this idea in mind the approach in this thesis will be to study equilibrium and non-equilibrium structural transitions of colloidal suspensions and discuss the related rheological phenomena. Experimental investigations will be carried out on one of these transitions in concentrated colloidal suspensions, by means of rheological and light scattering techniques.

In this chapter we will introduce the terminology that will be used throughout the book. The appropriate terms are emphasized by *italic letters*. Further we will give a short overview of the main ideas and some results of this work.

Structures

The *thermodynamic system* we will study is an assembly of colloidal particles dispersed in a medium without particle exchange (canonical ensemble). The rheology of such a colloidal suspension can be understood from the transport properties of structures formed by the colloidal particles. By a *structure* we understand the arrangements of the colloidal particles as distributed over space and time. The order of a structure can be characterized by its *symmetry properties*, i.e. the set of allowed symmetry operations that transforms the system into itself.

Depending on the magnitude of an applied shear perturbation we classify the structures in *equilibrium* and *non-equilibrium structures*. The first type is found in a colloidal suspension in equilibrium, while its transport properties can be determined from the stress response to small shear perturbations. The second type of structures occurs as a result of large shear perturbations.

Equilibrium Structures in Soft Sphere Suspensions

We will confine our considerations to *soft sphere* suspensions, which consist of particles with a repulsive interaction potential $U(r)$ that decreases with $U(r) \sim r^{-x}$, while $1 \leq x \leq 12$ [2]. While the interaction potential of *hard spheres* originates from a hard core repulsion (Born repulsion), soft sphere particles have a "long range" interaction.

The equilibrium structure is, amongst others, a function of the three variables: the temperature T , the volume fraction Φ of the particles, and the Debye screening parameter κ_D . Travelling through the space of the state variables a variety of structures appear together with a wide variation in the transport properties.

We restrict our considerations essentially to electrically stabilised colloidal suspensions, with an interaction potential composed of a Coulomb repulsion and a van der Waals attraction, as described by the standard DLVO-theory [3],[4]. In most

cases use was made of the repulsive interaction potential as derived from the DLVO-theory using the superposition approximation. The characteristic *two particle interaction potential* of electrically stabilized colloidal particles consists of a secondary minimum followed by a Coulomb barrier and a primary minimum formed by the van der Waals attraction.

The equilibrium phase diagram of soft sphere suspensions will be analyzed in this thesis in chapter II.3 An approximation of the interaction potential between electrically stabilized colloidal particles as introduced by Victor & Hansen [5] will be combined with a perturbation approach as developed by Gast et. al. [6]. The dependence of the transition lines in the κ - Φ phase diagram will be calculated for a number of interaction potentials.

The electrostatic stabilization leads to a rather complex phase diagram schematically depicted in Figure 1, for the condition of constant temperature. We will use the nomenclature for the different phases introduced by Pusey [7]. Colloidal particles at low salt concentrations are known to form a *bcc-crystal* structure, where the colloidal particles are arranged in a bcc-lattice [7],[8],[9],[10].

On increasing the salt concentration the bcc-crystal becomes unstable and is converted either into a *fcc-crystal* structure [11],[12] at high volume fractions, or at low volume fractions into a *colloidal fluid* phase [14]. The latter phase consists of freely moving hard-sphere-like colloidal particles (Brownian particles) distributed at random.

The colloidal fluid phase at intermediate volume fractions becomes unstable with increasing salt concentrations and separates into a colloidal gas and a colloidal liquid phase due to a flocculation into the secondary minimum [5]. The freely moving colloidal particles can form flocculation clusters when they collide. These flocculated, disordered clusters (colloidal gel) form the *colloidal liquid* phase. This phase differs from the fluid phase by the presence of an infinite percolation cluster built up of the colloidal particles dispersed in the medium. Due to this cluster the colloidal fluid has a non-zero elastic modulus. This phase can also be viewed as a less compact *colloidal*

glass, because a glass is an amorphous state formed here by the colloidal particles in the medium.

A further increase of the salt concentration lets the particles coagulate into the primary minimum, when the Coulomb barrier disappears.

Starting from the fluid phase on increasing the volume fraction a transition into a colloidal fcc-crystal occurs [13],[15],[16],[17]. For this first order transition the coexistence lines are drawn in Figure 1.

A further increase of the volume fraction leads to an increase of the relaxation times of internal fluctuations. Recent theories [18],[19],[20] and computer simulations have suggested that an assembly of hard spheres, when compressed rapidly enough to bypass crystallisation forms a *metastable glass* structure at $\Phi_g \approx 0.58$ [7]. Beyond this volume fraction of hard spheres only a closed packed crystal can survive up to the maximum volume fraction of $\Phi_m = 0.74$.

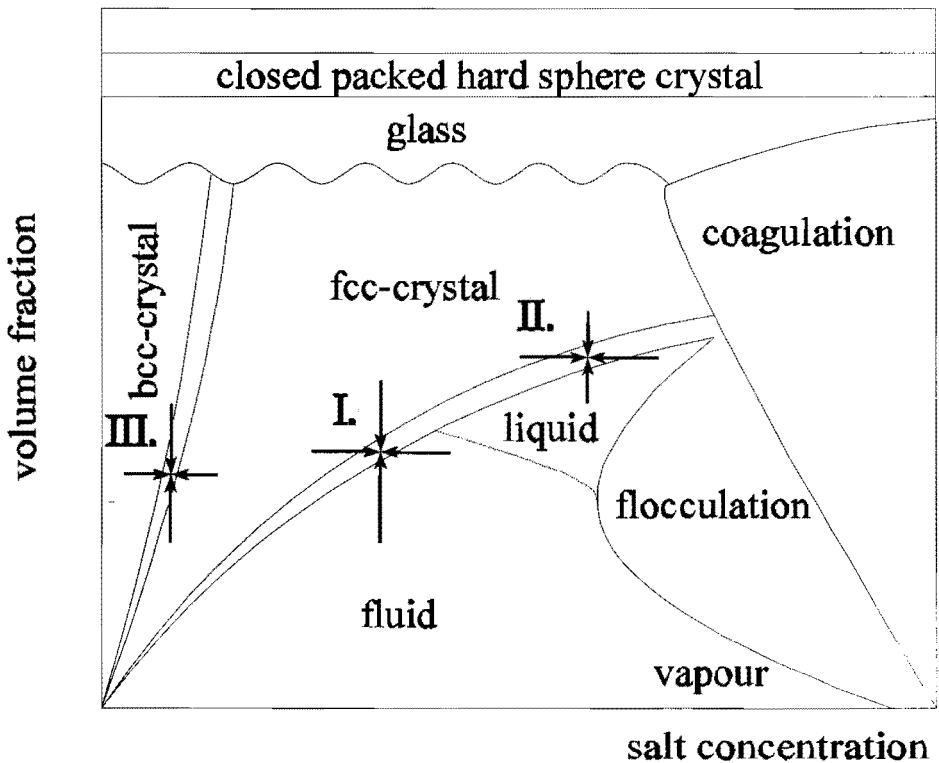


Figure 1 Schematic phase diagram of electrically stabilized colloidal suspensions.

Transport Processes and Structures

Let us consider a colloidal suspension under an external perturbation at a time scale τ_e . As a response, internal transport processes occur at a time scale τ_i by e.g. diffusion, convection etc. These processes can be classified into three groups (Fig.2) according to the ratio $De = \tau_i / \tau_e$, known as the *Deborah number*, with τ_i the characteristic relaxation time of the structure and the experimental time scale τ_e :

1. $De \gg 1$; i.e. the internal transport processes of these structures are on a macroscopic time scale if compared to τ_e . The structure will instantaneously follow the applied perturbation on the time scale of the measurement, without relaxation into the unperturbed structure. The internal relaxational transport and the resulting dissipation can be neglected to a large extent and the suspension behaves essentially as an elastic solid. A colloidal crystal structure behaves in that way.

2. $De \ll 1$; i.e. the internal transport processes occur at a microscopic time scale if compared with the time scale of the measurement. The suspension relaxes quasi-instantaneously into the unperturbed state and dissipates the applied perturbation energy into heat. This viscous response occurs with the colloidal fluid structure.

3. $De \approx 1$; i.e. the time scale of the internal transport processes are of the order of the time scale of the shear perturbation. On this mesoscopic time scale the transport processes are strongly influenced by the nature and the amount of the perturbation; a viscoelastic response will occur. Characteristic structures at this mesoscopic time scale are thermal and entropic fluctuations like e.g. the Brownian motion of the colloidal particles, fractal clusters (flocs), critical fluctuations etc.

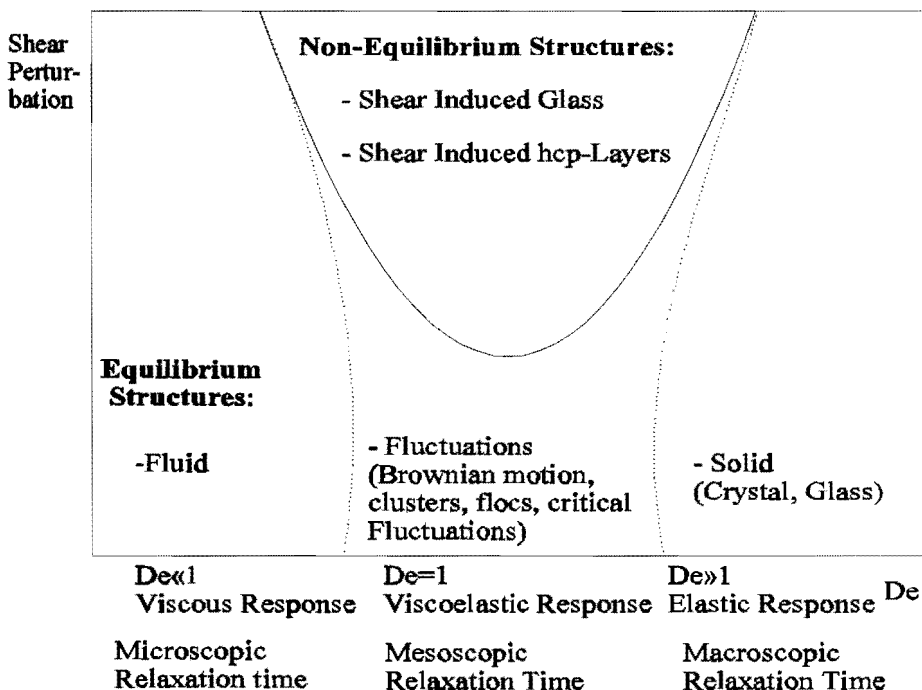


Figure 2 Equilibrium and non-equilibrium structures as a function of the magnitude of the shear perturbation and the Deborah number De .

The Rheology of the Equilibrium Structures

A viscous structure ($De \gg 1$) in the phase diagram is the colloidal fluid (gas) phase. A great number of authors have studied the transport properties of this phase, which can be treated by the motion of hard sphere particles. They usually employed hydrodynamic methods [21],[22],[23],[24]. The interaction of soft spheres in the fluid phase can be simplified by an effective hard sphere diameter for which one may apply the results by Einstein [25] and Batchelor & Green [26], who calculated the increase of the viscosity with the volume fraction [27],[28],[29],[30]. The mechanisms of transport processes in the fluid phase have been investigated also using colloidal hydrodynamic methods for both equal [31],[32] and unequal spheres [33],[34]. These

methods have been applied to the periodic colloidal crystal phase as well [35],[36].

The colloidal crystal and glass structures behave viscoelastically. The usual approach with these materials is to generate a phenomenological equation of state by combining the viscous and elastic responses in a rather simple way [37]. Such equations have no direct relation to the microscopic structure and we will therefore follow the other path of relating the microscopic transport processes to the corresponding internal structures; a similar approach was successful in the description of polymers [38],[39].

The fcc- and bcc-crystals can essentially be characterized as elastic solids. The rheology of these structures have been described by studying the deformation of a periodic assembly of colloidal particles on a macroscopic time scale [40],[41],[42].

The colloidal liquid phase is a viscoelastic, disordered glass containing an infinite network of flocculated colloidal particles. The transport processes of these aggregated structures are determined by the disruption of the network and the formation and break up of clusters (flocs) on a mesoscopic time scale [43], [44], [45], [46].

Near the transition regions of the equilibrium phases long scale fluctuations occur with transport processes on a mesoscopic timescale. A phase transition is accompanied by a softening of the thermodynamic potential leading to a pronounced increase of long scale fluctuations. These "critical" fluctuations having long relaxation times ("critical slowing down"), are of a universal nature and have been studied e.g. in connection with binary fluids [47], nematic liquid crystals [48] and polymers [39].

Structural Transitions

In this thesis we will focus our attention on the rheology near structural transitions between the equilibrium phases of soft sphere suspensions. We will employ methods developed in the statistical mechanics of structural phase transitions in solids [49]. The advantage of using these methods here is that a direct relation between the variation of the microscopic structure and the rheological properties can be established. Both can be measured independently and compared with the theoretical outcome.

A *structural transition* is characterized by a change of the global spatial arrangement of the colloidal particles. It can be characterized as a change of the degree of order within a suspension, the magnitude of which can be described by a so-called *order parameter*. All structural transitions are accompanied by a change of the symmetry properties, therefore denoted as *symmetry breaking transitions* (Chapter II.2). Three structural transitions exist in the equilibrium phase diagram of soft sphere suspensions (Figure.1):

- I. the order-disorder transition from a crystal into a fluid,
- II. the order-disorder transition from a crystal into a liquid and
- III. the order-order transition from an fcc lattice into a bcc lattice.

The flocculation transition in which the fluid separates into a liquid and a gas phase, is not a structural transition because the global structure remains disordered.

Landau Theory

Our interest lies in the rheological properties of systems close to structural transitions. For that purpose we introduce, in chapter II.2, the basic relationships of the *Landau theory* of symmetry breaking, first and second order phase transitions. In the Landau theory the degree of order of a structure is described by an *order parameter* q with the property of being non-zero in the ordered phase (*low symmetry phase*) and zero in the disordered phase (*high symmetry phase*) for the case of a order-disorder transition.

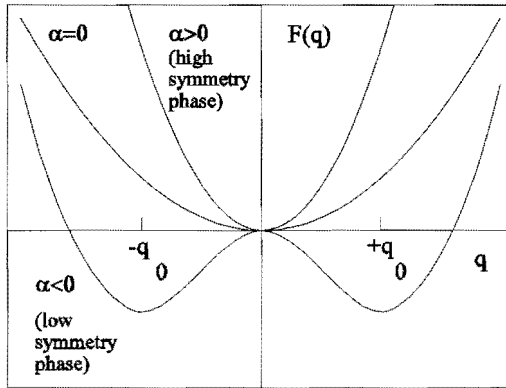


Figure 3 Landau free energy as a function of the order parameter q before ($\alpha>0$) at ($\alpha=0$) and after the transition ($\alpha<0$).

For small magnitudes of the order parameter q , close to a second order transition, the thermodynamic potential $F(q)$ can be expressed as a fourth order Taylor expansion in the order parameter q as displayed schematically in Figure 3 for different values of the second order Taylor coefficient α . For positive α the suspension is in the disordered phase (e.g. fluid phase) because the equilibrium value of the order parameter q_0 is 0 and for negative α it is in the ordered phase (crystal phase), while the minimum of the potential is at $q_0 \neq 0$. The thermodynamic potential softens approaching the transition, i.e. the slope at $q_0=0$ goes to zero. The transition occurs at $\alpha=0$ accompanied by pronounced *critical fluctuations*. The *parameter* α , characterizing the distance to the transition, can be expanded in a function of the state variables of the form $\alpha = \alpha_\Phi(\Phi - \Phi_{tr}) + \alpha_T(T - T_{tr}) + \alpha_C(C - C_{tr})$, where the index tr denotes the transitional values of the state variables.

The transport properties of a suspension near a symmetry breaking transition are dominated by the critical fluctuations, as described by the time dependent Ginzburg-Landau theory of phase transitions [50].

Rheology at a Structural Transition

The rheology is controlled by the internal transport properties determined by the thermal fluctuations of the equilibrium structure. The fluctuations grow, when a phase transition is approached. These critical fluctuations will strongly influence the transport processes near a transition. The critical slowing down due to the critical fluctuations leads to transport processes on a mesoscopic time scale and therefore to fluctuation-corrected transport coefficients.

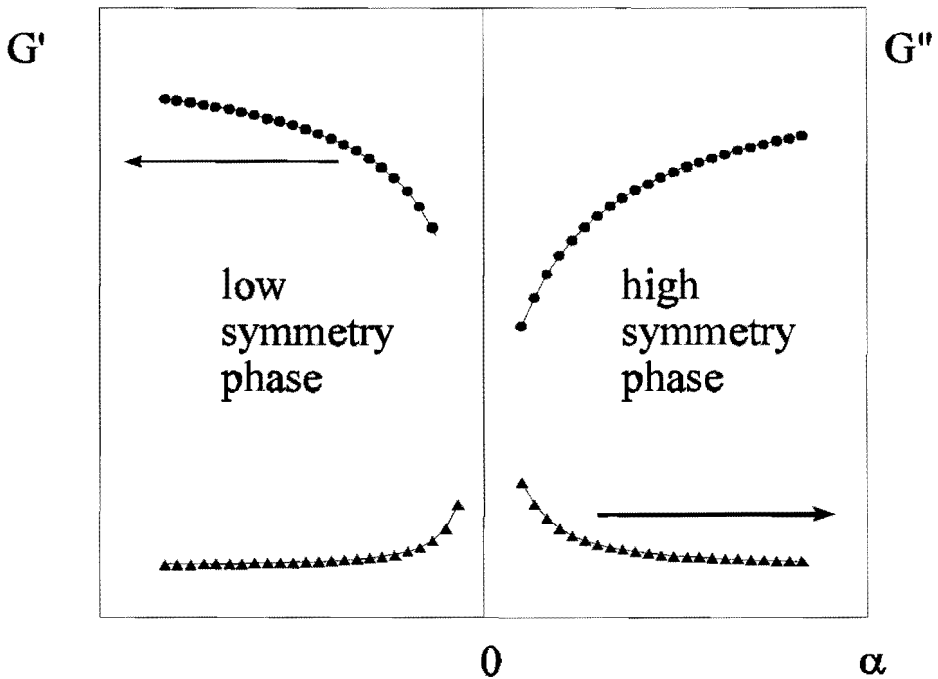


Figure 4 The storage modulus G' and the loss modulus G'' as a function of the parameter α characterizing the distance to the transition.

The transport of the mass, energy and momentum as determined by the conservation laws can be considered as the *slow modes* of a system, i.e. the slowly varying parameters determining the transport properties of the system. Close to a symmetry breaking transition another slow mode appears: the *order parameter mode*, i.e. the diffusive transport of the entropic fluctuations.

A coupling arises between the momentum mode and the order parameter mode near the transition. In this thesis the coupling will be introduced in chapter II.4 by making use of a *mode coupling model* introduced by Levanyuk [51].

According to the model developed here the storage modulus G' will exhibit a minimum and the loss modulus G'' will have a maximum at a structural transition, as the result of the critical fluctuations (Fig.4). A consequence of this result in the hydrodynamic limit is that the viscosity will increase at a transition and is expected to be of the form $\eta \sim (\Phi - \Phi_c)^{-1.5}$ while the elastic modulus rises with $G \sim (\Phi - \Phi_c)^{-0.5}$ near the transition.

Static Shear Melting Transition

Quasistatically applying a large shear perturbation on a colloidal crystal will change the equilibrium structure as discussed in chapter II.5. A colloidal crystal is not stable against an externally applied shear strain u_0 and will melt into a disordered structure. This shear-induced transition of a colloidal crystal will be denoted as *static shear melting transition*, because it occurs under a statically applied shear strain.

The rheology of this shear-induced structural transition [52],[53] is essentially given in Fig.4, while α is now interpreted as $\alpha \sim u_0 - u_0^{(c)}$ with a critical shear strain $u_0^{(c)}$. Experimental results indicated [54], that a concentrated colloidal crystal can sustain a critical shear strain up to $u_0^{(c)} \approx 0.05$ before it becomes unstable. Continuous-shear experiments reveal this transition by a slight discontinuity in the transport parameters at very small shear rates known from computer simulations [55] and from rheo-optical experiments [56],[57].

Shear Induced Order Transition

Unlike equilibrium structures, shear induced non-equilibrium structures occur only when the time scale of the perturbation is of the order of the characteristic relaxation time scale, because those structures are formed by the perturbation itself.

A non-equilibrium transition induced by increasing the shear rate has been observed in numerical simulations of molecular liquids [58],[2], and was observed in experimental investigations of soft sphere suspensions [59],[60]. It involves the formation of hexagonally close packed (hcp) layered particle structures oriented parallel to the direction of motion by the shear gradient, here denoted as the *shear induced order transition*.

Dynamic Shear Melting Transition

The most striking non-equilibrium transition is the disappearance of the hcp-layered structure at even higher shear rates accompanied by a dramatic increase of the viscosity (shear thickening). This transition is denoted here as the *dynamic shear melting transition* indicating the fact that this melting of a periodic structure occurs only at a non-zero shear rate. The dynamic shear melting transition can be described by a resonance between the periodic excitations of the sheared colloidal crystal and the eigen modes of the viscoelastic material. We will derive a theory that allows the calculation of the critical shear rate of this transition.

Based on assumptions made in [62],[63], we apply a two fluid model, where the colloidal suspension is treated as a viscoelastic medium. A critical shear rate $\dot{\gamma}_c$ independent of the system size will be derived of the form $\dot{\gamma}_c \sim G_0/\eta$, where G_0 is the elastic modulus and η is the viscosity of a sheared colloidal suspension.

As an illustration the critical shear rates of Hoffman's [64] and Boersma's [1] experiments are predicted with the present model. A single unknown quantity will be used as a fit parameter.

Viscosity of a Sheared Colloidal Suspension

The experimental results on the viscosity of sheared colloidal systems are described in Chapter III.7. They can be summarized as describing the dependence of the viscosity on the shear rate. Agreement on the viscosity-shear rate dependence of soft sphere colloidal suspensions has been found by a great number of investigators both experimentally [65],[66],[67],[68],[69], and by computer simulations [70],[55],[71],[72]. Its characteristic form is schematically displayed in Fig. 5. Together with an experimentally accessible measure for the *order parameter* OP_{60} [69] indicates the presence of a oriented hexagonal structure in the sample as can be probed by scattering techniques in the velocity direction.

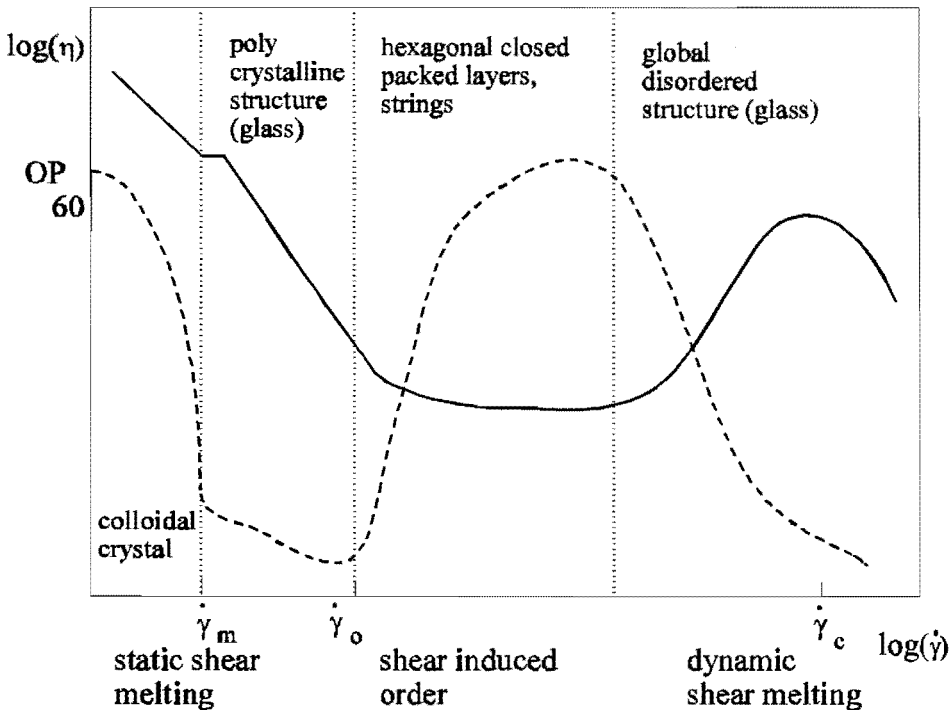


Figure 5. Qualitative dependence of the viscosity of a sheared suspension on the shear rate together with the value of the parameter OP_{60} indicating a periodic structure.

At small stresses the system responds as a deformed colloidal crystal. Beyond a critical stress (a corresponding shear rate $\dot{\gamma}_m$) the equilibrium ordered structure is thermodynamically unstable against the shear perturbation and melts. The value of OP_{60} decreases. This transition is accompanied by a downward jump in the stress tensor [73]. Passing this static shear melting transition the structure changes into a disordered structure. On increasing the shear rate, the shear induced order transition is approached at $\dot{\gamma}_o$. This non-equilibrium transition is accompanied by the formation of sliding hcp layers pointing in the flow direction, where OP_{60} increases again. Experimental and numerical investigations [70],[72],[74] established that the ordered structure decreases the dissipation and therefore the viscosity.

At high shear rates the dynamic shear melting transition caused by an acoustic resonance is accompanied by a viscosity increase and the disappearance of the global ordered structure at $\dot{\gamma}_c$ and the value of OP_{60} vanishes. Far beyond of the resonance region at very high shear rates the layered crystal structure probably occurs again.

Rheo-optical Experiments on Soft Sphere Suspensions

Since the investigations of Hoffman [59] a great deal of rheo-optical experiments were performed to determine simultaneously the microstructural transitions and the corresponding rheological variations [60],[73],[74],[75]. In this thesis we focus our attention on the static shear melting transition under dynamic shear perturbations, where a colloidal crystal melts into a disordered structure if the applied shear strain exceeds a critical value.

For that purpose a rheo-optical setup has been built to study simultaneously the microstructure and the rheological properties of colloidal suspensions under shear. The experimental results are reported in chapter III.7. They indicate qualitative agreement between the expected theoretical transport properties with the obtained experimental data. Especially the expected decrease of the elastic modulus as a result of the critical fluctuations could be observed.

Conventions

In the entire book we will denote the i -th vector element by x_i and a matrix element by x_{ik} , while we use only the indices i,k or l . The *Einstein convention* is applied, i.e. a summation has to be performed over indices occurring twice in a product (e.g. $x_i x_i = x_1^2 + x_2^2 + x_3^2$). The entire vector is written as \underline{x} , while a matrix (tensor) has the form \underline{x} .

A complex number is written by using $j^2 = -1$.

Definition of the Fourier transform

We introduce a Fourier transform by:

$$\delta q(\underline{k}, \omega) = \int_{-\infty}^{\infty} \int_{-\infty}^{\infty} e^{j(\underline{k} \cdot \underline{r} + \omega t)} \delta q(\underline{r}, t) d^3 r dt \quad (1)$$

and the reverse Fourier transform:

$$\delta q(\underline{r}, t) = \frac{1}{(2\pi)^4} \int_{-\infty}^{\infty} \int_{-\infty}^{\infty} e^{-j(\underline{k} \cdot \underline{r} + \omega t)} \delta q(\underline{k}, \omega) d^3 k d\omega \quad (2)$$

Literature

[1]

Boersma, W.H., *Shear Thickening of Concentrated Dispersions*, Ph.D. Thesis, Eindhoven University of Technology, 1990.

[2]

Hess, S., "Shear induced melting and reentrant positional ordering in a system of spherical particles," *Int. J. Thermophys.* **6** 657-671 (1985).

[3]

Verwey, E.J.W. and T.Th. G. Overbeek, *Theory of the Stability of Lyophobic Colloids* (Elsevier, Amsterdam, 1948).

[4]

Hunter, R.J., *Foundations of Colloid Science* (Clarendon Press-Oxford 1989) Vol. 1,2

[5]

Victor, J.M. and J-P. Hansen, "Spinodal Decomposition and the Liquid-Vapour Equilibrium in Charged Colloidal Dispersions," *J. Chem. Soc. Faraday Trans. 2* **81**, 43-61 (1985).

[6]

Gast, A.P., C.K. Hall and W.B. Russel, "Polymer-Induced Phase separation in Nonaqueous Colloidal Suspensions," *J. Colloid. Interface. Sci.* **96**, 251-267 (1983).

[7]

Pusey, P.N., "Colloidal Suspensions" in *Liquids, Freezing and the Glass Transition* edited by J.P. Hansen, D. Levesque and J. Zinn-Justin (North-Holland, Amsterdam, 1991).

[8]

Sirota, E.B., H.D. Ou-Yang, S.K. Sinha, P.M. Chaikin, J.D. Axe, Y. Fuji, "Complete Phase Diagram of a Charged Colloidal System: A Synchrotron X-Ray Scattering Study," *Phys. Rev. Lett.* **62** 1524-1527 (1989)

[9]

Sengupta, S. and A.K. Sood, "Theory of the liquid-bcc-fcc coexistence in charged-stabilized colloidal systems," *Phys. Rev. A* **44**, 1233-1236 (1991).

[10]

Salgi,P. and R.Rajagopalan, "Ordering in Charged Colloidal Dispersions and Macroionic Solutions: A Density-Functional Approximation," *Langmuir* **7**, 1383-1387 (1991).

[11]

Chaikin,P. M., P. Pincus, S. Alexander and D. Hone, "BCC-FCC, Melting and Reentrant Transition in Colloidal Crystals," *J. Colloid. Interface. Sci* **89**, 555-562 (1982).

[12]

Hone, D., S. Alexander, P.M. Chaikin and P.Pincus, "The phase diagram of charged colloidal suspensions,"*J. Chem. Phys.* **79**, 1474-1479 (1983).

[13]

Adler,B.J. and T.E. Wainwright, "Phase Transition for a Hard- Sphere System," *J. Chem Phys* **27**, 1208-1209 (1957).

[14]

Voegtli,L.P. and C.F.Zukoski IV, "A Perturbation treatment of the order-disorder phase transition in colloidal suspensions," *J. Colloid. Interface. Sci.* **141**, 79-91 (1991).

[15]

Adler,B.J. and T.E. Wainwright, "Phase Transition in Elastic Disks," *Phys. Rev.* **127**, 359-361 (1962).

[16]

Shih,W.H. and D. Stroud, "Theoretical study of the freezing of polystyrene sphere suspensions," *J. Chem Phys.* **79**, 6255-6260 (1983).

[17]

Baus,M. and J.L. Colot, "The freezing of hard spheres; The density functional theory revisited," *Molecular Physics* **55**, 653-677 (1985).

[18]

Leutheusser, E., "Dynamical model of the liquid-glass transition," *Phys. Rev. A* **29**, 2765-2780 (1984).

[20]

Kirkpatrick,T.R. , E.G.D. Cohen and J.R. Dorfman, "Fluctuations in nonequilibrium steady state: Basic equations," *Phys. Rev. A* **26**, 950-971 (1982).

[19]

Götze, W., "Aspects of Structural Glass Transitions," in *Liquids, Freezing and the Glass Transition*, edited by J.P. Hansen, D. Levesque and J. Zinn-Justin (North-Holland, Amsterdam, 1991).

[21]

van de Ven, T.G.M., *Colloidal Hydrodynamics* (Academic Press 1989).

[22]

Bedeaux, D., R. Karpal and P. Mazur, "The effective shear viscosity of a uniform suspension of spheres," *Physica A* **88** 88-121 (1977).

[23]

Felderhof, B.U., "The contribution of Brownian motion to the viscosity of suspensions of spherical particles," *Physica A* 533-543 (1988).

[24]

Ohtsuki, T., "Dynamical properties of strongly interacting Brownian particles." *Physica A* **108**, 441-458 (1981).

[25]

Einstein, A., *Investigations on the Theory of Brownian Movement*, edited by R. Fürth, (Dover Publications, Inc. 1956).

[26]

Batchelor, G.K. and J.T. Green, "The determination of the bulk stress in a suspension of spherical particles to the order c^2 " *J. Fluid. Mech.* **56** 401-427 (1972), *J. Fluid. Mech.* **56** 375-400 (1972).

[27]

Brady, J.F., "The rheological behaviour of concentrated colloidal dispersions," *J. Chem. Phys.* **99**, 567-581 (1993).

[28]

Russel, W.B. and A.P. Gast, "Nonequilibrium statistical mechanics of concentrated colloidal dispersions: Hard spheres in weak flows," *J. Chem. Phys.* **84**, 1815-1826 (1986).

[29]

Wagner, N.J. and W.B. Russel, "Non-equilibrium statistical mechanics of concentrated colloidal dispersions: Hard spheres in weak flows with many-body thermodynamic interactions," *Physica A* **155**, 475-518 (1989).

[30]

Beenakker, C.W.J., "The effective viscosity of a concentrated suspension of spheres," *Physica A* **128**, 48-81 (1984).

[31]

Kim, S. and R.T. Mifflin, "The resistance and mobility functions of two equal spheres in low-Reynold number flow," *Phys. Fluids* **28**, 2033-2045 (1985).

[32]

Arp, P.A. and S.G. Mason, "The kinetics of flowing dispersions," *J. of Coll. Int. Sci.* **61** 21-61 (1977).

[34]

Hanley, H.J.M., J. Pieper, G.C. Straty, R.P. Hjelm jr. and P.A. Seeger, "Structure of binary colloidal suspensions under shear," *Faraday Discuss. Chem. Soc.* **90**, 91-106 (1990).

[33]

Jeffrey, D.J. and Y. Onishi, "Calculation of the resistance and mobility functions for two unequal rigid spheres in low-Reynold-number flow," *J. Fluid Mech.* **139**, 261-290 (1984).

[35]

Adler, P.M. and H. Brenner, "Spatially periodic suspensions of convex particles in linear shear flow," *Journal de Physique* **C3**, 224-244 (1984).

[36]

Krieger, J.M., "Rheology of monodisperse latices," *Adv. Colloid. Interface. Sci.* **3**, 111-136 (1972).

[37]

Joseph, D.D. *Fluid Dynamics of Viscoelastic Liquids*, (Springer-Verlag, Berlin, 1990).

[38]

Doi, M. and S.F. Edwards, *The Theory of Polymer Dynamics*, (Clarendon Press, Oxford, 1986)

[39]

de Gennes, P.G *Scaling Concepts in Polymer Physics* (Cornell University Press, 1979)

[40]

Buscall,R., J.W. Goodwin, M.W. Hawkins and R.H. Ottewill, "Viscoelastic properties of concentrated latices," *J. Chem. Soc. Faraday Trans. 1* **78**, 2889-2899 (1982).

[41]

Russel,W.B. and D.W. Benzing, "The viscoelastic properties of ordered latices: A self- consistent field theory,"*J. Colloid. Interface. Sci.* **83**, 163-177 (1981).

[42]

Wagner,N.J., " The high-frequency shear modulus of colloidal suspensions and the effects of hydrodynamic interactions," *J. Colloid. Interface. Sci.* **161**, 169-181 (1993).

[43]

Schreuder,F.W.A.M. and H.N. Stein, "Rheology of concentrated coagulating suspensions in non- aqueous media," *Rheol. Acta* **26**, 45-54 (1987).

[44]

Potantin,A.A., "On the Mechanism of Aggregation in the Shear Flow of Suspensions," *J. Colloid. Interface. Sci.* **145**, 140-157 (1991).

[45]

Wouterson,A. T. J. M. *The rheology of adhesive hard sphere dispersions*, (Ph.D. Thesis Twente University 1993).

[46]

de Rooij,R., A.A. Potantin, D. van den Ende and J. Mellema "Steady shear viscosity of weakly aggregated polystyrene latex dispersions," *J. Chem. Phys.* **99**, 9213-9223 (1993).

[47]

Onuki,A. and K. Kawasaki, "Non-equilibrium steady state of critical fluids under shear flow: A renormalization group approach," *Ann. Phys. (N.Y.)* **121**, 456-528 (1979).

[48]

Bruinsma,R.F. and C.R. Safinya, "Landau theory of the nematic-smectic-A phase transition under shear flow," *Phys. Rev. A* **43**, 5377-5404 (1991).

[49]

Landau,L.D. and E.M. Lifshitz, *Statistical Physics* (Pergamon Press 1980) Vol. 5, Part 1.

[50]

Ma,S.K., *Modern Theory of Critical Phenomena* (W.A. Benjamin, Inc. 1976).

[51]

Levanyuk,A.P., "Contribution to a Phenomenological Theory of Sound Absorbtion near Second-Order Phase Transition Points," *Soviet Physics JETP* **22**, 901-906 (1966).

[52]

Bagchi,B. and D.Thirumalai, "Freezing of a colloidal liquid subjected to shear flow," *Phys. Rev. A* **37**, 2530-2538 (1988).

[53]

Ramaswamy, S. and S.R. Renn, "Theory of Shear-Induced Melting of Colloidal Crystals," *Phys. Rev. Lett.* **56**, 945-948 (1986).

[54]

Goodwin, J.W. "The rheology of polymer colloids," in *An Introduction to Polymer Colloids*, edited by F. Candau, R.H. Ottewill (Kluwer Academic Press 1990).

[55]

Barnes,H.A., M.F. Edwards and L.V. Woodcock, "Applications to computer simulations to dense suspensions rheology," *Chem. Eng. Sci.* **42**, 591-608 (1987).

[56]

Laun,H. M., "Rheological properties of aqueous polymer dispersions," *Angew. Makro. Chem.* **123**, 335-359 (1984).

[57]

Chen,L.B., C.F. Zukoski, B.J. Ackerson, H.J.M. Hanley, G.C. Strarty, J.Barker and C.J.Glinka, "Structural changes and orientational order in a sheared colloidal suspension," *Phys. Rev. Lett.* **69**, 688-691 (1992).

[58]

Erpenbeck,J. J., " Shear viscosity of the hard-sphere fluid via nonequilibrium molecular dynamics," *Phys. Rev. Lett.* **52**, 1333-1335 (1984).

[59]

Hoffman,R.L., "Discontinuous and dilatant viscosity behavior in concentrated suspensions," *Trans. Soc. Rheol.* **16**, 155-173 (1972).

[60]

Ackerson, B.J. and N.A. Clark, "Sheared colloidal suspensions," *Physica A* **118**, 221-249 (1983).

[61]

Loose, W. and S. Hess, "Rheology of dense fluids via nonequilibrium molecular dynamics: shear thinning and ordering transition," *Rheol. Acta* **28**, 91-101 (1989).

[62]

Harrowell, P. and M. Fixman, "The shear melting of colloidal crystals: a long wavelength driven transition," *J. Chem. Phys.* **87**, 4154-4161 (1987).

[63]

Ronis, D. and S. Khan, "Stability and fluctuations in sheared colloidal crystals," *Phys. Rev. A* **41** 6813- 6829 (1990)

[64]

Hoffman, R.L. "Discontinuous and dilatant viscosity behavior in concentrated suspensions III," *Adv. Colloid. Interface. Sci.* **17**, 161-184 (1982).

[65]

Barnes, H.A., " Shear-thickening ('dilatancy') in suspensions of nonaggregating solid particles dispersed in newtonian liquids," *J. Rheol.* **33**, 329-366 (1989).

[66]

Hoffman, R.L. "Discontinuous and dilatant viscosity behavior in concentrated suspensions II," *J. Colloid. Interface. Sci.* **46**, 491-506 (1974).

[67]

Boersma, W. H. and P.J.M. Baets, J. Laven and H.N. Stein, "Time-dependent behavior and wall slip in concentrated shear thickening dispersions," *J. Rheol.* **35**, 1093-1120 (1991).

[68]

Boersma, W. H., J. Laven and H.N. Stein, "Shear thickening (dilatancy) in concentrated dispersions," *AIChE J.* **36**, 321-332 (1990).

[69]

Chow, M.K. and C.F. Zukoski, "Non-equilibrium behavior of dense suspensions of uniform particles: volume fraction and size dependence of rheology and microstructure," *J. Rheol.* **39**, 33-59 (1995).

[70]

Boersma W.H., J. Laven, H.N. Stein, "Computer Simulations of Shear Thickening of Concentrated Dispersions" *J. Rheol.* **39**, 841-860 (1995).

[71]

Woodcock, L.V., "Origins of shear dilatancy and shear thickening phenomena," *Chem. Phys. Lett.* **111**, 455-461 (1984).

[72]

Heyes, D.M., "Shear thinning and thickening of Lennard-Jones liquids," *J. Chem. Soc. Faraday Trans. 2* **82**, 1365-1383 (1986).

[73]

Chen, L.B., B.J. Ackerson and C.F. Zukoski, "Rheological consequences of microstructural transitions in colloidal crystals," *J. Rheol.* **38**, 193-216 (1994).

[74]

Laun, H.M. and R. Bung, S. Hess, W. Loose, O. Hess, P. Lindner, "Rheological and small angle neutron scattering investigation of shear-induced particle structures of concentrated polymer dispersions submitted to Poiseuille and Couette flow," *J. Rheol.* **36**, 743-787 (1992).

[75]

Tomita, M. and T. G. M. van de Ven, "The structure of sheared ordered lattices," *J. Colloid. Interface. Sci.* **99**, 374-386 (1984).

CHAPTER II.

THEORY

2. Theoretical Background on Structural Transitions

2.1 Introduction

Chapter II.2. summarizes the theoretical background for readers, who are not familiar with structural transitions. Colloidal suspensions of soft spheres show a variety of transitions as indicated in the equilibrium phase diagram (Fig.1).

A non-structural phase transition is for example a gas-liquid transition, in which a parameter (e.g. the density) undergoes a change at the critical temperature, whereas the microscopic structure does not change [1] with regard to the symmetry properties. The characteristic property of structural transitions is, that they always involve a change ("breaking") of the symmetry properties of the system. In this thesis we will focus our attention on structural transitions, at which a change in the symmetry properties of the stationary microscopic structure of the particles takes place [2].

A structural transition in a colloidal suspension occurs, when the spatial configuration of the colloidal particles changes from one equilibrium phase to another. These transitions can be either of an order-order type as in the bcc-fcc transition or of an order-disorder type; e.g. the crystal-liquid transition.

A symmetry breaking transition in colloidal suspensions can be induced in two ways; either by travelling through the equilibrium phase diagram, varying the state variables such as the temperature T , the salt concentration C or the volume fraction Φ , or by applying a perturbation, such as a shear deformation. The first case is treated in Chapter II.4 and the latter in Chapter II.5.

The evolution of a system with energy exchange with the surrounding but with a constant number of particles is determined by a thermodynamic potential. We will consider the colloidal suspension as incompressible and take therefore the Helmholtz free energy as the appropriate potential.

In this thesis we focus our attention on the transport properties occurring at structural transitions. The transport properties of a suspension are given by a set of hydrodynamic equations corresponding to the conservation laws of mass, momentum and energy. They can be written as a product of a derivative of the thermodynamic potential and a constant transport parameter [3]. The transport parameter can be obtained from a time dependent correlation function (Green-Kubo equation) of the slightly disturbed equilibrium structure [4],[5].

Approaching a transition in the equilibrium phase diagram the thermodynamic potential softens and critical fluctuations appear, leading to a coupling between the linearized hydrodynamic equations and thus to fluctuation corrected transport parameters. Although the thermodynamic potential can be calculated from a perturbation theory in the (Chapter II.3), it is not in an analytic form applicable to investigate the transport properties near a phase transition. Instead we will use a qualitative form of the thermodynamic potential.

Fortunately the change of the free energy of a system of identical particles is known on approaching a phase transition. The free energy of such a transition can be written as an expansion of an order parameter characterizing the transition, as has been studied first by Landau [2]. The time dependent Ginzburg-Landau (Khalatnikov) theory [6] includes the dynamic behaviour of the order parameter using fluctuating hydrodynamic equations [7]. The application range of this mean field theory is given by the Ginzburg-criterion [7], taking into account the influence of fluctuations on the transition. Depending on the spatial dimensions and the range of the interaction forces it states that the Landau theory is generally only qualitatively applicable but can give quantitatively correct results in four dimensions, or in three dimensions in the case of long range forces [2] between the particles. A specific extension of the Landau theory, the renormalization group theory, delivers correct solutions also for three dimensions [8]. In our studies we will confine ourselves to the Ginzburg-Landau theory.

2.2 General Considerations on Structural Transitions and the Landau Theory

Symmetry Properties

We define a probability density $\rho(\underline{r}, T, \Phi, \dots)$ where ρd^3r is the probability of finding a particle in the elementary volume d^3r . To characterize a change in configuration we introduce the symmetry of a system, defined by a set of geometrical transformations s_{ij} (translations, rotations, reflections etc.), which leave the equilibrium density $\rho(\underline{r}, T, \Phi, \dots)$ invariant. The equilibrium density corresponds to the minimum of the variational free energy $F(\rho(\underline{r}), T, \dots)$ with respect to $\rho(\underline{r}, T, \Phi, \dots)$.

Let the symmetry operation s_{ij} be an element of the group g_0 if:

$$s_{ij}\rho(r_p, T, \Phi, \dots) = \rho(s_{ij}r_p, T, \Phi, \dots) = \rho(r_p, T, \Phi, \dots) = \rho(r_p, T, \Phi, \dots) \quad (3)$$

i.e. the equilibrium density $\rho(\underline{r}, T, \Phi, \dots)$ is invariant against all elements of g_0 . We denote the corresponding phase as the high symmetry phase. The group g_0 can be a continuous group (as in a fluid), an infinite discrete group (as in a crystal) or a finite group (if the crystal symmetry can be reduced to a point symmetry).

The phase transition is defined as the point where the number of allowed symmetry operations of the system is changed abruptly. This phenomenon is called symmetry breaking, because the symmetry of the system is lowered, when some symmetry operations disappear having passed the transition, at the transition values $(T_u, C_u, \Phi_u, \dots)$. The phase with a lower number of allowed symmetry operations is called the low symmetry phase. Such a symmetry breaking transition occurs for example in going from a liquid (high symmetry phase) to a crystal (low symmetry phase). Beyond the transition point the intensity of density waves with the periodicity of the crystal gradually rises with increasing distance to the transition point up to an amplitude corresponding to the fully evolved crystal structure.

On going from the high symmetry phase to the low symmetry phase, the equilibrium density in the low symmetry phase close to the structural phase transition can be written

as

$$\rho(\underline{r}) = \rho_{tr} + \delta\rho(\underline{r}) \quad (4)$$

where $\rho_{tr} = \rho(\underline{r}, T, C, \Phi, \dots)$ is the density at the transition and $\delta\rho(\underline{r})$ is the density increment not invariant under the action of all elements of the group g_0 , but only of a subgroup g_1 of g_0 (g_1 is the low symmetry group). An example of a symmetry breaking transition is given in Appendix A introducing some concepts of the group theory.

We will write the density increment $\delta\rho(\underline{r}_i)$ as a linear combination of orthogonal, normalized functions $\Psi_k^{(n)}(\underline{r})$, where n indicates the various irreducible sets involved:

$$\delta\rho(\underline{r}, T, \Phi, \dots) = \sum_n \lambda_k^{(n)}(T, \Phi, \dots) \Psi_k^{(n)}(\underline{r}) \quad (5)$$

and their amplitudes $\lambda_k^{(n)}$, while k runs over the set of the functions $\Psi_k^{(n)}(\underline{r})$.

Within a specific irreducible representation the functions $\Psi_k^{(n)}(\underline{r})$ will transform into one another under all transformations of the group g_1 . The matrices of the transformations form the representation of the group g_1 and the functions $\Psi_k^{(n)}(\underline{r}_i)$ are the basis of this representation (Appendix A). One can always select these functions in such a way that they split into a number of sets containing as few functions as possible, each set of functions being transformed into itself under all transformations of the group. The transformation matrices of the functions contained in each set form the irreducible representation of the group g_1 .

A structural transition is characterized by the appearance and disappearance of one or several irreducible sets. At the structural transition considered here, only by accident more than one irreducible set will change at the same critical value. Thus focusing on only one irreducible set, we can omit the sum over n in equation (5). Each of the basic functions of a irreducible set of a space group can be written as a periodic function of \underline{r} . We define $\Psi_k(\underline{r})$ as:

$$\Psi_k = e^{j \underline{G}(k) \cdot \underline{r}} \quad (6)$$

where $j^2 = -1$ and $\underline{G}(k)$ are the reciprocal lattice vectors [1],[2].

Ginzburg- Landau Free Energy

The basic idea of the Landau theory is to consider the free energy as a function of the structural alteration [2]. For that purpose we write the free energy as a function of the density

$$F(\rho(\mathbf{r}))=F(\rho_{\sigma}+\lambda_k\Psi_k(\mathbf{r})) \quad (7)$$

Note that throughout this book we will interpret F as the free energy per unit volume. Having defined the functions $\Psi_k(\mathbf{r})$ and keeping their form fixed at the transition, the equilibrium value of the free energy can be found by a variation of F with respect to λ_k . Close to the symmetry breaking transition, $\delta\rho$ is small and $F(\rho)$ can be expanded in a Taylor expansion in $\delta\rho$

$$F(\delta\rho)=F_{\sigma}(\rho_{\sigma})+\alpha^*(T,\Phi,..) \delta\rho+\alpha(T,\Phi..) (\delta\rho)^2+O((\delta\rho)^3) \quad (8)$$

or with equation (5) as

$$F(\delta\rho)=F_{\sigma}(\rho_{\sigma})+\alpha^*(T,p,..)(\lambda_k\Psi_k)+\alpha(T,\Phi..)(\lambda_k\Psi_k)^2+O((\lambda_k\Psi_k)^3) \quad (9)$$

We assume that Ψ_k have fixed values at the transition and write the λ_k as

$$\lambda_k=q*e_k \quad (10)$$

while q is a scalar and is called the order parameter of the transition; e_k is a unit vector in the space of the chosen irreducible representation.

Combining (5), (6) and (10) we arrive at the final form of the density increment:

$$\delta \rho(\mathbf{r}) = q \sum_{\mathbf{k}} e_{\mathbf{k}} e^{j\mathbf{G}(\mathbf{k})\mathbf{r}} \quad (11)$$

where \mathbf{k} runs over the reciprocal lattice vectors $\mathbf{G}(\mathbf{k})$ of the irreducible representation. The sum describes the density wave of the reciprocal lattice and q is its amplitude.

The equilibrium value of the order parameter q can be obtained by minimization of the free energy with respect to q .

$$\left(\frac{\partial F}{\partial q} \right)_{T, \phi, \dots} = 0 \quad (12)$$

and we obtain

$$\alpha^* + \alpha q_0 = 0 \quad (13)$$

For the high symmetry phase we demand that $q=0$ and therefore $\alpha^*=0$. Thus the first relevant term in the expansion of the free energy is of the second order. Additionally we demand that the free energy has a minimum and therefore $\alpha > 0$. Thus $\alpha > 0$ corresponds to $q=0$, i.e. the high symmetry phase.

For $\alpha < 0$ i.e. the low symmetry phase it is necessary to expand F up to higher order in q . A third order expression does not lead to a stable equilibrium state and thus the free energy will be supplemented by a fourth order term.

$$F(q) = F_0 + \frac{\alpha}{2} q^2 - \frac{\zeta}{3} q^3 + \frac{\nu}{4} q^4 \quad (14)$$

where we assume $\nu > 0$; otherwise we have to take into account higher order terms in q to find a minimum of the free energy. We will confine our theory to positive equilibrium values of the order parameter and thus demand $\zeta \geq 0$.

Order Parameter of a Second Order Transition

A special case of equation (14) is $\zeta=0$. In this situation the free energy takes the form

$$F(q) = F_0 + \frac{\alpha}{2} q^2 + \frac{\nu}{4} q^4 \quad (15)$$

By means of the equilibrium condition (12) we obtain the order parameter in the low symmetry phase ($\alpha < 0$) to be

$$q_0 = \pm \sqrt{-\frac{\alpha}{\nu}} \quad (16)$$

Since α is a function of the temperature, volume fraction etc, we require the coefficient $\alpha(T, \phi, \dots)$ to satisfy the condition $\alpha((T_{tr})_{\Phi}, (\Phi_{tr})_{T, \dots}) = 0$ at the transition values of the temperature volume fraction etc..

Because $\alpha(T, \Phi, \dots)$ is small close to the transition, we can expand $\alpha(T, \Phi, \dots)$ as a function of the temperature T , volume fraction Φ etc. around the transition coordinates; α can be written as

$$\alpha(T, \Phi, \dots) = \alpha_T (T - T_{tr})_{\Phi, \dots} + \alpha_{\Phi} (\Phi - \Phi_{tr})_{T, \dots} + \dots \quad (17)$$

where α_T, α_{Φ} are positive constants.

The absence of a jump in the order parameter and the infinite correlation length at the transition value $\alpha_{tr} = 0$ is in the literature referred to as a second order transition. Thus while $\zeta=0$ corresponds to a second order phase transition, the condition $\zeta > 0$ will be shown to describe a first order transition.

Order Parameter of a First Order Phase Transition

The case $\zeta > 0$ of the free energy (14) leads to the characteristic properties of a first order phase transition, such as a jump in the order parameter and the coexistence of two phases, which implies the possibility of metastability.

The equilibrium values can be obtained from equation (12) leading to three solutions:

$$\begin{aligned}
 q_{00} &= 0 \\
 q_{01} &= \frac{\zeta}{2\nu} + \sqrt{\left(\frac{\zeta}{2\nu}\right)^2 - \frac{\alpha}{\nu}} \\
 q_{02} &= \frac{\zeta}{2\nu} - \sqrt{\left(\frac{\zeta}{2\nu}\right)^2 - \frac{\alpha}{\nu}}
 \end{aligned}
 \tag{18}$$

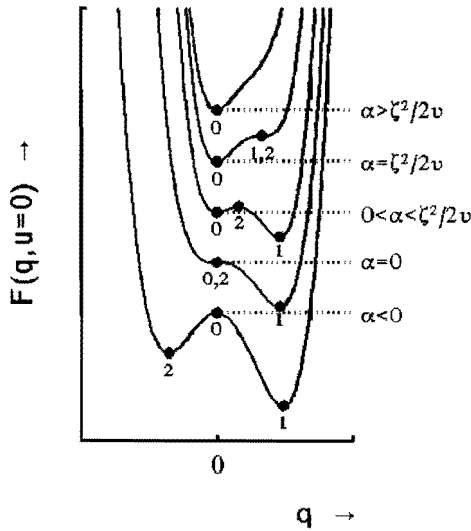


Figure 6 The Helmholtz free energy for different values of α .

The stability of the solutions of equation (14) depends on the second derivatives of the free energy with respect to the order parameter. The solution $q = q_{00} = 0$ represents

the high symmetry phase, whereas $q = q_{01} > 0$ is the low symmetry phase. The high symmetry phase is thermodynamically stable when $\alpha \geq \alpha_{01} = \zeta^2/4\nu$. The low symmetry phase is stable when $\alpha < \alpha_{00} = 0$; in that case $q = q_{01}$. The coexistence region is bounded by α_{00} and α_{01} (Fig.6).

The value of the order parameter depends on the history of the system. The system stays in the high symmetry phase q_{00} if $\alpha \gg 0$. Decreasing α down to α_{01} the system jumps from the high symmetry phase at $q_{00} = 0$ to the low symmetry phase at $q_{01} \neq 0$. At negative α the system is in the low symmetry phase and jumps back into the high symmetry phase at $\alpha = \alpha_{00}$ on increasing α . Thus the system exhibits a hysteresis between $\alpha_{01} \geq \alpha \geq \alpha_{00}$. Two minima at equal values of the free energy appear at $\alpha = \alpha_c$. The value of α_c can be determined from $F(q_{00}) = F(q_{01}) = 0$ and thus

$$\alpha_c = \frac{2\zeta^2}{9\nu} \quad (19)$$

For second order transitions the hysteresis disappears and the transition occurs at $\alpha = 0$.

Free Energy Density

The contributions of spatial fluctuations to the free energy have been neglected up to now. In order to take them into account we have to introduce a local free energy density $f(\underline{r})$:

$$F = \int_V d^3r f(\underline{r}) \quad (20)$$

The free energy density takes the form

$$f(\underline{r}) = f_0 + \frac{\lambda}{2} (\nabla q(\underline{r}))^2 + \frac{\alpha}{2} q(\underline{r})^2 - \frac{\zeta}{3} q(\underline{r})^3 + \frac{\nu}{4} q(\underline{r})^4 \quad (21)$$

where we introduced a space dependent order parameter density $q(\underline{r})$ and a term $\lambda(\text{grad}(q(\underline{r})))^2$. The latter term takes into account homogeneous fluctuations, i.e. fluctuations on a length scale large compared to the length scale of the crystal lattice [2].

Validity of the Landau Theory

The validity of this approach is determined by the influence of the fluctuations on the transition, as given by the Ginzburg criterion [2]. It indicates that the Landau theory describes the transition quantitatively correct for a D -dimensional space with $D \geq D_c$ but that is at least qualitatively correct for dimensions of the system $D < D_c$. The universality hypothesis claims that the critical dimension D_c of the transition depends on the range of the interaction. The Landau theory is quantitatively valid for interaction forces decreasing slower than $F(r) \sim r^{-(\beta D)}$ with $\beta < 3/2$ ($D=3$). Thus the critical dimension is

$$D_c = \frac{3}{2}D \quad (22)$$

[8]. Because the screened Coulomb potential as used in our model is of the form e^{-r}/r , the Landau theory will be only qualitatively applicable to electrically stabilized colloidal suspensions.

Appendix A

Example of a symmetry breaking [1]

In this Appendix we describe some concepts of the group theory concerning the symmetry breaking. Let us consider a crystalline substance in which a phase transition is assumed to take place at a given temperature and pressure (T_u, p_u). The unit cell of phase 1 is shown in Figure 7. Phase 2 differs from phase 1 by the fact that the centre particle is displaced by the vector \underline{q} . Thus phase 1 is characterized by $\underline{q}=0$, while phase 2 has a non-zero value of \underline{q} . The configuration of particles in phase 1 is unchanged by a set of rotations and reflections with respect to the centre of a cell.

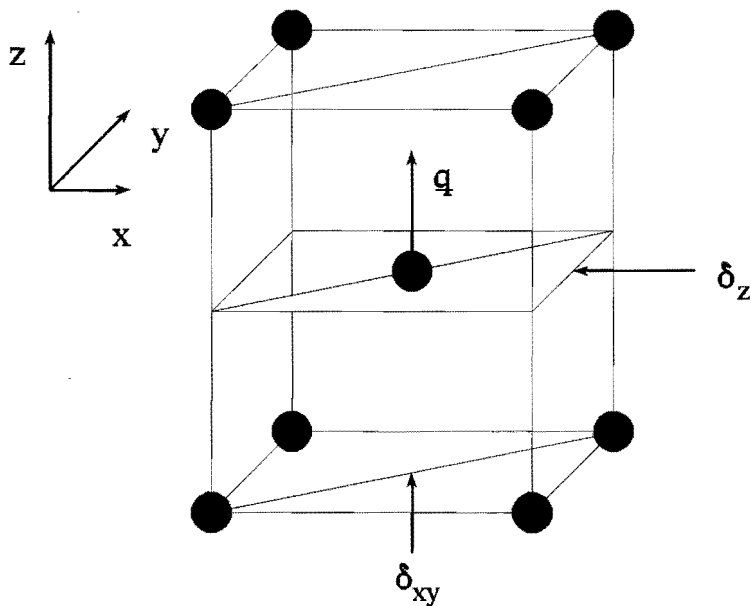


Figure 7 Unit cell of a phase1 with vector $\underline{q}=0$ and phase2 with $\underline{q}\neq 0$.

Phase 1 is left invariant by:

- fourfold ($\pi / 2$) rotations around the z- axis
- reflections about planes δ_y , δ_z or δ_{xy} perpendicular to the coordinate axes y or z or to the diagonals of the square basis of the unit cell
- inversion I about the centre of the cell

The product of any two of these geometrical transformations also leaves the structure unchanged. The corresponding set of symmetry transformations that leaves the structure invariant is called the high symmetry group g_0 which contains 16 elements (the crystallographic label is $4/mm$ or D_{4h}).

The set of transformations leaving phase 2 invariant is the group g_1 , which depends on the direction of the displacement of \underline{q} . If \underline{q} is associated for example to a displacement q_z along the z direction $\underline{q}=(0,0,q_z)$; g_1 contains the fourfold rotations around z as well as the reflections $\delta_x, \delta_y, \delta_{xy}$ in planes containing the z direction. It does not include other elements of g_0 such as the inversion I or the reflection δ_z . In this case the low symmetry group g_1 is a subgroup of g_0 containing 8 elements (C_{4v}).

Table A-1 indicates the way in which $\underline{q}=(q_x, q_y, q_z)$ transforms under the action of the generators of g_0 .

Table A-1

g_0	C_4	σ_x	I
q_x	q_y	$-q_x$	$-q_x$
q_y	$-q_x$	q_y	$-q_y$
q_z	q_z	q_z	$-q_z$

We note that q_z is transformed into itself or into its opposite. If we consider the direction q_z as a vector space we can see that this vector space is invariant by the transformations belonging to g_0 . However the direction q_x does not constitute an invariant vector space since elements of g_0 can transform q_x into q_y . The vector space constituted by the directions

(q_x, q_y) is invariant by g_0 .

The entire set (q_x, q_y, q_z) constitutes a 3-dimensional vector space invariant by g_0 and contains smaller spaces $(q_z, (q_x, q_y))$ which also possess the property of invariance by g_0 . We characterize this situation by saying that (q_x, q_y, q_z) is a reducible invariant space with respect to g_0 , while (q_z) and (q_x, q_y) are irreducible invariant spaces with respect to g_0 . It is well known that if a vector space is invariant under a linear transformation belonging to g_0 , this transformation can be represented by a matrix indicating the action of that element of g_0 on the basic vectors of the space. The Table A-2 shows the matrices representing the generators of g_0 .

Table A-2

g_0	C_4	σ_x	I
(q_x, q_y, q_z)	$\begin{pmatrix} 0 & 1 & 0 \\ -1 & 0 & 0 \\ 0 & 0 & 1 \end{pmatrix}$	$\begin{pmatrix} -1 & 0 & 0 \\ 0 & 1 & 0 \\ 0 & 0 & 1 \end{pmatrix}$	$\begin{pmatrix} -1 & 0 & 0 \\ 0 & -1 & 0 \\ 0 & 0 & -1 \end{pmatrix}$
(q_x, q_y)	$\begin{pmatrix} 0 & -1 \\ 1 & 0 \end{pmatrix}$	$\begin{pmatrix} -1 & 0 \\ 0 & 1 \end{pmatrix}$	$\begin{pmatrix} -1 & 0 \\ 0 & -1 \end{pmatrix}$
(q_z)	1	1	-1

The set of all matrices of a group g_0 constitute a representation of g_0 in the vector space involved. The two sets of matrices for the spaces (q_z) and (q_x, q_y) constitute an irreducible representation of g_0 , since the corresponding spaces are irreducible invariant spaces by g_0 . The order parameter of the considered symmetry breaking transition coincide either with (q_z) or (q_x, q_y) belonging to the different basic symmetry properties but not with the entire set (q_x, q_y, q_z) .

The basic idea of the Landau theory is to consider this order parameter as a variational degree of freedom of the system, and to note that the equilibrium value can be determined by minimizing the variational free energy $F(T, p, q_x, q_y, q_z)$ with respect to the components of q .

We expand the free energy up to second degree terms in q :

$$F(T,p,q) = F_0(T,p) + a_i(T,p)q_i + b_{ij}(T,p)q_iq_j \quad (\text{A.1.})$$

Considering the reflections δ_y , δ_z , δ_x of g_0 , each δ_i reverses the corresponding component q_i and leaves unchanged the two other components. The action of these transformations shows that the linear term is absent in the Taylor expansion since F only depends on the "internal" state of the system, and not on its absolute orientation. That is, F must be invariant under all geometrical transformations of the group g_0 .

Because (q_x) and (q_x, q_y) are linearly independent, F can be written as:

$$F(T,p,q) = F_0(T,p) + \frac{\alpha_2(T,p)}{2}(q_x^2 + q_y^2) + \frac{\alpha_1}{2}q_z^2 \quad (\text{A.2.})$$

Literature

[1]

Toledano, J.C. and P. Toledano, *Landau Theory of Phase Transitions* (World Scientific 1987).

[2]

Landau, L.D. and E.M. Lifshitz, *Statistical Physics* (Pergamon Press, Oxford, 1980) (Vol.5) Part 1.

[3]

de Groot, S.R. and P. Mazur, *Non-equilibrium Thermodynamics* (North-Holland Publishing Company, 1962)

[4]

Kadanoff, L.P. and P.C. Martin, "Hydrodynamic equations and correlation functions," *Annals of Phys.* **24**, 419-469 (1963).

[5]

Hansen, J.P. and I.R. McDonald *Theory of Simple Liquids* (Academic Press 1986).

[6]

Hohenberg, P.C. and B.I. Halperin, "Theory of Dynamical Critical Phenomena," *Rev. Mod. Phys.* **49**, 435-479 (1977).

[7]

Ma, S.K., *Modern Theory of Critical Phenomena* (W.A. Benjamin, Inc., Massachusetts, 1976).

[8]

Binney, J.J., N.J. Dowrick, A.J. Fisher and M.E.J. Newman, *The Theory of Critical Phenomena* (Clarendon Press, Oxford, 1992).

3. The Equilibrium Phase Diagram of Suspensions of Electrically Stabilised Colloidal Particles

3.1 Introduction

Colloidal particles may repel each other, either electrostatically (by electric charges on their surfaces) or sterically (by polymers attached to their surfaces and protruding into the continuous phase). The effective interaction potential, due to double layers surrounding the colloidal particles in an electrolyte solution, can be represented by a screened Coulombic potential. For the spherical particles investigated here we will use a Debye interaction potential. Thus the present treatment neglects deviations from the Boltzmann-distribution (with electrostatic interaction between point charges as sole energy term) of the ions around the particles, e.g. by hydrated ions on the surface or chemisorption.

The Coulomb potential can be progressively screened at constant surface potential by subsequent addition of electrolyte and under these conditions the van der Waals attraction becomes important. The resulting interaction potential can be described by the standard DLVO theory [1],[2],[3]. A "primary" minimum of the potential close to the particle surface may be separated from a "secondary" minimum at larger distances by a Coulombic barrier as depicted in Figure 8.

Dilute suspensions form a random distribution of electrostatically stabilized colloidal particles ("fluid phase"). However, at higher volume fractions a colloidal crystal may be more favourable. Two ordered crystal phases, a body centred cubic lattice (bcc) and a face centred cubic lattice (fcc) have been found in a number of experimental [4],[5],[6] and theoretical [7],[8],[9] investigations. The bcc crystal was only found at very low ionic strengths. The transition line between them has been calculated by using a density functional approach [10],[11],[12].

Victor & Hansen [13] theoretically predicted that on increasing the ionic strength a reversible 'liquid-vapour' spinodal decomposition appears into a flocculated

phase ("liquid") and a low density phase of non-flocculated particles ("vapour"). This flocculation takes place into the secondary minimum. It is reversible and occurs as long as irreversible coagulation is prevented by a Coulomb barrier.

The limitation of the approach by Victor & Hansen however is that they calculated the spinodal lines of the liquid-vapour transition disregarding the presence of the colloid crystal phase. Including the crystal phase allows to determine the phase diagram also at high volume fractions and low Debye screening parameters. Our approach can lead to qualitatively different results if compared to that of Victor & Hansen. The expected liquid-vapour spinodal decomposition disappears for example for low attractive forces. Their analysis was confined to a first order perturbation approach.

The objective of this paper is to improve the approximations made by Victor & Hansen. For that purpose we start from the interaction potential introduced by Victor & Hansen [13] for electrostatically stabilized colloidal particles, which consists of a superposition of a repulsive hard sphere potential and an attractive perturbation. Using this interaction potential we apply a second order perturbation approach to determine the free energy of the colloidal fluid and the crystal phase based on statistical thermodynamics as developed originally by Gast et. al. [14]. The latter approach was originally developed for predicting the phase diagram of non-aqueous, colloidal suspensions in the presence of non-adsorbing polymers. By comparing the free energies of the fluid and the crystal phase, the coordinates of the coexistence lines in the phase diagram can be determined. Employing a numerical scheme we will calculate the coexistence lines as a function of the salt concentration for different temperatures, surface potentials and particle sizes.

3.2 Theory

Interaction Potential

We consider a suspension of N charged, monodisperse, colloidal spheres. The spheres are surrounded by counter ions and additional electrolyte forming an electrical double layer around them. The total DLVO-potential energy $\tilde{U}(r)$ is the sum of the electric repulsion of the double layers and the van der Waals attraction between two colloidal particles:

$$\tilde{U}(r) = \tilde{U}_R(r) + \tilde{U}_A(r) \tag{23}$$

where r is the centre to centre distance between the colloidal particles.

In the linear superposition approximation the electrostatic term can be calculated from the Poisson Boltzman theory [1], [15] to be:

$$\tilde{U}_R(r) = \frac{16\pi\epsilon_0\epsilon_r\sigma_0^2}{e_0^2} \left[k_B T \tanh\left(\frac{e_0\Psi_0}{4k_B T}\right) \right]^2 \frac{\exp(-\kappa_0(r-\sigma_0))}{r} \tag{24}$$

where Ψ_0 is the surface potential of a colloidal particle, σ_0 is its diameter, ϵ_0 is the permittivity of vacuum, ϵ_r is the relative dielectric constant of the solvent, e_0 is the elementary charge, k_B is Boltzmann's constant, T is the temperature and κ_0^{-1} is the 'Debye screening length' of the ions.

The 'Debye screening parameter' κ_0 , can be written as:

$$\kappa_0 = \sqrt{\frac{2e_0^2 z^2 C}{\epsilon_0 \epsilon_r k_B T}} \quad (25)$$

where C is the added salt concentration of a $z:z$ electrolyte based on the liquid volume.

For not too large surface potentials (less than $\Psi_0 \approx 25$ mV), the hyperbolic tangent in (24) can be linearized and the potential reduces to

$$\tilde{U}_R(r) = \pi \epsilon_0 \epsilon_r \sigma_0^2 \Psi_0^2 \frac{\exp(-\kappa_0(r - \sigma_0))}{r} \quad (26)$$

This dimensionless Coulomb potential, scaled by the thermal energy $k_B T$, takes the form

$$U_K(x) = \frac{T_R \exp(-\kappa(x-1))}{x} \quad (27)$$

where we introduced $x = r/\sigma_0$ as the reduced centre-to-centre distance, $\kappa = \kappa_0 \sigma_0$ is the reduced Debye reciprocal length and

$$T_R = \frac{\pi \epsilon_0 \epsilon_r \sigma_0^2 \Psi_0^2}{k_B} \quad (28)$$

The van der Waals attraction energy between spherical particles is of the form [13]

$$U_A(x) = -\frac{Ah(x)}{12} \tag{29}$$

where A is Hamaker's constant and

$$h(x) = \frac{1}{x^2 - 1} + \frac{1}{x^2} + 2 \ln\left(1 - \frac{1}{x^2}\right) \tag{30}$$

Thus the total potential scaled by the thermal energy becomes:

$$U(x) = \frac{1}{T} \left(T_R \frac{\exp(-\kappa(x-1))}{x} - T_A \frac{h(x)}{12} \right) \tag{31}$$

with $T_A = A/(k_B)$. The interaction potential may exhibit a positive maximum at $x_M > 1$ and has a secondary minimum at x_m where $x_m > x_M$ (Fig.8).

The secondary minimum in $U(x)$ becomes more pronounced either on increasing the van der Waals attraction or on screening the Coulomb repulsion by increasing the concentration of salt. This leads to flocculation into the secondary minimum, if the thermal energy is the only energy of motion of the dispersed particles. Coagulation into the primary minimum will be prevented as long as the

Coulomb barrier $U(x_M)$ is substantially larger than the thermal energy $k_B T$. Victor & Hansen assumed, somewhat arbitrarily, that the suspension is charge-stabilized if

$$U(x_M) > \frac{10T}{T_R} \tag{32}$$

Their results with respect to the phase diagram of such suspensions are rather insensitive to the precise value of the assumed potential barrier.

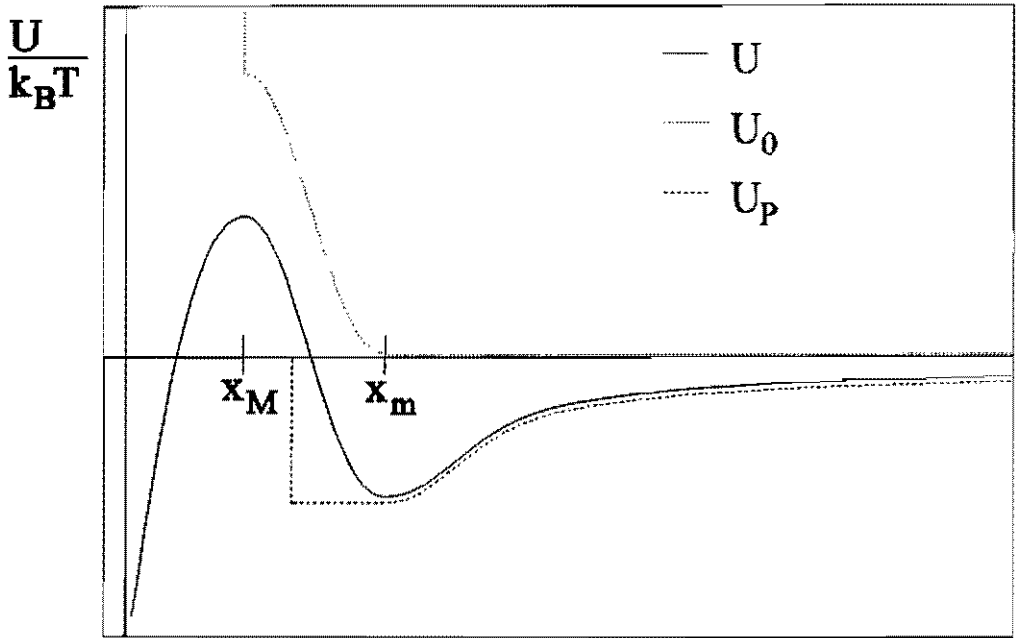


Figure 8 The total two-particles interaction potential (solid line) $U(x)/k_B T$ scaled by the thermal energy as a function of the centre-to-centre distance x .

U_0 is the repulsive contribution to the potential and U_p is the attractive perturbation.

In order to calculate the thermodynamic properties of charge-stabilized colloidal particles, we make use of the perturbation theory developed by Gast et al. [14] based on a hard sphere reference state. For that purpose the total potential is transformed into an effective hard sphere part and an attractive perturbation.

Separation of the Potential

According to Weeks et al. [16] the total potential is attractive for large distances and repulsive for small distances. This can be written as:

$$U(x) = U_0(x) + W(x) \tag{33}$$

while U_0 and W are:

$$\begin{aligned} U_0(x) &= \infty && ; x < x_M \\ U_0(x) &= U(x) - U(x_m) && ; x_M < x < x_m \\ U_0(x) &= 0 && ; x > x_m \end{aligned} \tag{34}$$

and

$$\begin{aligned} W(x) &= U(x_m) && ; x < x_m \\ W(x) &= U(x) && ; x > x_m \end{aligned} \tag{35}$$

Following Victor & Hansen $U_0(x < x_M)$ in Eq.(34) is replaced by a hard sphere potential provided the condition Eq. (32) is satisfied. This is justified, because the high Coulomb barrier will practically speaking prevent particles from getting as close

as x_M and coagulation is negligible.

A system of particles interacting by the purely repulsive potential $U_0(x)$ constitutes the reference system, while the attractive component $W(x)$ will be looked upon as a perturbation.

The Effective Hard Sphere Diameter

Weeks et. al. neglected the repulsion at distances $x_M < x < x_m$. However, the potential $U_0(x)$ gives an extra contribution to the effective hard sphere potential of the particles. According to Victor & Hansen, the properties of the reference system with the interaction $U_0(x)$ can be related to those of an 'equivalent' fluid containing hard spheres of diameter σ . For that purpose they calculated the Barker-Henderson parameter S [17], which is given by $S = \sigma/\sigma_0$. Its value can be derived from a functional Taylor expansion of the Helmholtz free energy in powers of the difference between the Boltzmann factors associated with the reference system (e^{-U_0}) and the equivalent hard-sphere fluid. The leading term in this expansion is:

$$S = \frac{\sigma}{\sigma_0} = x_M + \int_{x_M}^{\infty} [1 - \exp(-U_0(x))] dx \quad (36)$$

Because $S \geq 1$, the volume fraction of the particles in the equivalent hard sphere system Φ will be larger than the true volume fraction Φ^0 : $\Phi = S^3 \Phi^0$ with

$$\Phi^0 = \frac{\pi \rho \sigma_0^3}{6} \quad (37)$$

where $\rho = N/V$ is the number density.

Perturbation Theory

The basic idea of the perturbation approach is to write the potential energy of a 2-particle system as the sum of two terms

$$U(x) = U_{HS}(x) + U_p(x) \tag{38}$$

in which $U_{HS}(x)$ is the potential energy of the unperturbed effective hard sphere reference system. According to Victor & Hansen [13] the two particle interaction potential can be written as:

$$\begin{aligned} U_{HS}(x) &= \infty & ; x < S \\ U_{HS}(x) &= 0 & ; x \geq S \end{aligned} \tag{39}$$

$U_p(x)$ is the attractive perturbation potential. This has the form:

$$\begin{aligned} U_p(x) &= 0 & ; x < S \\ U_p(x) &= U(x_m) & ; S \leq x < x_m \\ U_p(x) &= W(x) = \frac{1}{T} \left(\frac{T_R \exp(-\kappa(x-1))}{x} - \frac{T_A h(x)}{12} \right) & ; x \geq x_m \end{aligned} \tag{40}$$

This potential is shown in Figure 8. Note that the attractive potential is kept constant in the region $S \leq x < x_m$.

According to Zwanzig [18] and Barker and Henderson [17] the Helmholtz free energy of a thermodynamic system of particles with an attractive two particle interaction potential can be written as a perturbation expansion in $1/k_b T$ (high temperature expansion). Because the high temperature case is equivalent to the hard sphere system, the expansion of the Helmholtz free energy including the second order

takes the form:

$$\frac{F}{Nk_B T} = \frac{F_{HS}}{Nk_B T} + \frac{\rho}{2} \int_0^\infty U_p(r) g_{HS}(r) 4\pi r^2 dr - \frac{\rho}{4} \left(\frac{\partial \rho}{\partial p} \right)_{HS} k_B T \int_0^\infty (U_p(r))^2 g_{HS}(r) 4\pi r^2 dr \quad (41)$$

where F_{HS} is the free energy of the undisturbed hard sphere system and g_{HS} is the hard sphere pair distribution function. This equation is valid for both for colloidal fluids and colloidal crystals. The free energy as a function of the effective diameter is derived in Appendix B.

The thermodynamic relations between the Helmholtz free energy, the Gibbs free energy G and the osmotic pressure p are given by

$$\frac{G}{k_B T} = \frac{\partial}{\partial \rho} \left(\frac{\rho F}{k_B T} \right)_{p,T} \quad (42)$$

and

$$\frac{p}{k_B T} = \frac{\rho G}{k_B T} - \frac{\rho F}{k_B T} \quad (43)$$

Note that the screened Coulomb interaction potential is also a function of the density. The intersection of the curves of the Gibbs free energies of the colloidal fluid and the crystal phase determines the coexistence pressure and thus the coexistence densities of these phases.

3.3 Numerical Procedure

The volume fraction dependent Barker-Henderson parameter S is obtained by numerical integration of equation (36). All numerical integrations are carried out by a Runge-Kutta procedure as described in [19].

After rescaling the distance r with the effective hard sphere diameter σ we arrive at an alternative form of the interaction potential (see Appendix B). For the numerical integration of the contributions to the Helmholtz free energy of the crystal and the fluid phase (B.5), the equations of state and the correlation functions of the hard sphere reference system for both the fluid and the crystal phase were taken as summarized in reference [14].

The Gibbs free energies are obtained by numerical differentiation of (41) according to (42). The intersection of the fluid and the solid Gibbs free energies $G/(k_B T)$ as plotted versus the pressure determines the coexistence pressure p' of the transition.

Substituting the pressure p' in equation (43) gives the coexistence densities of the fluid and the solid phases. Plotting the coexisting volume fractions for varying salt concentrations maps out the phase diagram. The independent parameter set of a given particle-solvent system consists of the surface potential, the particle diameter, the temperature, the dielectric constant of the solvent, the Hamaker constant and the concentration of added electrolyte. These parameters are combined into three independent parameters that determine the phase diagram: T_A, T_R and κ . To test the proper functioning of the computer program one of the phase diagrams as calculated by Gast et al. [14] was evaluated. It well reproduced their original result.

3.4 Results and Discussion

A number of phase diagrams has been calculated for electrically stabilized particles in water as a function of the Debye screening parameter κ . In order to compare our formalism with the results of Victor & Hansen [13] we have chosen similar parameters of T_A and T_R as summarized in Tables 1 and 2. These Tables also

also give the corresponding values of the surface potential and the Hamaker constant. We restricted our calculations to polystyrene particles with a diameter $\sigma_0 = 1\mu\text{m}$, dispersed in water ($\epsilon_r = 80.37$) surrounded by monovalent ions.

T_R / K	Ψ_0 / mV
60000	19.2
65000	20
70000	20.8
75000	21.6

Table 3.1

T_A / K	$A / 10^{20} \text{ J}$
1800	2.5
3500	4.9
4000	5.5
4500	6.2

Table 3.2

In Figure 9 the phase diagram of a latex suspension with $T_A = 4000 \text{ K}$ and $T_R = 70000 \text{ K}$ is displayed. For low salt concentrations the fluid-crystal transition starts at the origin.

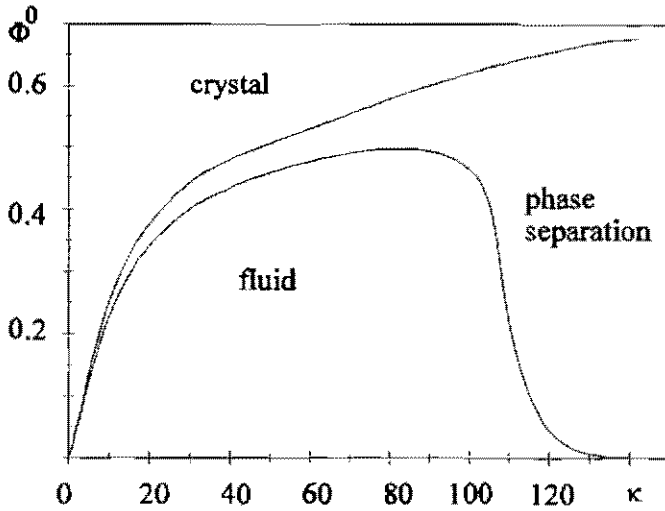


Figure 9 The phase diagram of electrically stabilized colloidal particles for the parameter values $T_R=60000$ K and $T_A=1800$ K.

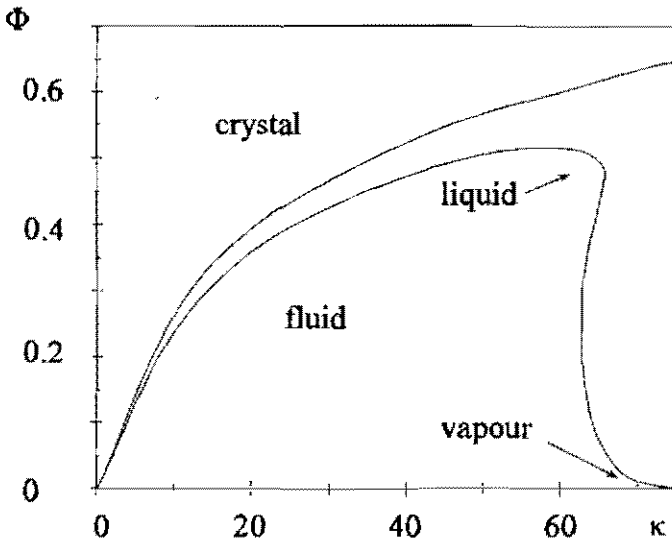


Figure 10 The phase diagram of electrically stabilized colloidal particles for the parameter values $T_R=70000$ K and $T_A=4000$ K.

The coexistence lines rise monotonically in the volume fraction with increasing screening by increasing κ . The further increase of the screening lets the transition finally occur at almost the values of the fcc-fluid transition of hard spheres ($\Phi_{\text{fluid}}^0 = 0.49$ $\Phi_{\text{solid}}^0 = 0.54$). This result is in agreement with the theoretical [15] and experimental [20],[21],[22] investigations.

On increasing the screening κ further, the fluid becomes unstable against flocculation. It decomposes into a liquid (flocculated structure) and a vapour phase. At $\Phi^0 = 0.47$, $\kappa = 66$ we arrive at a triple point, where the liquid, gas and solid (crystal) phases are in thermodynamic equilibrium. The spinodal decomposition into a flocculated liquid and a gas phase as predicted by us is shifted by nearly a factor two to lower values of the Debye screening length κ if compared with the results of Victor & Hansen on the basis of their first order perturbation theory. This deviation can be ascribed to main differences between our approach and that of Victor & Hansen: (i) we acknowledge the occurrence of a crystal phase and (ii) our perturbation approach is of second order.

In Figure 10 the attractive and repulsive forces were decreased applying the parameter set $T_A = 1800$ K and $T_R = 60000$. Disregarding the crystal phase the approach by Victor & Hansen expected for this parameter set a phase separation into a liquid and a gas phase. However the liquid phase, made up of aggregated colloidal particles, disappears and a phase separation takes place into a fluid and a crystal phase. Similar results have been obtained recently by Mederos & Navascues [23], while they applied a density functional theory. In agreement with our investigations they found that the liquid phase will only appear in the case of fairly large attractive potential. Tejero et al. [24], [25] systematically investigated colloidal suspensions with a double-Yukawa pair potential, and found that the liquid phase occurs only for long range attractive forces and disappears for intermediate-range attractions.

To study the influence of the attractive and repulsive forces of the interaction potential on the phase diagram, the parameters T_A and T_R were varied.

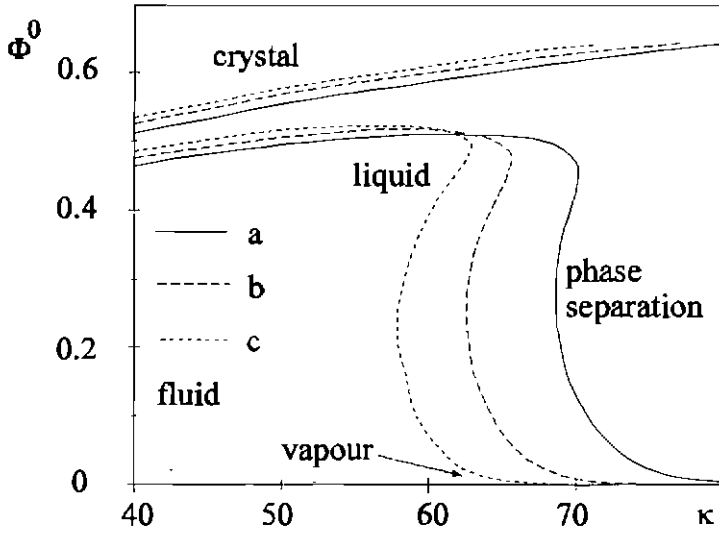


Figure 11 The phase diagram of elect. stabilized colloidal particles for the parameter values $T_R=70000$ K and (a) $T_A= 4500$ K, (b) $T_A= 4000$ K and (c) $T_A= 3500$ K .

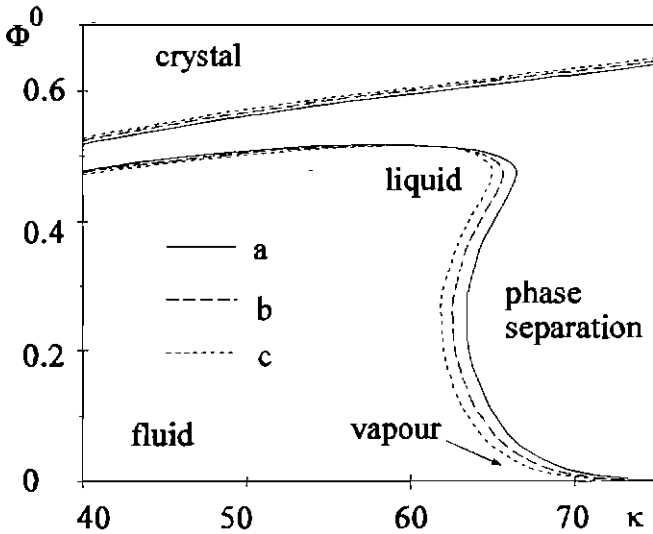


Figure 12 The phase diagram of electrically stabilized colloidal particles for the parameter values $T_A=4000$ K and (a) $T_R= 75000$ K, (b) $T_R= 70000$ K and (c) $T_R= 65000$ K .

Figure 11 shows the dependence of the phase diagram on the attractive forces. Keeping $T_R=70000$, the value of T_A was varied: $T_A=4500$, (a) $T_A=4000$ (b) and $T_A=3500$ (c). On increasing the attraction the critical point also shifts to slightly lower values of Φ , while the triple point shifts to slightly larger values of Φ . On increasing the attraction the fluid-crystal coexistence region broadens. This is in agreement with calculations of other investigators [14], [25] with interaction potentials using a constant effective diameter and varying attractive potentials.

In Figure 12 the attractive forces are kept constant at $T_A=4000$ and the repulsive interaction was varied: $T_R=75000$ (a), $T_R=70000$ (b) and $T_R=65000$ (c). On increasing the repulsion T_R the critical and triple points shift to larger values of κ and will coincide eventually. With increasing repulsion the liquid phase becomes less pronounced. The fluid-crystal coexistence lines shift to lower values of the volume fraction on increasing the repulsion, because the effective diameter of the colloidal particles is increased.

3.5 Conclusion

In order to calculate the phase diagram of electrically stabilized colloidal suspensions we applied a second order perturbation theory [14] in the attractive perturbation potential. For that purpose we approximate the two particle interaction potential by a repulsive effective hard sphere potential and a attractive perturbation potential according to Victor & Hansen [13]. The numerical calculations showed that for not too large surface potentials a flocculation transition into a colloidal fluid occur accompanied by the appearance of a triple point, where the fluid, crystal and liquid (flocculated structures) phases are in equilibrium. Applying a higher order perturbation approach than that used by Victor & Hansen [13] and taking into account the possibility of the occurrence of a crystal phase leads to a shift of the prediction of the critical point to lower values of the Debye screening parameter. For small attractive forces the liquid phase disappears.

Appendix B

Scaled Helmholtz Free Energy

The centre-to centre distance of two colloidal particles can be scaled by the effective hard sphere diameter:

$$R = \frac{r}{\sigma} = \frac{r}{\sigma_0 S} = \frac{x}{S} \tag{B.1}$$

The total potential, scaled by the thermal energy $k_b T$, can be written as a function of the scaled distance R as:

$$U(R) = U_{HS}(R) + U_p(R) \tag{B.2}$$

where

$$\begin{aligned} U_{HS}(R) &= \infty && ; R < 1 \\ U_{HS}(R) &= 0 && ; R > 1 \end{aligned} \tag{B.3}$$

and the perturbation potential takes the form

$$\begin{aligned}
 U_p(R) &= 0 && ; R < 1 \\
 U_p(R) &= U(R_m) && ; 1 \leq R < R_m \\
 U_p(R) &= \frac{1}{T} \left(T_R \frac{\exp(-\kappa(R-1))}{R} - \frac{T_A}{12} \left(\frac{1}{R^2-1} + \frac{1}{R^2} + 2 \ln \left(1 + \frac{1}{R^2} \right) \right) \right) && ; R \geq R_m
 \end{aligned} \tag{B.4}$$

with $R_m = x_m/S$.

The second order perturbation Helmholtz free energy (41) can, with $r = R\sigma$, $dr = \sigma dR$ and the density $\rho = (6\Phi)/(\pi\sigma)$, be written as

$$\frac{F}{Nk_B T} = \frac{F_{HS}}{Nk_B T} + 12\Phi \int_1^\infty U_p(R) g_{HS}(R) R^2 dR - 6\Phi \left(\frac{\partial \rho}{\partial \rho} \right)_{HS} k_B T \int_1^\infty (U_p(R))^2 g_{HS}(R) R^2 dR \tag{B.5}$$

with

$$\left(\frac{\partial \rho}{\partial \rho} \right)_{HS} k_B T = \frac{1}{Z_{HS} + \Phi \frac{\partial Z_{HS}}{\partial \Phi}} \tag{B.6}$$

while Z_{HS} is the hard sphere function of state.

Literature

[1]

Verwey, E.J.W.; Overbeek, T.T.H. G. *Theory of the Stability of Lyophobic Colloids*; Elsevier: Amsterdam, 1948.

[2]

Lyklema, J. *Fundamentals of Interface and Colloid Science (vol.1)*; Academic Press Limited: London, 1993.

[3]

Hunter, R. J. *Foundations of Colloid Science (vol.1,2)*; Clarendon Press: Oxford, 1989.

[4]

Shih, W. Y.; Aksay, J.A.; Kikuchi, R. *J. Chem. Phys.* **1987**, *86*, 5127.

[5]

Monovoukas, Y.; Gast, A.P. *J. Colloid Interface Sci.* **1989**, *128*, 533.

[6]

Sirota, E.B.; Ou-Yang, H.D.; Sinha, S.K.; Chaikin, P.M.; Axe, J.D.; Fujii, Y. *Phys. Rev. Lett.* **1989**, *62*, 1524.

[7]

Castillo, C.A.; Rajagopalan, R.; Hirtzel, C.S. *Rev.Chem. Engineering* **1984**, *2*, 237.

[8]

Kesavamoorthy, R.; Tata, B.V.R.; Arora, A.K.; Sood, A.K. *Phys. Lett. A* **1989**, *138*, 208.

[9]

Van Meegen, M.; Snook, J. *Adv. Colloid Interface Sci.* **1984**, *21*, 119.

[10]

Baus, M.; Colot, J.L. *Mol. Phys.* **1985**, *55*, 653.

[11]

Laird, B.B.; McCoy, J.; Haymet, A.D.J. *J. Chem. Phys.* **1987**, *87*, 5449.

[12]

Saigi, P.; Rajagopalan, R. *Langmuir* **1991**, *7*, 1383.

[13]

Victor, J.M.; Hansen, J-P. *J. Chem. Soc. Faraday Trans. 2* **1985**, *81*, 43.

[14]

Gast, A.P.; Hall, C.K.; Russel, W.B. *J. Colloid Interface Sci.* **1983**, *96*, 251.

[16]

Weeks, J.D.; Chandler, D.; Anderson, H.C. *J. Chem. Phys.* **1971**, *54*, 5237.

[15]

Russel, W.B.; Saville, D.A.; Schowalter, W.R. *Colloidal dispersions*; Cambridge University: Cambridge, 1989, Equation 4.10.13.

[17]

Barker, J.A.; Henderson, D. *J. Chem. Phys.* **1967**, *47*, 2856.

[18]

Zwanzig, R.W. *J. Chem. Phys.* **1954**, *22*, 1420.

[19]

Bronstein, J.N.; Semedejajew, K.A. *Taschenbuch der Mathematik*; Grosche, G., Ziegler, V., Ziegler, D. Eds.; Verlag Nauka, BSB B.G. Teubner Verlagsgesellschaft: Leipzig, 1983.

[20]

Hachisu, S.; Kobayashi, Y.; Kose, A. *J. Colloid Interface Sci.* **1973**, *22*, 342.

[21]

Takano, K.; Hachisu, S. *J. Colloid Interface Sci.* **1978**, *66*, 124.

[22]

Takano, K.; Hachisu, S. *J. Colloid Interface Sci.* **1978**, *66*, 130.

[23]

Mederos, L.; Navascues, G. *J. Chem. Phys.* **1994**, *101*, 9841.

[24]

Tejero, C.F.; Daanoun A.; Lekkerkerker H.N.W.; Baus M. *Phys Rev. Lett.* **1994**, *73*, 752.

[25]

Tejero, C.F.; Daanoun, A.; Lekkerkerker, H.N.W.; Baus, M. *Phys. Rev. E* **1994**, *51*, 558.

4. The Rheology of Equilibrium Colloidal Suspensions Close to Structural Transitions

4.1 Introduction

Stabilized colloidal suspensions show a variety of phases, like e.g. a colloidal fluid (disordered, non-flocculated), a colloidal liquid (disordered, flocculated) and a colloidal crystal phase. The physical state of a suspension is governed by the competition between electrostatic, steric and van der Waals forces. These phases have different symmetry properties concerning the arrangement of the colloidal particles. The symmetry is determined by the set of symmetry operations (translations, rotations, reflections etc.), which leave the density distribution of the colloidal particles invariant. When studying a phase transition the phase with the higher number of allowed symmetry operations is denoted as the high symmetry phase and the other as the low symmetry phase. A disordered phase like the fluid or the liquid phase can be transformed into itself by an infinite number of transformations (we restrict ourselves here to time averaged distribution functions). Therefore in the case of an order-disorder transition the disordered phase is the high symmetry phase, while the crystal phase is the low symmetry phase. The degree of symmetry will be captured in the 'order parameter' to be defined below. Three different symmetry breaking transitions exist, at which the symmetry properties change according to the phase transition involved. According to the schematic equilibrium phase diagram (Figure 1) [1], we distinguish:

- I. the fluid-crystal transition
- II. the liquid-crystal transition
- III. the fcc-bcc transition.

In all cases the first phase is the high symmetry phase and the latter the low symmetry phase. While I. and II. are order-disorder transitions is III. an order-order

transition. It follows from the equilibrium phase diagram, that these transitions are of first order (Chapter 3). The difference in the solid volume fraction between the crystalline and the disordered states is however relatively small. The colloidal suspension is therefore treated here as incompressible, while we confine our treatment to the behaviour of transversal shear waves through the suspension.

A quantitative satisfactory statistical theory for the long time dynamics of such first order transitions has, to the knowledge of the present authors, not yet been developed. The description of the dynamics of first order transitions in colloidal suspensions by a Cahn-Hilliard like theory has been suggested by Dhont et.al. [2]; this treatment however is restricted to the very first stages of the phase separation from an initial fluid state into a liquid state.

A symmetry breaking (structural) transition can be described qualitatively by the Landau theory of phase transitions [3],[4]. The basic idea of the Landau theory is to consider the free energy of a system as a function of the structural alteration at the transition. The dimensionless order parameter describing a symmetry breaking transition in a colloidal suspension is chosen to be the amplitude of the density wave characterizing the colloidal lattice.

In this paper we focus our attention on a description of the rheological behaviour of a colloidal suspension near a structural transition. We will start with establishing a general model in analogy to the approach of Levanyuk [5] and we will analyze the frequency dependent transport parameters G' and G'' , while the system is supposed to be sufficiently close to equilibrium. By 'sufficiently close' we mean that the perturbations are small enough for the equilibrium structure to persist. In Chapter 5 the case of a symmetry breaking transition induced by an externally applied static perturbation will be considered.

The dynamic behaviour of a suspension of colloidal particles on a long time scale can be described by slow modes. A mode is defined here as a time dependent parameter characterizing the transport in the suspension, which is treated as a viscoelastic continuum, both in the ordered and in the disordered phases. Close to a transition the dynamics of the suspension are determined by two slow modes [6],[7],[8] given by the transport equations of the momentum and of the order parameter. It is

known that the order parameter mode influences all other slow modes close to a phase transition because its relaxation time goes to infinity (critical slowing down [9]). The coupling between the slow modes determines the properties of the transport parameters near the transition.

4.2 Theory

In order to include the coupling between the two slow modes we will construct a free energy density near a symmetry breaking transition. It consists of a reference free energy density, a contribution from the order parameter and two terms related to the strain:

- a contribution from the elastic energy
- a contribution from the coupling between the order parameter and the strain.

The Free Energy and the Equilibrium Values of the Order Parameter

We introduce an order parameter q that is associated with the amplitude of the density wave and with the wavelength of the colloidal lattice. The order parameter is zero in the high symmetry phase and becomes positive in the low symmetry phase. The free energy of the transition is given by the standard Ginzburg-Landau free energy, which can be written for a first order structural phase transition [4]:

$$F(q) = F_0 + \frac{\alpha}{2}q^2 - \frac{\zeta}{3}q^3 + \frac{\nu}{4}q^4 \quad (44)$$

where α and ν are free parameters. Here F is taken per unit volume. The values of ν and ζ are assumed positive. The Ginzburg criterion [3] states that this theory fails at the transition. Thus this model will

only be applicable close to but not too close to the transition.

The deformation w of a body is given by the spatial derivation of the displacement \underline{X} . For an arbitrary deformation the components of the deformation tensor \underline{w} can be calculated by:

$$w_{ik} = \frac{dX_i}{dx_k} \quad (45)$$

The strain tensor \underline{u} is of the form

$$\underline{u} = \frac{1}{2}(\underline{w} + \underline{w}^T) \quad (46)$$

The contribution of the strain to the free energy can generally be given by the product of the square of the tensor \underline{u} (\underline{u}, t) with the corresponding elastic modulus G_0 . We will confine our considerations here to simple shear, in which $u = 1/2(w_{xz} + w_{zx})$. The contribution to the free energy of a mechanically deformed system is thus $G_0/2 u^2$. Taking into account the elastic energy, the following expression for the free energy of a mechanically deformed system is obtained:

$$F(u, q) = F_0 + \frac{\alpha}{2} q^2 - \frac{\zeta}{3} q^3 + \frac{\nu}{4} q^4 + \frac{G_0}{2} u^2 \quad (47)$$

In this expression no coupling between q and u has been assumed as yet.

We cannot neglect however the coupling between the slow modes of the order parameter and the momentum close to the transition. We will write the contribution of this coupling to the free energy as an expansion of F up to the second order in the order parameter q and the strain u , with the free parameter γ . Terms of uneven order (e.g. linear terms) of the order parameter have no average contribution to the

transport equation of the momentum and are thus omitted. The first non-negligible term is of second order in q and linear in the strain. Taking only this lowest order into account we obtain

$$F(u, q) = F_0 + \frac{\alpha}{2} q^2 - \frac{\zeta}{3} q^3 + \frac{\nu}{4} q^4 + \frac{\gamma}{2} u q^2 + \frac{G_0}{2} u^2 \tag{48}$$

while γ is the coupling parameter. This simple generalization of the free energy couples the relaxation processes of the order parameter and of the elastic deformation field (mode coupling) and will lead to an elastic modulus and a dynamic shear viscosity corrected for the order parameter fluctuations.

Equation (48) describes qualitatively a first order phase transition, of which q is the corresponding order parameter. This can be illustrated by determining the equilibrium values q_0 of the order parameter by minimizing the Helmholtz free energy with respect to the order parameter q :

$$\left(\frac{\partial F}{\partial q} \right)_u = \alpha q - \zeta q^2 + \nu q^3 + \gamma u q = 0 \tag{49}$$

Focusing our attention to the case $u=0$, leads to:

$$q_{00} = 0$$

$$q_{01} = \frac{\zeta}{2\nu} + \sqrt{\left(\frac{\zeta}{2\nu} \right)^2 - \frac{\alpha}{\nu}} \tag{50}$$

$$q_{02} = \frac{\zeta}{2\nu} - \sqrt{\left(\frac{\zeta}{2\nu} \right)^2 - \frac{\alpha}{\nu}}$$

Whereas q_{01} always represents a maximum in F , the other minimum is either at q_{00} or q_{02} , depending on the value of α .

The solution $q = q_{00} = 0$ represents the high symmetry phase, whereas $q = q_{01} > 0$ is the low symmetry phase. The high symmetry phase is thermodynamically stable when $\alpha > \zeta^2/4\nu$. The low symmetry phase is stable when $\alpha < 0$; in that case $q = q_{01}$. The coexistence region is bounded by $\alpha = 0$ and $\alpha = \zeta^2/4\nu$ (Fig.6).

Our calculations on the rheology of colloidal suspensions are restricted to

systems not too close to the coexistence region. In that case the value of the terms containing ζ in Eq. (48) can be considered to be small as compared to the term containing ν . For $\zeta=0$ the first order transition simplifies to a second order transition.

With a second order transition we can exactly expand α up to the first order as a function of the free state variables volume fraction Φ of the dispersed solid particles, the salt concentration C and the temperature T around their 'transition' values [3],[4]:

$$\alpha(\Phi, C, T) = \alpha_{\Phi}(\Phi - \Phi_{tr})_{T,C} + \alpha_C(C - C_{tr})_{\Phi,T} + \alpha_T(T - T_{tr})_{\Phi,C} \quad (51)$$

The transition values are denoted by a subscript tr. In the case of a first order transition considered here the transitional values of Φ , C and T depend on the way the phase transition is approached. Starting at the low (high) symmetry phase the high (low) symmetry coexistence line defines the transition value. The coexistence values are known from the equilibrium phase diagram, as derived e.g. for electrically stabilized colloidal particles in Chapter 3.

The Helmholtz Free Energy Density

In order to take into account space and time dependent variations in the system we define a free energy density $f(q(\underline{r},t), u(\underline{r},t))$ by writing :

$$F(q, u, t) = \frac{1}{V} \int_V d^3r f(q(\underline{r},t), u(\underline{r},t)) \quad (52)$$

while the integration is taken over the entire space of the system V .

The free energy density can be written similar to (48) as:

$$\begin{aligned}
 f(q(\underline{r},t),u(\underline{r},t)) = & f_0 + \frac{\lambda}{2}(\nabla q(\underline{r},t))^2 + \frac{\alpha}{2}q^2(\underline{r},t) - \frac{\zeta}{3}q^3(\underline{r},t) + \frac{\nu}{4}q^4(\underline{r},t) \\
 & + \frac{\gamma}{2}u(\underline{r},t)q^2(\underline{r},t) + \frac{G_0}{2}u^2(\underline{r},t)
 \end{aligned}
 \tag{53}$$

where λ is a positive parameter. The term $\lambda/2 (\nabla q(\underline{r},t))^2$ accounts for the contribution of homogeneous space-dependent order parameter fluctuations to the free energy [3]. These fluctuations occur on length scales much larger than the colloidal distances.

We further assume that the time and space dependent order parameter $q(\underline{r},t)$ and the strain $u(\underline{r},t)$ are composed of a constant value and small time and space dependent deviations $\delta u(\underline{r},t)$ and $\delta q(\underline{r},t)$ around the equilibrium values u_0 and q_0 :

$$\begin{aligned}
 u(\underline{r},t) = & u_0 + \delta u(\underline{r},t) \\
 q(\underline{r},t) = & q_0 + \delta q(\underline{r},t)
 \end{aligned}
 \tag{54}$$

We confine our study here to the case $u_0=0$, i.e. the system will be disturbed by small strain deviations $\delta u(\underline{r},t)$ only. The case $u_0 \neq 0$ leads to a shear induced symmetry breaking transition, that will be discussed in Chapter 5.

Substituting (54) into (53) and taking into account only terms up to the second order in $\delta u(\underline{r},t)$ and $\delta q(\underline{r},t)$ we obtain:

$$\begin{aligned}
 f(\delta q, \delta u) = & f_0 + \frac{\alpha}{2}q_0^2 - \frac{\zeta}{3}q_0^3 + \frac{\nu}{4}q_0^4 \\
 & + (\alpha q_0 - \zeta q_0^2 + \nu q_0^3)\delta q + \left(\frac{\alpha}{2} - \zeta q_0 + \frac{3}{2}\nu q_0^2\right)\delta q^2 \\
 & + \frac{\gamma}{2}\delta u \delta q^2 + \frac{\gamma}{2}q_0^2 \delta u \\
 & + \frac{G_0}{2}\delta u^2 + \gamma q_0 \delta u \delta q + \frac{\lambda}{2}(\nabla \delta q)^2
 \end{aligned}
 \tag{55}$$

The terms of the order $\delta u(\underline{r},t)$ and $\delta q(\underline{r},t)$ disappear, because the system is in a minimum of the thermodynamic potential. The Helmholtz free energy density depends on the value of q_0 and α . For the high symmetry phase ($q_0=0$) we arrive at:

$$f(\delta q, \delta u) = f_0 + \frac{\lambda}{2} (\nabla q)^2 + \frac{1}{2} \alpha \delta q^2 + \frac{1}{2} G_0 \delta u^2 + \frac{1}{2} \gamma \delta q^2 \delta u \quad (56)$$

and for the low symmetry phase ($q_0 \neq 0$) we get:

$$f(\delta q, \delta u) = f'_0 + \frac{\lambda}{2} (\nabla q)^2 + \frac{1}{2} (-2\alpha + \zeta q_0) \delta q^2 + \frac{1}{2} G_0 \delta u^2 + 2\gamma q_0 \delta q \delta u + \frac{1}{2} \gamma \delta q^2 \delta u \quad (57)$$

with

$$f'_0 = f_0 + \frac{\alpha}{2} q_0^2 - \frac{\zeta}{3} q_0^3 + \frac{\nu}{4} q_0^4 \quad (58)$$

Having derived the free energy density for the high and the low symmetry phase we will now describe the influence of the fluctuations of the order parameter on the transport parameters. The two slow modes describing the dynamics of the system are given by a Langevin equation for the relaxation transport of the order parameter [7]

$$\frac{\partial \delta q}{\partial t} = -\frac{1}{\chi} \frac{\delta f(\delta q, \delta u)}{\delta q} + \frac{g(\underline{r}, t)}{\chi} \quad (59)$$

and by the momentum conservation law

$$\rho \frac{\partial^2 \delta X_x}{\partial t^2} = \frac{\partial}{\partial z} \left(\frac{\delta f(\delta q, \delta u)}{\delta u} + \eta_0 \delta \dot{u} \right) \quad (60)$$

while ρ is the density of the suspension and δX_x is a displacement deviation in x -direction. η_0 is the viscosity of the suspension far from the transition, which is different for the high and the low symmetry phase. The Langevin term $g(\underline{r}, t)$ is a fluctuating term ('white noise') obeying the fluctuation-dissipation theorem for the correlation function:

$$\langle g(\underline{r}, t) g(\underline{r}', t') \rangle = 2\chi k_B T \delta(t-t') \delta(\underline{r}-\underline{r}') \quad (61)$$

while χ is a damping parameter. In Equation (60) the influence of thermal fluctuations on the strain relaxation process has been neglected, because the order

parameter fluctuations predominantly determine the behaviour of the system close to a phase transition.

Generally speaking the transport coefficients G_0 and η_0 are frequency dependent both in the high and in the low symmetry phase. The transport coefficients depend on the interparticle interaction determined a.o. by the relaxation process of the electric double layer of the colloidal particles. Close to a phase transition however the low frequency critical fluctuations determine the transport processes (critical slowing down). Therefore close to the transition only the low frequency values $G(\Omega=0)$ and $\eta(\Omega=0)$ of the high and low symmetry phase are important, denoted as G_0 and η_0 . These values of the transport coefficients are valid under conditions far removed from the phase transition, and will be specified later for the high and the low symmetry phase. Close to a transition they are modified by the presence of fluctuations. To describe this phenomenon we will study the propagation of shear waves for a viscoelastic medium with strong fluctuations [11].

Transport Equations Near a Symmetry Breaking Transition

Substituting the free energy of the high (56) and the low (57) symmetry phase into equations (59) and (60) we get a set of coupled differential equations that depend on α . These equations of the order parameter mode and the momentum mode are given,

for the high symmetry phase $q_0=0$, by:

$$\chi \delta \dot{q} + \alpha \delta q + \gamma \delta q(\underline{r}, t) \delta u - \lambda \nabla^2 \delta q = g \quad (62)$$

$$\rho \delta \ddot{X}_x = \frac{\partial}{\partial z} (G_0 \delta u + \frac{1}{2} \gamma \delta q^2 + \eta \delta \dot{u}) \quad (63)$$

and for the low symmetry phase $q_0=q_{0z}$, by:

$$\chi \delta \dot{q} + (-2\alpha + \zeta q_0) \delta q + 2\gamma q_0 \delta u + \gamma \delta q \delta u - \lambda \nabla^2 \delta q = g \quad (64)$$

$$\rho \delta \ddot{X}_x = \frac{\partial}{\partial z} (G_0 \delta u + \frac{1}{2} \gamma \delta q^2 + 2\gamma q_0 \delta q + \eta \delta \dot{u}) \quad (65)$$

To find a solution for the order parameter equations (64) and (62) we expand δq in a series

$$\delta q(\underline{r}, t) = \delta q^0(\underline{r}, t) + \delta q^1(\delta u, \underline{r}, t) + \mathcal{O}(\delta u^2) \quad (66)$$

where δq^0 is the solution of the uncoupled set of the equations (62)-(65), that means that terms in $\delta q \delta u$ are omitted. In analogy to Levanyuk [5] we will only consider first order corrections. Note that by using a more sophisticated treatment of a similar problem Ma [7] obtained higher order correction terms to transport parameters.

The solution of δq^1 can be determined by means of a Green function $h_1(\underline{r}, t)$:

$$\delta q^1(\delta u, \underline{r}, t) = -\gamma \int h_1(t-t', \underline{r}-\underline{r}') \delta q^0(t', \underline{r}') \delta u(t', \underline{r}') dt' d^3r' \quad (67)$$

Now we derive a solution for the δq -perturbed momentum equation. Here we will consider only the high symmetry case $q_0=0$. The low symmetry case can be treated in a similar way (Appendix D).

To proceed, Equation (66) is substituted into (63). In order to find the correction of the transport coefficients G_0 and η_0 with respect to the perturbation in δq we take into account only terms up to the first order in δu . Because we are not interested in the entire solution of the latter equation but only in the fluctuation-corrected transport coefficients G and η we omit the u -independent inhomogeneity of the latter equation, and end up with:

$$\begin{aligned} \rho \delta \ddot{X}_x(\underline{r}, t) - \frac{\partial}{\partial z} (G_0 \delta u(\underline{r}, t) + \eta_0 \delta \dot{u}) \\ - \gamma^2 \delta q^0(\underline{r}, t) \int h_1(t-t', \underline{r}-\underline{r}') \delta q^0(t', \underline{r}') \delta u(t', \underline{r}') dt' d^3r' = 0 \end{aligned} \quad (68)$$

We consider a sinusoidal deformation wave in the system with frequency Ω and wave vector $\underline{K} = (0, 0, k_z)$:

$$\delta X_x = U e^{-j(\underline{K} \cdot \underline{r} + \Omega t)} \quad (69)$$

while $(\underline{K})^2 = \underline{K} \cdot \underline{K}$ is the scalar product of the vectors. By averaging over the fluctuations in δq and dividing by

$$U e^{-j(\underline{K} \cdot \underline{r} + \Omega t)} \quad (70)$$

we obtain a dispersion relation in $\underline{K}(\Omega)$

$$-\rho \Omega^2 + (\underline{K})^2 (G_0 + j \Omega \eta_0 - J(\underline{K}, \Omega)) = 0 \quad (71)$$

with

$$J(\underline{K}, \Omega) = \gamma^2 \int h_1(t-t', \underline{r}-\underline{r}') (\delta q^0(\underline{r}, t) \delta q^0(\underline{r}', \underline{r}')) e^{-j(\underline{K}(\underline{r}-\underline{r}') + \Omega(t-t'))} dt' d^3 r' \quad (72)$$

This integral takes into account the influence of the critical fluctuations on the propagation of shear waves through a suspension near a phase transition. The value of the integral is essentially determined by the correlation function of the order parameter, which increases on approaching the transition. The explicit calculation of the integral $J(\underline{K}, \Omega)$ for the high symmetry phase is performed in Appendix C. The calculation of this integral for the low symmetry phase is given in Appendix D in view of its lengthy character. It turns out that the dependence of $J(\underline{K}, \Omega)$ on \underline{K} can be neglected if $\text{abs}(\underline{K}^{-1}) \gg \xi$, where ξ is the correlation length of the order parameter fluctuations. This condition is valid if the system is not too close to the phase transition. Therefore we study here only systems outside the coexistence region. Under this condition Equation (72) can be solved both for the high and the low symmetry phase by writing:

$$J(\Omega, \underline{K} \rightarrow 0) = J(\Omega) = J_1(\Omega) + j J_2(\Omega) \quad (73)$$

From inspection of (71) and (73) it is evident that in the high symmetry phase the fluctuation corrected elastic storage modulus and loss modulus take the form:

$$G'_{Hl}(\Omega) = G_{H0} - J_{Hl}(\Omega) \quad (74)$$

$$G''_H(\Omega) = \Omega \eta_{H0} - J_{H2}(\Omega) \quad (75)$$

where G_{H0} and η_{H0} are the undisturbed values of the elastic modulus and the viscosity of the high symmetry phase. In Appendix C is been derived that the function J for the high symmetry phase can be written as (C.16),(C.17):

$$J_{H1}(\Omega) = \frac{2\sqrt{2}\pi^3\gamma^2k_B T\lambda}{\chi\Omega} \sqrt{\sqrt{\left(\frac{\alpha^2}{\lambda^2} + \frac{\chi^2\Omega^2}{4\lambda^2}\right)} - \frac{\alpha}{\lambda}} \quad (76)$$

$$J_{H2}(\Omega) = \frac{-4k_B T \pi^3\gamma^2\lambda^2}{\chi\Omega} \left(\sqrt{\frac{1}{2} \sqrt{\left(\frac{\alpha^2}{\lambda^2} + \frac{\chi^2\Omega^2}{4\lambda^2}\right)} + \frac{\alpha}{2\lambda}} - \sqrt{\frac{\alpha}{\lambda}} \right) \quad (77)$$

while their low symmetry equivalents (index L) Appendix D (D.35.) and (D.36.) take the form:

$$J_{L1}(\Omega) = (-2\alpha + \zeta q_0) 4\gamma^2 q_0^2 \frac{1}{\Omega^2 \chi^2 + (-2\alpha + \zeta q_0)^2} + \frac{2\sqrt{2}\pi^3\gamma^2k_B T\lambda}{\chi\Omega} \sqrt{\sqrt{\left(\frac{(-2\alpha + \zeta q_0)^2}{\lambda^2} + \frac{\chi^2\Omega^2}{4\lambda^2}\right)} + \frac{(-2\alpha + \zeta q_0)}{\lambda}} \quad (78)$$

and

$$J_{L2}(\Omega) = \chi\Omega 4\gamma^2 q_0^2 \frac{1}{\Omega^2 \chi^2 + (-2\alpha + \zeta q_0)^2} - \frac{4k_B T \pi^3\gamma^2\lambda^2}{\chi\Omega} \left(\sqrt{\frac{1}{2} \sqrt{\left(\frac{(-2\alpha + \zeta q_0)^2}{\lambda^2} + \frac{\chi^2\Omega^2}{4\lambda^2}\right)} + \frac{-2\alpha + \zeta q_0}{2\lambda}} - \sqrt{\frac{-2\alpha + \zeta q_0}{\lambda}} \right) \quad (79)$$

On approaching a symmetry breaking transition, $G_0(\alpha)$, $\eta_0(\alpha)$ and the correction term $J(\Omega, \alpha)$ are functions of the distance α to the transition (see Eq. (51)). In a not too wide range outside the coexistence region the reference values G_0 and η_0 can be viewed as independent of α . Under such conditions the behaviour of the transport coefficients is displayed in Fig. 13, where we have chosen the same G_0 and η_0 for the high and the low symmetry phase, which is not necessarily the case.

The theory is not valid at and very close to the transition. However, the trend in the curve of the storage modulus $G'(\alpha)$ at fixed frequency suggests a minimum at the transition ($\alpha=0$), whereas for the loss modulus $G''(\alpha)$ at a fixed frequency a maximum is expected at the transition due to the critical fluctuations. For the transport parameters, in the low symmetry phase α is replaced by $-2\alpha + \zeta q_0$ thus the parameters are asymmetric with regard to the transition point.

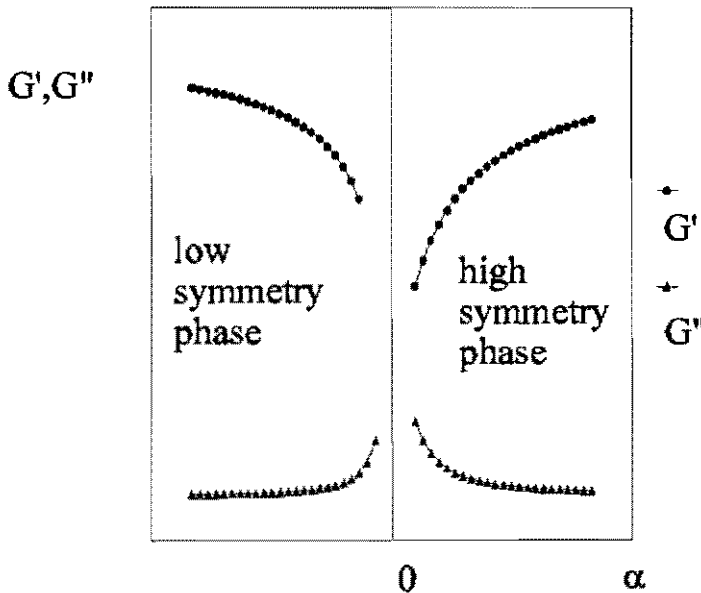


Figure 13 G' and G'' of a suspension as a function of the distance to the transition α occurring at $\alpha=0$, in arbitrary units.

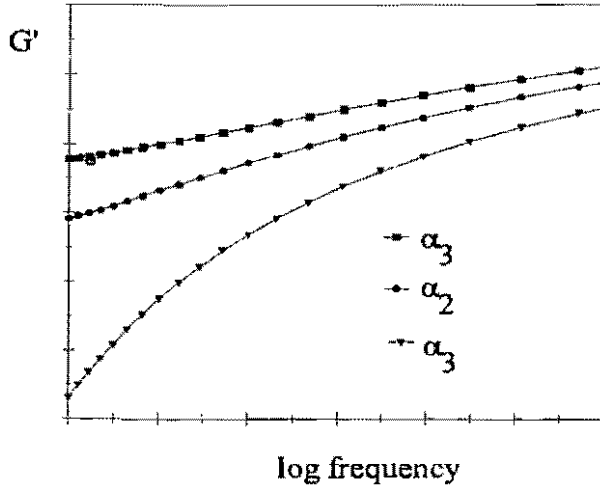


Figure 14 The storage modulus G' of a colloidal suspension having a non-zero elastic modulus, as a function of the frequency with $|\alpha_1| < |\alpha_2| < |\alpha_3|$.

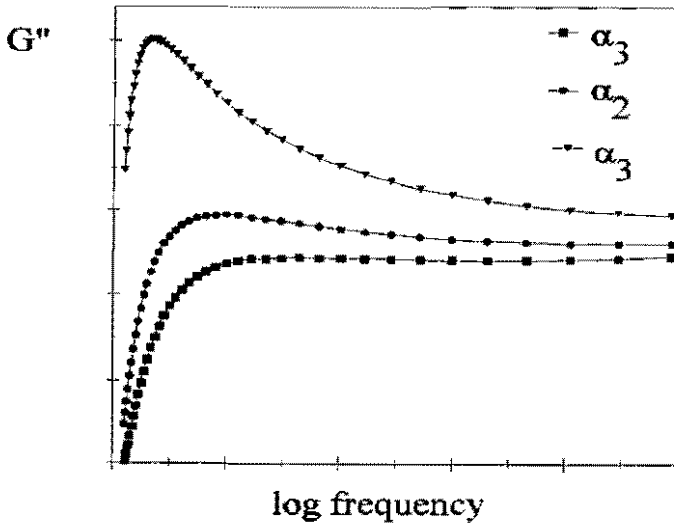


Figure 15 The loss modulus G'' of a colloidal suspension having a non-zero elastic modulus, as a function of the frequency with $|\alpha_1| < |\alpha_2| < |\alpha_3|$.

As an illustration Fig.14 and Fig.15 display how of G' and G'' vary with the applied frequency Ω , for different values of the parameter α . All curves of G' attain the value G_0 at high Ω and decrease with decreasing Ω . The slope of the $G'(\Omega)$ curve increases on approaching the phase transition (decreasing α). The height of the maximum of G'' at $\alpha=0$ depends on the relaxation time $\tau=\chi/\alpha$ of deviations of δq from its equilibrium value. The maximum in G'' rises and shifts to larger time scales (smaller frequencies) on approaching the transition, due to the phenomenon of the critical slowing down. At high frequencies the influence of the critical fluctuations can be ignored.

In the hydrodynamic limit, with $|\underline{K}| \rightarrow 0$ and $\Omega \rightarrow 0$ [12], equations (76), (77), (78) and (79) reduce to more simple expressions. These results in the hydrodynamic limit are applicable to quasi-statically applied shear deformations. In other words the hydrodynamic limit is comparable to the low shear rate limit $\dot{\gamma} \rightarrow 0$. For the high symmetry phase we get:

$$G(\Omega=0) = G_{H0} - \pi^3 \gamma^2 k_B T \sqrt{\frac{\lambda}{\alpha}} \tag{80}$$

$$\eta(\Omega=0) = \eta_{H0} + \frac{\pi^3 \gamma^2 k_B T \chi}{8} \left(\frac{\lambda}{\alpha}\right)^{\frac{3}{2}} \tag{81}$$

and for the low symmetry phase:

$$G(\Omega=0) = G_{L0} + \frac{4\gamma^2}{v} - \pi^3 \gamma^2 k_B T \sqrt{\frac{\lambda}{-2\alpha + \zeta q_0}} \quad (82)$$

$$\eta(\Omega=0) = \eta_{L0} - \frac{4\chi\gamma^2}{v} + \frac{\pi^3 \gamma^2 k_B T \chi}{8} \left(\frac{\lambda}{-2\alpha + \zeta q_0} \right)^{\frac{3}{2}} \quad (83)$$

Note that the model is not applicable close to the transition region. We therefore consider suspensions only far away from the coexistence region, i.e. that $|\alpha| > \zeta q_0$. In that case the ζ -correction in the Equations (82) and (83) can be neglected.

4.3 Discussion

We will compare the model presented here with experimental data taken from the literature. The parameter α (see Eq. (51)) can be considered as the distance to the transition in the phase diagram. We will confine our discussion to suspensions outside the coexistence region i.e. $|\zeta q_0| \ll \alpha$, because with the approximations made this model is not applicable too close to the transition. A symmetry breaking transition can occur by varying either of the three independent state variables; the temperature T , the volume fraction Φ , and the salt concentration C , which is related to the chemical potential. Each of the possibilities will be discussed separately below.

Phase Transition by Change in Volume Fraction

The parameter α can be written as a function of the volume fraction of the dispersed particles, when keeping the temperature and the salt concentration constant (51):

$$\alpha = \alpha_\Phi(\Phi_r - \Phi)_{T,C} \quad (84)$$

with $\alpha_\Phi > 0$ and Φ_r is the high symmetry coexistence volume fraction at the structural

transition.

I. The fluid-crystal transition

The high symmetry phase formed by the colloidal fluid is converted into the low symmetry phase of a colloidal fcc or bcc crystal on increasing the volume fraction. Φ_v is given by the equilibrium phase diagram of soft spheres. This transition (Kirkwood-Adler transition) was first observed in computer simulations of hard spheres. Note that the change from a colloidal crystal into a disordered structure (glass) with further increasing volume fractions at $\Phi \approx 0.6$ (Fig.1) is due to the freezing of density-fluctuations and can be viewed as a dynamic transition [1],[13] not manageable within the present model.

low shear rate viscosity

The expectation based on our theory is, that the shear viscosity in the hydrodynamic limit becomes infinite on approaching the fluid-crystal transition from the low symmetry phase (i.e. the crystal phase) and has the form

$$\eta \sim (\Phi - \Phi_c)^{-1.5} \quad (85)$$

This equation results from introducing (84) into (83). Note that η can not be measured by steady state techniques in the low symmetry phase because this phase is crystalline.

The viscosity decreases on going into the fluid phase. Although very close to the transition a similar dependence in the fluid phase can be expected as in the crystal phase, the model applied is not valid in the fluid phase far away from the transition, because the low frequency elastic modulus of the fluid phase is zero. G_0 in the fluid phase cannot be taken to be zero in this theory, because this would bring us into conflict with the starting point of the model. However by going away from the transition any non-zero value of the elastic modulus in the fluid phase allows the application of the presented model.

The increase of the low shear viscosity near the symmetry breaking transition on going from a colloidal fluid into a colloidal crystal was investigated by Allain et.al. [15] with Ludox particles in water. They were able to scale all acquired measurements for different salt concentrations on a master curve of the form

$$\eta = \eta_0 \left(1 - \frac{\Phi}{\Phi_c}\right)^{-K} \quad (86)$$

with $\Phi_c = 0.53 \pm 0.03$ and $K = 1.9 \pm 0.1$. Note however that the values of K and Φ_c are very sensitive to measuring errors which are easily made near Φ_c . The fact that the coexistence volume fraction Φ_c is close to the expected value of the hard sphere coexistence ($\Phi_c = 0.54$) confirms our approach of a structural transition. The agreement between (86) and (85) is reasonable because we would expect K to be $K = 1.5$ according to Equation (85). Buscall et.al. [14] investigated electrically stabilized polystyrene particles in water and obtained a similar value for K viz. 1.99.

Note the similarity between equation (85) and the Krieger-Dougherty-equation [16], which is claimed to be a fairly good description of the viscosity of a suspension

of a hard spheres:

$$\eta = \eta_0 \left(1 - \frac{\Phi}{\Phi_g} \right)^{-[\eta]\Phi_g} \quad (87)$$

with $\Phi_g = 0.64$ the maximum theoretical random packing fraction and the intrinsic viscosity $[\eta] = 2.5$, which gives an exponent 1.6. Although the phenomenon of an infinite increase of the viscosity is not a structural transition it incidentally gives an exponent that is close to the value derived for this model (85).

storage modulus of the crystal phase

In the low symmetry phase (crystal) far from the transition the elastic modulus is $G = G_{L0}$. On approaching the transition G' drops according to Eq. (82):

$$G'(\Omega \rightarrow 0) \sim G_{L0} - R(\Phi - \Phi_{rep})^{-0.5} \quad (88)$$

while R is an appropriate constant.

When considering a wide range of Φ the dependence of the elastic modulus $G_0(\Phi)$ on the volume fraction can no longer be neglected. From the interaction energy U between colloidal particles Buscall et.al. [17] determined the value of the low frequency elastic modulus

$$G_{L0} = \frac{I}{M} \frac{\partial^2 U}{\partial d^2} \quad (89)$$

where $d = 2a + h$ is the centre to centre distance between the particles and

$$I = \frac{3}{32} \Phi_m N_n \quad (90)$$

while N_n is the number of the next nearest neighbours and Φ_m the maximum volume fraction of the suspension. The values of I and M depend on the crystal structure and are $I = 0.833$, $M = 2a(0.74/\Phi)^{1/3}$ for an fcc-crystal and $I = 0.5$, $M = 2a(0.68/\Phi)^{1/3}$ for a bcc-crystal. While the pair interaction potential was taken independent of the volume fraction by Buscall et. al. [17], Russel and Benzing [18] improved this approach by

calculating a self consistent interaction potential. They found good agreement between experiments on colloidal crystals and Equation (89) over a wide range of Φ values. Only close to the crystal-fluid transition the experimental G' drops sharply [18],[14] in accordance with our model. The results of Lindsay & Chaikin [19] confirm the results reported by Buscall et. al.

loss modulus of the crystal phase

The theoretical expectation is that the low frequency loss modulus G'' decreases with increasing volume fractions according to (83) as:

$$G''(\Omega \rightarrow 0) \sim G''_{L0} + R(\Phi - \Phi_c)^{-1.5} \tag{91}$$

Dynamic shear measurements on electrically stabilized colloidal particles were performed by the group of Tadros and coworkers [22]-[25]. However not enough data close to the transition are available to compare their results with the present model.

frequency dependence

Experimental data on the frequency dependence of dispersions of soft polystyrene particles in water are shown e.g. in Figure 1 of [25]. G' increases with the frequency, while the loss modulus G'' slightly decreases, in qualitative accordance with our model for conditions not too close to the phase transition.

II. The liquid-crystal transition

Concentrated dispersions are expected to exhibit a transition from a colloidal crystal into an aggregated structure (colloidal liquid) due to attractive forces into the secondary minimum of the interaction potential. The symmetry properties change by decreasing the volume fraction at a coexistence value Φ_c . At this flocculation transition the expected dependence of G' and G'' on Φ is of the form shown in Figure 13. Here the high symmetry phase is a colloidal liquid structure while a colloidal

crystal is the low symmetry phase. No experimental investigations of this transition in soft spheres suspensions are available.

III. The bcc-fcc-transition

The expected variation of the transport properties of an order-order transition between two colloidal crystals is of the form displayed in Figure 13. No experimental data exists for the changes on passing the phase transition between the two forms of colloidal crystals.

Phase Transition by a Change of the Electrolyte Concentration

Another option to move around in the equilibrium phase diagram is by keeping the volume fraction and the temperature constant and varying the salt concentration in the suspension. In this case α can be written as

$$\alpha = \alpha_C(C - C_r)_{T,\phi} \quad (92)$$

with C_r the coexistence salt concentration from the high into the low symmetry phase and $\alpha_C > 0$.

I. The fluid-crystal transition

A colloidal crystal is formed by decreasing the salt concentration in a soft sphere suspension starting from the colloidal fluid phase. This is known as the Kirkwood-Adler transition for particles with an effective volume fraction equal to that of the hard sphere freezing volume fraction [27],[28].

low shear rate viscosity

The dependence of the low shear viscosity on the salt concentration in the crystal phase (low symmetry phase) near a structural transition according to our model has the form

$$\eta \sim (C - C_m)^{-1.5} \tag{93}$$

obtained by introducing (92) into (83). The low shear viscosity dependence in the crystal phase cannot be measured because of the presence of a yield stress. In the liquid phase (high symmetry phase) a number of authors investigated the low shear viscosity.

Lindsay & Chaikin [19] were able to measure the low shear viscosity of low volume fractions colloidal crystals. As can be seen e.g. from Figure 7 of ref. [19] the low shear viscosity becomes infinite on approaching the fluid-crystal transition due to a change in the salt concentration. This divergence was interpreted as the occurrence of a yield stress.

A similar result has been obtained earlier by Okano & Mitaku [26] and Mitaku et.al. [29]. The divergence in the viscosity could be fitted fairly well by using a modified Brinkman formula [30]

$$\eta = \eta_0 (1 - \Phi')^{-2.5} \tag{94}$$

while Φ' is called the "relative volume fraction"

$$\Phi' = \Phi \left(1 + \frac{\beta'}{\kappa a} \right) \tag{95}$$

κ_D is the Debye parameter and β' a constant of the order unity.

This result was improved by Mitaku et. al. [31] and by Ohtsuki [32]. Both authors explained the viscosity increase as the result of the disorder-order transition from a colloidal fluid into a colloidal crystal. Although our model is strictly speaking not valid in the low symmetry phase, we were able to fit the results of Ohtsuki [32] with equation (93) quite satisfactorily, as can be seen in Figure 16. This supports the use of the statistical theory presented here in the case of the fluid-crystal transition.

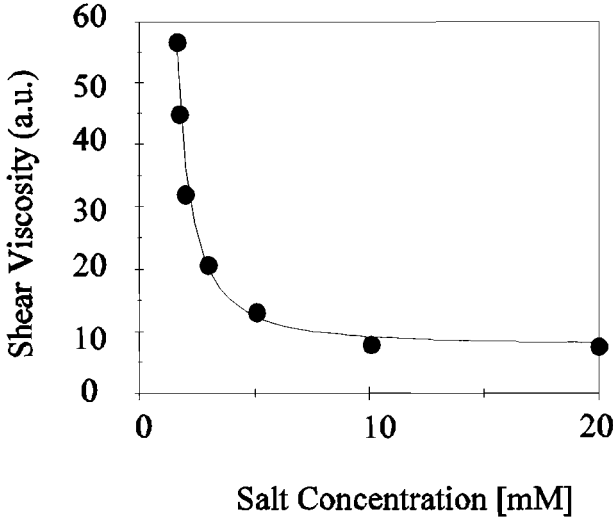


Figure 16 Experimental viscosity data obtained by Ohtsuki [32] for a latex suspension. The fit of Equation (93) to this data is quite satisfactory.

storage modulus of the crystal phase

The elastic modulus of the crystal phase is theoretically expected (82) to be of the form:

$$G'(\Omega \rightarrow 0) \sim G_{L0} - R(C - C_r)^{-0.5} \tag{96}$$

with an appropriate constant R.

The experimental evidence is that a change in salt concentration has a pronounced influence on the elastic modulus. Such a transition has been investigated by a number of authors e.g. Buscall et.al. [14], Lindsay & Chaikin [19] and Mitaku et. al. [29]. The elastic modulus $G_{L0}(C)$ far from the transition can be obtained from equation (89); together with the self consistent field model of the interaction potential by Russel & Benzing [18]. The latter theory agrees well with experiments of Russel & Benzing [20], except for conditions close to the fluid-crystal transition. Our fluctuation-corrected elastic modulus (96) will only lead to appreciable deviations

from the dynamic behaviour as predicted by these authors under conditions that are very close to the transition. However the number of data reported by Russel & Benzing near the transition does not allow a reliable fit of equation (96) to their data.

loss modulus of the crystal phase

The loss modulus of the crystal phase at low frequencies is expected to increase at the coexistence salt concentration according to (82)

$$G''(\Omega \rightarrow 0) \sim G''_0 + R(C_r - C)^{-1.5} \tag{97}$$

The only available dynamic measurements are those by Mitaku et. al. [29]. These were carried out in the high frequency limit (40 kHz) and are not comparable with the calculated low frequency transport properties of the present model.

II. The liquid-crystal transition

Another symmetry breaking transition occurs for concentrated dispersions, when the salt concentration is increased and the structure changes into an aggregated glass structure (flocculated structure) as a result of the van der Waals attraction. The model predicts a variation of the transport coefficients G' and G'' as indicated in Figure 13 with a minimum of the storage modulus and a maximum of the loss modulus at the coexistence salt concentration C_v of the liquid-crystal transition.

Unfortunately no experimental investigations are available for electrostatically stabilized spheres. However, our model is also applicable to nearly hard spheres, e.g. colloidal particles that are stabilized sterically with long 'hairs' (long polymers), provided they form single crystals.

Sterically stabilized polystyrene particles were investigated by Tadros et. al. [23]. In Figure 5 of ref. [23] his results are presented of dynamic shear measurements as a function of the salt concentration. With increasing salt concentrations at relatively low values the colloidal crystal structure is converted into an aggregated structure

(colloidal liquid). At the critical flocculation concentration (CFC) a minimum of G' can be found in accordance with our model. G'' is expected to have a maximum, but a minimum has been observed. However the phase angle shows a maximum at the coexistence salt concentration C_r . The phase transition may be shifted by a deformation. This implies that during an oscillation the viscoelastic properties may change if the amplitude is not small enough (Chapter 5). In other words, the linear viscoelastic region is reduced considerably near a phase transition. Tadros et. al. did not specify the applied amplitude. The amplitude used by these authors near the transition may not have been small enough to be in the linear viscoelastic region. This may have disturbed the trend in G'' .

III. The bcc-fcc transition

No experimental rheological data concerning the bcc-fcc transition by varying the salt concentration are known.

Phase Transition by a Change in the Temperature

Symmetry breaking transitions are expected to occur as a result of a variation of the temperature with

$$\alpha = \alpha_T(T - T_r)_{\phi, C} \tag{98}$$

We confine our discussion to the fact that the predicted rheological behaviour close to a symmetry breaking transition resembles the dependencies of the volume fraction and salt concentration discussed above.

Unfortunately very little is known about the melting of colloidal crystals by heating. Schaefer & Ackerson [33] reported a melting transition in crystalline suspensions of polystyrene particles and Williams et. al. [34] investigated the melting transition as a function of the salt concentration and established an equation for $T_{ref}(C)$. Tadros [23] investigated the dynamic rheological properties of sterically stabilized polystyrene particles. The results indicate that for the chosen salt

concentration irreversible alternations appear. The experimental results are not sufficiently specific to compare them with the theoretical model.

4.4 Conclusion

The model presented here is based on an extension of the Landau theory of phase transitions and takes into account the effects of the critical fluctuations on the rheological properties of colloidal suspensions near symmetry breaking transitions. The storage modulus is expected to have a minimum and the loss modulus a maximum at the transition. The model is applicable if the system is not too close to structural transitions in colloidal suspensions induced by varying the state variables, such as the temperature, salt concentration or the volume fraction of the solid particles. Its predictions agree qualitatively with the available experimental data near fluid-crystal and liquid-crystal transitions.

Appendix C

The Integral $J(\underline{K}, \Omega)$

Here we will perform in this appendix the integral $J(\underline{K}, \Omega)$ (72) for $q_0 = 0$:

$$J(\underline{K}, \Omega) = \gamma^2 \int h_1(t-t', \underline{r}-\underline{r}') \langle q^0(\underline{r}, t), q^0(\underline{r}', t') \rangle e^{-j(\underline{K}(\underline{r}'-\underline{r}) + \Omega(t'-t))} d^3r' dt' \tag{C.1}$$

This integral can be transformed with

$$t-t' = \tau \quad \underline{r}-\underline{r}' = \underline{R} \tag{C.2}$$

into

$$J(\underline{K}, \Omega) = \gamma^2 \int h_1(\tau, \underline{R}) \langle q^0(\underline{r}, t), q^0(\underline{r}-\underline{R}, t-\tau) \rangle e^{j(\underline{K} \cdot \underline{R} + \Omega \tau)} d\tau d^3R \tag{C.3}$$

This is a Fourier transform over \underline{R} and τ of the product of the Green function and the correlation function. A product in real space becomes a convolution integral in Fourier space. Therefore we need the Fourier transform of the Green function and the correlation function.

Fourier transform of the correlation function

The Fourier transform of the order parameter equation to order q^0 is:

$$-j\omega \chi q^0(\underline{k}, \omega) + \alpha q^0(\underline{k}, \omega) + \lambda(\underline{k})^2 q^0(\underline{k}, \omega) = g(\underline{k}, \omega) \tag{C.4}$$

and thus

$$q^0(\underline{k}, \omega) = \frac{g(\underline{k}, \omega)}{-j\omega \chi + \alpha + \lambda \underline{k}^2} \tag{C.5}$$

With the fluctuation- dissipation theorem in the Fourier space :

$$\langle g(\underline{k}, \Omega) g(\underline{k}', \Omega') \rangle = 2\chi k_B T \delta(\underline{k} + \underline{k}') \delta(\Omega + \Omega') \tag{C.6}$$

the correlation function in q^0 is:

$$\langle q^0(\underline{k}, \omega), q^0(\underline{k}', \omega') \rangle = \frac{\langle g(\underline{k}, \omega), g(\underline{k}', \omega') \rangle}{(\alpha + \lambda(\underline{k})^2 + j\omega\chi)(\alpha + \lambda(\underline{k})^2 - j\omega\chi)} = \frac{2\chi k_B T \delta(\underline{k} + \underline{k}') \delta(\omega + \omega')}{(\alpha + \lambda(\underline{k})^2)^2 + \omega^2 \chi^2} \quad (C.7)$$

Fourier Transform of the Green Function

The Green function $h_1(\underline{r}, t)$ is defined by

$$\chi \frac{\partial h_1(\underline{r}, t)}{\partial t} + \alpha h_1(\underline{r}, t) - \lambda \nabla^2 h_1(\underline{r}, t) = \delta(\underline{r}, t) \quad (C.8)$$

Performing a Fourier transform we obtain

$$h_1(\underline{k}, \omega) = \frac{1}{\lambda(\underline{k})^2 + \alpha - j\omega\chi} \quad (C.9)$$

Convolution integral

With this results equation (C.1) can be written as:

$$J(\underline{K}, \Omega) = \gamma^2 \int \frac{\chi k_B T d\Omega' d^3 K'}{((\lambda(\underline{K}')^2 + \alpha)^2 + \Omega'^2 \chi^2)(\lambda(\underline{K}' - \underline{K})^2 + \alpha - j(\Omega' - \Omega)\chi)} \quad (C.10)$$

Under the condition that we confine our treatment to long wavelength deformations we can approximate $\underline{K} = 0$.

$$J(0, \Omega) = J(\Omega) = \gamma^2 \chi k_B T \int \frac{d\Omega' d^3 K'}{((\lambda(\underline{K}')^2 + \alpha)^2 + \Omega'^2 \chi^2)(\lambda(\underline{K}')^2 + \alpha - j(\Omega' - \Omega)\chi)} \quad (C.11)$$

Performing the integration over Ω' using Jordans Lemma by calculating the residues

of the upper half of the complex plane we obtain:

$$J(\Omega) = 2\pi^2 \gamma^2 k_B T \int_0^\infty dK' \frac{(\underline{K}')^2}{(2(\alpha + \lambda(\underline{K}')^2) + j\Omega\chi)(\alpha + \lambda(\underline{K}')^2)} \quad (\text{C.12})$$

Separating the integral in real and imaginary part we find

$$J(\Omega) = J_1(\Omega) + jJ_2(\Omega) \quad (\text{C.13})$$

with

$$J_1(\Omega) = \pi^2 \gamma^2 k_B T \int_{-\infty}^\infty \frac{2(\underline{K}')^2 dK'}{4(\alpha + \lambda(\underline{K}')^2)^2 + \Omega^2 \chi^2} \quad (\text{C.14})$$

$$J_2(\Omega) = -\pi^2 \gamma^2 k_B T \chi \Omega \int_{-\infty}^\infty \frac{\underline{K}'^2 dK'}{(4(\alpha + \lambda(\underline{K}')^2)^2 + \Omega^2 \chi^2)(\alpha + \lambda(\underline{K}')^2)} \quad (\text{C.15})$$

Performing the integration over K' we obtain for the real part:

$$J_1(\Omega) = \frac{2\sqrt{2}\pi^3 \gamma^2 k_B T \lambda}{\chi \Omega} \sqrt{\sqrt{\left(\frac{\alpha^2}{\lambda^2} + \frac{\chi^2 \Omega^2}{4\lambda^2}\right)} - \frac{\alpha}{\lambda}} \quad (\text{C.16})$$

and for the imaginary part:

$$J_2(\Omega) = \frac{-4k_B T \pi^3 \gamma^2 \lambda^2}{\chi \Omega} \left(\sqrt{\frac{1}{2} \sqrt{\left(\frac{\alpha^2}{\lambda^2} + \frac{\chi^2 \Omega^2}{4\lambda^2}\right)} + \frac{\alpha}{2\lambda}} - \sqrt{\frac{\alpha}{\lambda}} \right) \quad (\text{C.17})$$

Appendix D

Low Symmetry Phase

Here we study the perturbation approach for the low symmetry phase $q_0 = q_{01}$. The set of modecoupling equations (64) and (65) are:

$$\chi \delta \dot{q}(\underline{r}, t) + (-2\alpha + \zeta q_0) \delta q(\underline{r}, t) + 2\gamma q_0 \delta u(\underline{r}, t) + \gamma \delta q(\underline{r}, t) \delta u(\underline{r}, t) - \lambda \nabla^2 \delta q(\underline{r}, t) = g(\underline{r}, t) \quad (\text{D.1.})$$

$$\rho \delta \ddot{\bar{X}}_x(\underline{r}, t) = \frac{\partial}{\partial z} (G_0 \delta u(\underline{r}, t) + \frac{1}{2} \gamma \delta q(\underline{r}, t)^2 + 2\gamma q_0 \delta q(\underline{r}, t) + \eta \delta \dot{u}(\underline{r}, t)) \quad (\text{D.2.})$$

Again we find the solution of the orderparameter equation by a series expansion in $\delta q(\underline{r}, t)$.

$$\delta q(\underline{r}, t) = \delta q^0(\underline{r}, t) + \delta q^1(\underline{r}, t) + \dots \quad (\text{D.3.})$$

with δq^0 - the uncoupled equation in δq and δq^1 taking into account the first contribution in δu (modecoupling) as disturbance of δq^0 . Thus $\delta q(\underline{r}, t)$ can be written as:

$$\delta q(\underline{r}, t) = \delta q^0(\underline{r}, t) - \gamma \int (2q_0 + \delta q^0) h_2(\underline{r} - \underline{r}', t - t') \delta u(\underline{r}', t') d^3 r' dt' \quad (\text{D.4.})$$

Substituting δq in (D.2.) while taking into account first order terms in δu and δq^0 we obtain

$$0 = \rho \delta \bar{X}_x + \frac{\partial}{\partial z} (-G_0 \delta u - \eta_0 \delta \dot{u} + \gamma^2 \delta q^0(\underline{r}, t)) \int (2q_0 + \delta q^0(\underline{r}', t')) h_2(\underline{r} - \underline{r}', t - t') \delta u(\underline{r}', t') d^3 r' dt' + 2\gamma^2 q_0 \int (2q_0 + \delta q^0(\underline{r}', t')) h_2(\underline{r} - \underline{r}', t - t') \delta u(\underline{r}', t') d^3 r' dt' \quad (D.5)$$

We rearrange the equation in orders of $\delta q^0(\underline{r}, t)$:

$$0 = \rho \delta \bar{X}_x + \frac{\partial}{\partial z} (-G_0 \delta u - \eta_0 \delta \dot{u} + 4\gamma^2 q_0^2 \int h_2(\underline{r} - \underline{r}', t - t') \delta u(\underline{r}', t') d^3 r' dt' + 2\gamma^2 q_0 \int (\delta q^0(\underline{r}', t') + \delta q^0(\underline{r}, t)) h_2(\underline{r} - \underline{r}', t - t') \delta u(\underline{r}', t') d^3 r' dt') + \gamma^2 \int \delta q^0(\underline{r}, t) \delta q^0(\underline{r}', t') h_2(\underline{r} - \underline{r}', t - t') \delta u(\underline{r}', t') d^3 r' dt' \quad (D.6)$$

Equation (D.6.) is an Operator equation to 0. 1. and 2. order in $\delta q^0(\underline{r}, t)$ and can be written as:

$$L \delta u = 0 \quad (D.7)$$

with

$$L = L_0 + L_1 + L_2 \quad (D.8)$$

and thus

$$L_0 \delta u = \rho \delta \bar{X}_x + \frac{\partial}{\partial z} (-G_0 \delta u - \eta_0 \delta \dot{u} + 4\gamma^2 q_0^2 \int h_2(\underline{r} - \underline{r}', t - t') \delta u(\underline{r}', t') d^3 r' dt') \quad (D.9)$$

$$L_1 \delta u = \frac{\partial}{\partial z} (2\gamma^2 q_0 \int (\delta q^0(\underline{r}', t') + \delta q^0(\underline{r}, t)) h_2(\underline{r} - \underline{r}', t - t') \delta u(\underline{r}', t') d^3 r' dt') \quad (D.10)$$

$$L_2 \delta u = \frac{\partial}{\partial x} (\gamma^2 \int \delta q^0(x,t) \delta q^0(x',t') h_2(x-x', t-t') \delta u(x',t') d^3 r' dt') \quad (\text{D.11.})$$

First we study the general operator equation

$$(L_0 + \epsilon L_1 + \epsilon^2 L_2) u = g \quad (\text{D.12.})$$

with ϵ small.

We try to find an equation of the average strainfield $\langle u \rangle$ were the 0. order operator determine the meanfield u_0 by:

$$u_0 = L_0^{-1} g \quad (\text{D.13.})$$

We obtain

$$\begin{aligned} L_0 u &= g - \epsilon L_1 u - \epsilon^2 L_2 u \\ u &= L_0^{-1} g - \epsilon L_0^{-1} L_1 u - \epsilon^2 L_0^{-1} L_2 u \\ u &= u_0 - L_0^{-1} (\epsilon L_1 - \epsilon^2 L_2) u \end{aligned} \quad (\text{D.14.})$$

and can find the solution of the selfconsistent equation by means of successive approximations.

The first approximation is $u \approx u_0$, thus

$$\begin{aligned} u &= u_0 - L_0^{-1} (\epsilon L_1 - \epsilon^2 L_2) u_0 \\ u &= u_0 - \epsilon L_0^{-1} L_1 u_0 - \epsilon^2 L_0^{-1} L_2 u_0 \end{aligned} \quad (\text{D.15.})$$

and substitution in u

$$\begin{aligned} u &= u_0 - L_0^{-1} (\epsilon L_1 - \epsilon^2 L_2) (u_0 - L_0^{-1} (\epsilon L_1 - \epsilon^2 L_2) u_0) \\ u &= u_0 - \epsilon L_0^{-1} L_1 u_0 - \epsilon^2 L_0^{-1} L_2 u_0 + L_0^{-1} (\epsilon L_1 - \epsilon^2 L_2) L_0^{-1} (\epsilon L_1 - \epsilon^2 L_2) u_0 \end{aligned} \quad (\text{D.16.})$$

Rearranging in orders of ϵ we obtain

$$\begin{aligned}
 u &= u_0 - \epsilon L_0^{-1} L_1 u_0 - \epsilon^2 L_0^{-1} L_2 u_0 + \epsilon^2 L_0^{-1} L_1 L_0^{-1} L_1 u_0 + \dots \\
 u &= u_0 - \epsilon L_0^{-1} L_1 u_0 + \epsilon^2 (L_0^{-1} L_1 L_0^{-1} L_1 - L_0^{-1} L_2) u_0 \\
 u &= u_0 - \epsilon L_0^{-1} L_1 u_0 + \epsilon^2 L_0^{-1} (L_1 L_0^{-1} L_1 - L_2) u_0
 \end{aligned}
 \tag{D.17.}$$

By averaging both sides of the equation

$$\langle u \rangle = u_0 - \epsilon L_0^{-1} \langle L_1 \rangle u_0 + \epsilon^2 L_0^{-1} (\langle L_1 L_0^{-1} L_1 \rangle - \langle L_2 \rangle) u_0
 \tag{D.18.}$$

and express u_0 in terms of $\langle u \rangle$ by

$$u_0 = \langle u \rangle + \epsilon L_0^{-1} \langle L_1 \rangle u_0
 \tag{D.19.}$$

We can substitute this result in the latter equation for $\langle u \rangle$:

$$\begin{aligned}
 \langle u \rangle &= u_0 - \epsilon L_0^{-1} \langle L_1 \rangle (\langle u \rangle + \epsilon L_0^{-1} \langle L_1 \rangle u_0) + \epsilon^2 L_0^{-1} (\langle L_1 L_0^{-1} L_1 \rangle - \langle L_2 \rangle) (\langle u \rangle + \epsilon L_0^{-1} \langle L_1 \rangle u_0) \\
 \langle u \rangle &= u_0 - \epsilon L_0^{-1} \langle L_1 \rangle \langle u \rangle + \epsilon^2 L_0^{-1} \langle L_1 \rangle L_0^{-1} \langle L_1 \rangle \langle u \rangle + \epsilon^2 L_0^{-1} \langle L_1 L_0^{-1} L_1 \rangle \langle u \rangle - \epsilon^2 L_0^{-1} \langle L_2 \rangle \langle u \rangle \\
 \langle u \rangle &= u_0 - \epsilon L_0^{-1} \langle L_1 \rangle \langle u \rangle + \epsilon^2 L_0^{-1} (\langle L_1 L_0^{-1} L_1 \rangle - \langle L_1 \rangle L_0^{-1} \langle L_1 \rangle - \langle L_2 \rangle) \langle u \rangle
 \end{aligned}
 \tag{D.20.}$$

By applying L_0 on $\langle u \rangle$ we obtain:

$$\begin{aligned}
 L_0 \langle u \rangle &= g - \epsilon \langle L_1 \rangle \langle u \rangle + \epsilon^2 (\langle L_1 L_0^{-1} L_1 \rangle - \langle L_1 \rangle L_0^{-1} \langle L_1 \rangle - \langle L_2 \rangle) \langle u \rangle \\
 g &= (L_0 + \epsilon \langle L_1 \rangle + \epsilon^2 (\langle L_1 L_0^{-1} L_1 \rangle + \langle L_1 \rangle L_0^{-1} \langle L_1 \rangle + \langle L_2 \rangle)) \langle u \rangle
 \end{aligned}
 \tag{D.21.}$$

It is known that in most cases we can set $\langle L_1 \rangle = 0$ and thus

$$g=(L_0+\epsilon^2(-L_1L_0^{-1}L_1)+(L_2))(u) \quad (D.22.)$$

Back to our initial conditions $g=0$, $\epsilon=1$ and $u=\delta u$ we arrive at

$$0=(L_0+\epsilon^2(-L_1L_0^{-1}L_1)+(L_2))(\delta u) \quad (D.23.)$$

where L_0^{-1} is the inverse operator of L_0 , which can be written by means of a Greenfunction $H(r,t)$ as:

$$L_0^{-1}\delta u=\int H(\underline{r}-\underline{r}',t-t')\delta u(\underline{r}',t')d^3r'dt' \quad (D.24.)$$

Now we can write the explicite equation of the average strainfield using the incompressibility condition:

$$\begin{aligned} 0 &= \rho(\delta \bar{\chi}_2) + \frac{\partial}{\partial z}(-G_0\langle \delta u \rangle - \eta_0\langle \delta \dot{u} \rangle) \\ &+ 4\gamma^2 q_0^2 \int h_2(\underline{r}-\underline{r}',t-t')\langle \delta u(\underline{r}',t') \rangle d^3r'dt' + \gamma^2 \int \delta q^0(\underline{r},t)\delta q^0(\underline{r}',t')h_2(\underline{r}-\underline{r}',t-t')\langle \delta u(\underline{r}',t') \rangle d^3r'dt' \\ &- 4q_0^2 \gamma^4 \int h_2(\underline{r}-\underline{r}',t-t')H(\underline{r}'-\underline{r}'',t'-t'')\nabla_{\underline{r}'}h_2(\underline{r}''-\underline{r}''',t''-t''') \\ &(\delta q^0(\underline{r},t) + \delta q^0(\underline{r}',t'))(\delta q^0(\underline{r}'',t'') + \delta q^0(\underline{r}''',t'''))\langle \delta u(\underline{r}''',t''') \rangle dt'dt''dt''dr'dr''dr''') \end{aligned} \quad (D.25.)$$

Neglecting the last integral because it is small (at least if γ is small) and taking the average over $\delta q(\underline{r},t)$:

$$\begin{aligned} 0 &= \rho(\delta \bar{\chi}_2) - \frac{\partial}{\partial z}(G_0\langle \delta u \rangle + \eta_0\langle \delta \dot{u} \rangle - 4\gamma^2 q_0^2 \int h_2(\underline{r}-\underline{r}',t-t')\langle \delta u(\underline{r}',t') \rangle d^3r'dt') \\ &- \gamma^2 \int \delta q^0(\underline{r},t)\delta q^0(\underline{r}',t')h_2(\underline{r}-\underline{r}',t-t')\langle \delta u(\underline{r}',t') \rangle d^3r'dt') \end{aligned} \quad (D.26.)$$

Considering a monochromatic strain wave we obtain a similar dispersion relation to (71)

$$-\rho\Omega^2 + \frac{1}{2}K^2(G_0 + j\Omega\eta_0 - J(\underline{K}, \Omega)) = 0 \quad (\text{D.27.})$$

with

$$J(\underline{K}, \Omega) = 4\gamma^2 q_0^2 \int h_2(\underline{r}-\underline{r}', t-t') e^{j(\underline{K}(\underline{r}-\underline{r}') + \Omega(t-t'))} d^3r' dt' \quad (\text{D.28.})$$

$$+ \gamma^2 \int h_2(\underline{r}-\underline{r}', t-t') (\delta q^0(\underline{r}, t) \delta q^0(\underline{r}', t')) e^{j(\underline{K}(\underline{r}-\underline{r}') + \Omega(t-t'))} d^3r' dt'$$

The solution of the second integral is known from appendix F (C.16) ,(C.17) except that the Green function $h_1(\underline{r}, t)$ has to be substituted by $h_2(\underline{r}, t)$ and the first integral is the Fouriertransform of $h_2(\underline{r}, t)$.

Fouriertransform of the Green function $h_2(\underline{r}, t)$

The Greenfunction $h_2(\underline{r}, t)$ is defined by

$$\chi \frac{\partial h_2(\underline{r}, t)}{\partial t} + (-2\alpha + \zeta q_0) h_2(\underline{r}, t) + \lambda \nabla^2 h_2(\underline{r}, t) = \delta(\underline{r}, t) \quad (\text{D.29.})$$

and in the Fourier space

$$-j\Omega\chi h_2(\underline{K}, \Omega) + (-2\alpha + \zeta q_0) h_2(\underline{K}, \Omega) + \lambda K^2 h_2(\underline{K}, \Omega) = 1 \quad (\text{D.30.})$$

Thus we find for $h_2(\underline{K}, \Omega)$:

$$h_2(\underline{K}, \Omega) = \frac{1}{-j\Omega\chi + (-2\alpha + \zeta q_0) + \lambda K^2} \quad (\text{D.31.})$$

The result of the first integral is:

$$I(\underline{K}, \Omega) = 4\gamma^2 q_0^2 \frac{1}{-j\Omega\chi + (-2\alpha + \zeta q_0) + \lambda K^2} \quad (\text{D.32.})$$

Separating the integral in a real and a imaginary part for $\underline{K}=0$ we obtain

$$I_1(0, \Omega) = (-2\alpha)4\gamma^2 q_0^2 \frac{1}{\Omega^2 \chi^2 + (-2\alpha + \zeta q_0)^2} \quad (\text{D.33.})$$

$$I_2(0, \Omega) = \chi \Omega 4\gamma^2 q_0^2 \frac{1}{\Omega^2 \chi^2 + (-2\alpha + \zeta q_0)^2} \quad (\text{D.34.})$$

Results:

Using the fact that in the second integral of (D.28.) is the same as in Appendix C, we finally obtain for the low symmetry phase:

the real part:

$$J_{L1}(\Omega) = (-2\alpha + \zeta q_0)4\gamma^2 q_0^2 \frac{1}{\Omega^2 \chi^2 + (-2\alpha + \zeta q_0)^2} + \frac{2\sqrt{2}\gamma^2 k_B T \pi^3 \lambda}{\chi \Omega} \sqrt{\sqrt{\frac{(-2\alpha + \zeta q_0)^2}{\lambda^2} + \frac{\chi^2 \Omega^2}{4\lambda^2} + \frac{(-2\alpha + \zeta q_0)}{\lambda}}}$$

(D.35.)

the imaginary part

$$J_{L2}(\Omega) = \chi \Omega 4\gamma^2 q_0^2 \frac{1}{\Omega^2 \chi^2 + (-2\alpha + \zeta q_0)^2} - \frac{4k_B T \pi^3 \gamma^2 \lambda^2}{\chi \Omega} \left(\sqrt{\frac{1}{2} \left(\sqrt{\frac{(-2\alpha + \zeta q_0)^2}{\lambda^2} + \frac{\chi^2 \Omega^2}{4\lambda^2} + \frac{(-2\alpha + \zeta q_0)}{\lambda}} \right)} - \sqrt{\frac{(-2\alpha + \zeta q_0)}{\lambda}} \right)$$

(D.36.)

Literature

- [1]
P.N. Pusey, in *Liquids, Freezing and the Glass Transition* edited by J.P. Hansen, D. Levesque and J. Zinn-Justin (North-Holland, Amsterdam, 1991) Chapter 10.
- [2]
J.K.G. Dhont, A.F.H. Duyndam and B.J. Ackerson, *Physica A* 189 (1992) 503.
- [3]
L.D. Landau and E.M. Lifshitz, *Statistical Physics* (Pergamon Press, Oxford, 1980) chapter 14.
- [4]
J.C. Toledano and P. Toledano, *Landau Theory of Phase Transitions* (World Scientific, New York, 1987) Chapter 2.
- [5]
A.P. Levanyuk, *Soviet Physics JETP* 22 (1966) 901.
- [6]
H. Grabert, *Projection Operator Techniques in Nonequilibrium Statistical Mechanics*, (Springer Verlag, Berlin, 1982) Chapter 1.
- [7]
S.K. Ma, *Modern Theory of Critical Phenomena* (W.A. Benjamin, Inc. Massachusetts, 1976) Chapter 13.
- [8]
P.C. Hohenberg and B.I. Halperin, *Rev. Mod. Phys.* 49 (1977) 435.
- [9]
H.E. Stanley, *Introduction to Phase Transitions and Critical Phenomena* (Oxford University Press, Oxford, 1971) Chapter 11.
- [10]
D. Lawrie and S. Sarbach, *Theory of Tricritical Points, in Phase Transitions and Critical Phenomena* edited by C. Domb, J.L. Lebowitz (Academic Press, Boston,

[11]

K. Sobczyk, Stochastic wave propagation (PWN- Polish Scientific Publishers, Warsaw, 1985)

[12]

J.P. Hansen and I.R. McDonald, Theory of Simple Liquids (Academic Press, Boston, 1986).

[13]

W. Götze, Aspects of Structural Glass Transitions, in Liquids, Freezing and the Glass Transition edited by J.P. Hansen, D. Levesque and J. Zinn-Justin (North-Holland, Amsterdam, 1991) Chapter 5.

[14]

R. Buscall, J.W. Goodwin, M.W. Hawkins and R.H. Ottewill, J. Chem. Soc. Faraday Trans. 1, 78 (1982) 2873.

[15]

C. Allain, M.Cloitre, B. Lacoste and I. Marsonne, J. Chem. Phys. 100 (1994) 4537.

[16]

I.M. Krieger and T.J. Dougherty, Trans. Soc. Rheol. 3 (1959) 137.

[17]

R. Buscall, J.W. Goodwin, M.W. Hawkins and R.H. Ottewill, J. Chem. Soc. Faraday Trans. 1, 78 (1982) 2889.

[18]

W.B. Russel and D.W. Benzing, J. Colloid Interface Sci. 83 (1981) 163.

[19]

H.M. Lindsay and P.M. Chaikin, J. Chem. Phys. 76 (1982) 3774.

[20]

D.W. Benzing and W.B. Russel, J. Colloid Interface Sci. 83 (1981) 178.

[21]

L.B. Chen, B.J. Ackerson and C.F. Zukoski, J. Rheol. 38 (1994) 193.

[22]

D. Hearth and T.F. Tadros, *Faraday Discuss. Chem. Soc.* 76 (1983) 203.

[23]

T.F. Tadros, *Prog. Colloid. Polym. Sci.* 79 (1989) 120.

[24]

W. Liang, T.F. Tadros and P.F. Luckham, *J. Colloid Interface Sci.* 160 (1993) 183.

[25]

T.F. Tadros, W.Liang, B. Costello and P.F. Luckham, *Colloids and Surfaces* 79 (1993) 105.

[26]

K. Okano and S. Mitaku, *J. de Physique* 41 (1980) 585.

[27]

B.J. Adler and T.E. Wainwright, *J. Chem Phys* 27 (1957) 1208.

[28]

B.J. Adler and T.E. Wainwright, *Phys. Rev.* 127 (1962) 359.

[29]

S. Mitaku, T. Ohtsuki and K. Okano, *Jap. J. Appl. Phys.* 19 (1980) 439.

[30]

H.C. Brinkman, *J. Chem. Phys.* 20 (1952) 571.

[31]

S. Mitaku, T.Ohtsuki and K.Okano, *J. de Physique* 40 (1979) C3-481.

[32]

T. Ohtsuki, *Physica A* 108 (1981) 441.

[33]

D.W. Schaefer and B.J. Ackerson, *Phys. Rev. Lett.* 35 (1975) 1448.

[34]

R. Williams, R.S. Crandall and P.J. Wojtowicz, *Phys. Rev. Lett.* 37 (1976) 348.

5. A Theory for the Melting of Colloidal Crystals Induced by Static Shear

5.1 Introduction

A number of authors discussed theoretically the thermodynamic stability of colloidal crystals against steady-state shear perturbations. Ramaswamy & Renn [1] treated this shear induced melting transition as an extension of the equilibrium melting by using a generalized Hansen-Verlet criterion to the non-equilibrium case of a sheared colloidal crystal. With this concept they calculated a shift in the fluid-crystal coexistence curve. Bagchi & Thirumalai [2] applied a non-equilibrium generalization of the density functional theory of freezing under shear to colloidal suspensions. They constructed a free energy functional taking into account the effect of shear. Their results confirmed the results of Ramaswamy & Renn: if in the absence of shear the system is at the coexistence curve, then in the presence of shear it will be in the fluid phase. The shift ΔC_c of the salt concentration under coexistence conditions has been determined for small shear rates $\dot{\gamma}$ to be $\Delta C_c \sim -\dot{\gamma}^2$. This qualitative picture has also been found in a molecular dynamics simulation of soft sphere particles reported by Stevens et. al. [3]. These models, however, do not permit of calculating rheological parameters (storage and loss moduli).

In this paper a model is presented to describe the shear melting transition of colloidal crystals under an applied constant shear strain ($\dot{\gamma}=0$). It is based on an extension of the derivation in Chapter 4, in which the melting of a colloidal crystal is treated as a symmetry breaking transition. The basic idea of the present chapter is that the application of a critical shear strain on a colloidal crystal close to a symmetry breaking transition will change its free energy thereby leading to an instability, thus changing the symmetry properties of the system. This shear induced symmetry breaking will be treated here by using the model equations of Chapter 4, while we

include a constant shear, in order to obtain the variation of the transport parameters as reflected in the viscoelastic properties close to the transition.

5.2 Theory

The Helmholtz Free Energy Close to the Phase Transition

Starting point of the present model is a generalized local Helmholtz free energy density $f(q,u)$ of a colloidal suspension close to a symmetry breaking transition as introduced in Chapter 4:

$$f(q(\underline{r},t),u(\underline{r},t))=f_0+\frac{\lambda}{2}(\nabla q(\underline{r},t))^2+\frac{\alpha}{2}q^2(\underline{r},t)-\frac{\zeta}{3}q^3(\underline{r},t)+\frac{\nu}{4}q^4(\underline{r},t) \\ +\frac{\gamma}{2}u(\underline{r},t)q^2(\underline{r},t)+\frac{G_0}{2}u^2(\underline{r},t) \quad (99)$$

In this equation the positional and time dependent free energy density f is a function of the local order parameter $q(\underline{r},t)$ and of the local strain $u(\underline{r},t)$. We will confine our considerations here to simple shear, in which $u=(w_{xz}+w_{zx})/2$, while the deformation w of a body is given by the spatial derivation of the displacement vector \underline{X} :

$$w_{xz}=\frac{\partial X_x}{\partial z} \quad (100)$$

The contribution to the free energy density of a mechanically deformed system is thus $G_0/2 u(\underline{r},t)^2$ with an elastic modulus G_0 , which is assumed to be isotropic.

The degree of symmetry will be captured in the 'order parameter' q . The phase with the higher number of allowed symmetry operations is denoted as the high symmetry phase and the other as the low symmetry phase. Disordered phases such as the fluid or the liquid phase can be transformed into itself by an infinite number of transformations, as long as we restrict ourselves to time-average distribution functions. Therefore in the case of an order-disorder transition the disordered phase is the high symmetry phase, while the crystal phase is the low symmetry phase. The order parameter $q(\underline{r},t)$ is associated here with the change of the amplitude of the density

wave in the incompressible colloidal crystal (low symmetry phase) during the transition. The term $(\nabla q(\underline{r},t))^2$ takes into account the contribution of homogeneous (i.e. long ranged), space-dependent order parameter fluctuations to the free energy. The expansion of the order parameter up to the fourth order on the right hand side represents the Landau free energy close to a first order equilibrium phase transition, where λ , ζ and ν are positive parameters while α is positive in the high symmetry phase and negative in the low symmetry phase [4]. This can be illustrated by determining the equilibrium values of the order parameter by minimizing the Helmholtz free energy density f with respect to the order parameter q , while the term in Eq. (99) containing the $(\nabla q(\underline{r},t))^2$ has no influence on the average value of the order parameter and is thus neglected. The stability of the solutions depends on the second derivative of the free energy with respect to q . Whereas q_{00} and q_{01} represent minima of the free energy, q_{02} is a maximum.

$$\left(\frac{\partial F}{\partial q}\right)_u = \alpha q - \zeta q^2 + \nu q^3 + \gamma u q = 0 \quad (101)$$

The equilibrium values of the order parameter q_0 are:

$$q_{00} = 0$$

$$q_{01} = \frac{\zeta}{2\nu} + \sqrt{\left(\frac{\zeta}{2\nu}\right)^2 - \frac{\alpha + \gamma u}{\nu}} \quad (102)$$

$$q_{02} = \frac{\zeta}{2\nu} - \sqrt{\left(\frac{\zeta}{2\nu}\right)^2 - \frac{\alpha + \gamma u}{\nu}}$$

The solution $q=0$ represents the high symmetry phase, whereas $q \neq 0$ corresponds to the low symmetry phase. The system is in the high symmetry phase $q_{00}=0$ if $\alpha + \gamma u > 0$. At negative $\alpha + \gamma u$ the system is in the low symmetry phase $q_{01} \neq 0$. The coexistence region is given by the values $\alpha_{01} = \zeta^2/4\nu - \gamma u$, where the high symmetry phase becomes unstable and $\alpha_{00} = -\gamma u$, where the low symmetry is the only possible state. Our calculations on the rheology of colloidal suspensions are restricted to systems not too close to the coexistence region. In this case the parameter ζ is considered to be small compared to α . For $\zeta=0$ a second order transition takes place.

The term $1/2 \gamma u(\underline{r},t) q(\underline{r},t)^2$, [5] is a simple generalization of the free energy

and couples the relaxation processes of the order parameter and the elastic deformation field (mode coupling). It will lead to an elastic modulus and a shear viscosity both corrected for the influence of fluctuations.

We will write the time and space dependent order parameter $q(\underline{r},t)$ and the strain field $u(\underline{r},t)$ as the sum of the equilibrium values and small space and time dependent variations:

$$\begin{aligned} u(\underline{r},t) &= u_0 + \delta u(\underline{r},t) \\ q(\underline{r},t) &= q_0 + \delta q(\underline{r},t) \end{aligned} \tag{103}$$

For reasons of brevity we will not always indicate the dependence of δu and δq on \underline{r} and t . Inserting (103) into (99) and taking into account only terms up to the second order in δu and δq we arrive at:

$$\begin{aligned} f(\delta q, \delta u) &= f_0 + \frac{\alpha}{2} q_0^2 - \frac{\zeta}{3} q_0^3 + \frac{\nu}{4} q_0^4 + \frac{\gamma}{2} u_0 q_0^2 + \frac{G_0}{2} u_0^2 + \\ &+ (\alpha q_0 - \zeta q_0^2 + \nu q_0^3 + \gamma u_0 q_0) \delta q + \left(\frac{\alpha}{2} - \zeta q_0 + \frac{3}{2} \nu q_0^2 + \frac{\gamma}{2} u_0 \right) \delta q^2 \\ &+ \frac{\gamma}{2} \delta u \delta q^2 + \left(\frac{\gamma}{2} q_0^2 + G_0 u_0 \right) \delta u \\ &+ \frac{G_0}{2} \delta u^2 + \gamma q_0 \delta u \delta q + \frac{\lambda}{2} (\nabla \delta q)^2 \end{aligned} \tag{104}$$

The terms linear in δu and δq disappear, because the system is in a minimum of the thermodynamic potential. Note that in difference to the model discussed in Chapter 4 is that we take into account a constant quasi statically applied external shear strain $u_0 \neq 0$.

The Helmholtz free energy density depends on the value of q_0 . In the high symmetry phase, with $\alpha > 0$ and $q_0 = 0$, it can be written as:

$$f(\delta q, \delta u) = f' + \frac{\lambda}{2} (\nabla \delta q)^2 + \frac{1}{2} (\alpha + \gamma u_0) \delta q^2 + \frac{1}{2} G_0 \delta u^2 + \frac{1}{2} \gamma \delta q^2 \delta u \tag{105}$$

with

$$f' = f_0 + \frac{G_0}{2} u_0^2 \quad (106)$$

The free energy density in the low symmetry phase with $\alpha + \zeta q_0 < 0$ and $q_0 \neq 0$ becomes after substitution of the q_0^2 term by the solution of Equation (101):

$$\begin{aligned} f(\delta q, \delta u) = & f_0'' + \frac{\lambda}{2} (\nabla \delta q)^2 + \frac{1}{2} (-2\alpha + \zeta q_0 + 2\gamma u_0) \delta q^2 + \frac{1}{2} G_0 \delta u^2 \\ & + \gamma q_0 \delta q \delta u + \frac{1}{2} \gamma \delta q^2 \delta u \end{aligned} \quad (107)$$

where we used

$$f_0'' = f_0 + \frac{\alpha}{2} q_0^2 - \frac{\zeta}{3} q_0^3 + \frac{\gamma}{4} q_0^4 + \frac{\gamma}{2} u_0 q_0^2 + G_0 (u_0)^2 \quad (108)$$

The break of the symmetry leading to a transition occurs when the sign of $\alpha + \gamma u_0$ changes. This takes place at the transitional value of the external strain

$$u_0^{(C)} = |\alpha| \gamma^{-1} \quad (109)$$

We assume that γu_0 imparts a positive contribution to the free energy. This means that a change in the sign and thus a symmetry breaking transition can only occur for negative values of $\alpha + \zeta q_0$, i.e. in the low symmetry phase (colloidal crystal).

A colloidal crystal in equilibrium has a minimum in the thermodynamic potential $F(q)$ at a non-zero order parameter q . Applying a strain u_0 on the crystal (low symmetry phase) increases the thermodynamic potential but the structure remains stable for strains $u_0 < u^{(C)}$. For strains $u_0 > u^{(C)}$ the crystal phase is thermodynamically unstable and turns back into the high symmetry phase of a disordered structure with a zero-valued order parameter. This is a shear induced instability, where the order parameter turns back to the value of the high symmetry phase $q=0$ at $u_0 > u^{(C)}$. The value of the critical strain has been estimated e.g. for electrically stabilized colloidal particles in a hexagonal layered structure by Boersma [6].

The Viscoelastic Properties Close to a Phase Transition

Having derived the free energy density for the high and the low symmetry phase we are now able to describe the influence of the fluctuations of the order parameter on the transport parameters G_0 and η_0 . The two slow modes describing the dynamics of the system are given by the transport equations of the order parameter

$$\frac{\partial \delta q}{\partial t} = -\frac{1}{\chi} \frac{\delta f(\delta q, \delta u)}{\delta q} + \frac{g(r,t)}{\chi} \quad (110)$$

and the momentum

$$\rho \frac{\partial^2 \delta X_x}{\partial t^2} = \frac{\partial}{\partial z} \left(\frac{\delta f(\delta q(r,t), \delta u(r,t))}{\delta u} + \eta_0 \delta \dot{u}(r,t) \right) \quad (111)$$

where $g(r,t)$ is a fluctuating term with white noise obeying the fluctuation-dissipation theorem :

$$\langle g(r,t), g(r',t') \rangle = 2\chi k_B T \delta(t-t') \delta(r-r') \quad (112)$$

while χ is a damping coefficient. Generally speaking the transport coefficients G_0 and η_0 are frequency dependent both in the high and in the low symmetry phase. The transport coefficients depend on the interparticle interaction determined a. o. by the relaxation process of the electric double layer of the colloidal particles. Close to a phase transition however the low frequency critical fluctuations determine the transport processes (critical slowing down). Therefore close to the transition only the low frequency values $G(\Omega=0)$ and $\eta(\Omega=0)$ of the high and low symmetry phase are important, denoted as G_0 and η_0 . These values of the transport coefficients are valid under conditions far removed from the phase transition, and will be specified later for the high and the low symmetry phase. Close to a transition they are modified by the presence of fluctuations.

The equations (105) and (107) have exactly the same form as the model free energy density in Chapter 4, except for the shifts of the reference free energies f , f' and of α by the value γu_0 . The transport parameters in the presence of small periodic

perturbations in $\delta u(\underline{r}, t)$ and $\delta q(\underline{r}, t)$ can be calculated by the same procedure as in the previous chapter. Applying a shear perturbation by a controlled quasi-static strain u_0 , the model indicates that a colloidal crystal is thermodynamically unstable against a quasi-statically applied shear strain $u_0 > u_0^{(c)}$, where $u_0^{(c)}$ is given by equation (109).

The expected storage and loss moduli are given by (Chapter 4):

$$G'_H(\Omega) = G_{H0} - J_{H1}(\Omega) \quad (113)$$

$$G''_H(\Omega) = \Omega \eta_{H0} - J_{H2}(\Omega) \quad (114)$$

where G_{H0} and η_{H0} are the undisturbed values of the elastic modulus and the viscosity of the high symmetry phase (index H), where J_{H1} and J_{H2} are given by:

$$J_{H1}(\Omega) = \frac{2\sqrt{2}\pi^3\gamma^2 k_B T \lambda}{\chi \Omega} \sqrt{\sqrt{\frac{(\alpha + \gamma u_0)^2}{\lambda^2} + \frac{\chi^2 \Omega^2}{4\lambda^2}} - \frac{\alpha + \gamma u_0}{\lambda}} \quad (115)$$

$$J_{H2}(\Omega) = \frac{-4k_B T \pi^3 \gamma^2 \lambda^2}{\chi \Omega} \left(\sqrt{\frac{1}{2} \left[\sqrt{\frac{(\alpha + \gamma u_0)^2}{\lambda^2} + \frac{\chi^2 \Omega^2}{4\lambda^2}} + \frac{\alpha + \gamma u_0}{\lambda} \right]} - \sqrt{\frac{\alpha + \gamma u_0}{\lambda}} \right) \quad (116)$$

while their low symmetry equivalents (index L) takes the form:

$$J_{L1}(\Omega) = 4(-2\alpha + 2\gamma u_0 + \zeta q_0) \gamma^2 q_0^2 \frac{1}{\Omega^2 \chi^2 + (-2\alpha + 2\gamma u_0 + \zeta q_0)^2}$$

$$+ \frac{2\sqrt{2}\pi^3 \gamma^2 k_B T \lambda}{\chi \Omega} \sqrt{\sqrt{\frac{(-2\alpha + 2\gamma u_0 + \zeta q_0)^2}{\lambda^2} + \frac{\chi^2 \Omega^2}{4\lambda^2}} + \frac{(-2\alpha + 2\gamma u_0 + \zeta q_0)}{\lambda}}$$
(117)

and

$$J_{L2}(\Omega) = \chi \Omega 4 \gamma^2 q_0^2 \frac{1}{\Omega^2 \chi^2 + (-2\alpha + 2\gamma u_0 + \zeta q_0)^2}$$

$$- \frac{4k_B T \pi^3 \gamma^2 \lambda^2}{\chi \Omega} \left(\sqrt{\frac{1}{2} \left[\sqrt{\frac{(-2\alpha + 2\gamma u_0 + \zeta q_0)^2}{\lambda^2} + \frac{\chi^2 \Omega^2}{4\lambda^2}} + \frac{-2\alpha + 2\gamma u_0 + \zeta q_0}{\lambda} \right]} - \sqrt{\frac{-2\alpha + 2\gamma u_0 + \zeta q_0}{\lambda}} \right)$$
(118)

The transport properties of a colloidal suspension of a shear induced symmetry breaking transition can be determined by applying a constant strain u_0 and superimposing on it a small deformation with a low frequency Ω . This permits to determine the storage modulus $G'(\Omega)$ and loss modulus $G''(\Omega)$.

Because the position of the system in the equilibrium phase diagram in the absence of the strain has not changed, the occurrence of a shear induced transition can be viewed as a shift of the equilibrium transition lines due to the applied shear strain. The phase with the lower free energy is the disordered fluid phase, with a non-zero elastic modulus denoted here as a glass. Applying a shear strain on a colloidal crystal, it will break into pieces of smaller crystals delivering a global disordered structure with a non-zero elastic modulus.

Starting with a colloidal crystal $(G_{1,0}, \eta_{1,0})$, the storage modulus decreases and has a minimum at the critical strain $u_0^{(c)}$, while the loss modulus G'' has a maximum there. The high symmetry phase is a suspension with the transport parameters G_{H0}, η_{H0} of the glass phase. This behaviour as shown in Figure 17 is the result of the critical fluctuations and the destruction of the colloidal crystal. The model equations for the transport parameters are not correct at the critical strain $u_0^{(c)}$, i.e. at the transition, because the approximations made in the previous chapter are not applicable to this region. Therefore we consider only cases outside the coexistence region with $\alpha \gg \zeta q_0$.

The model presented here is therefore restricted for strain deformations not too close to the transition.

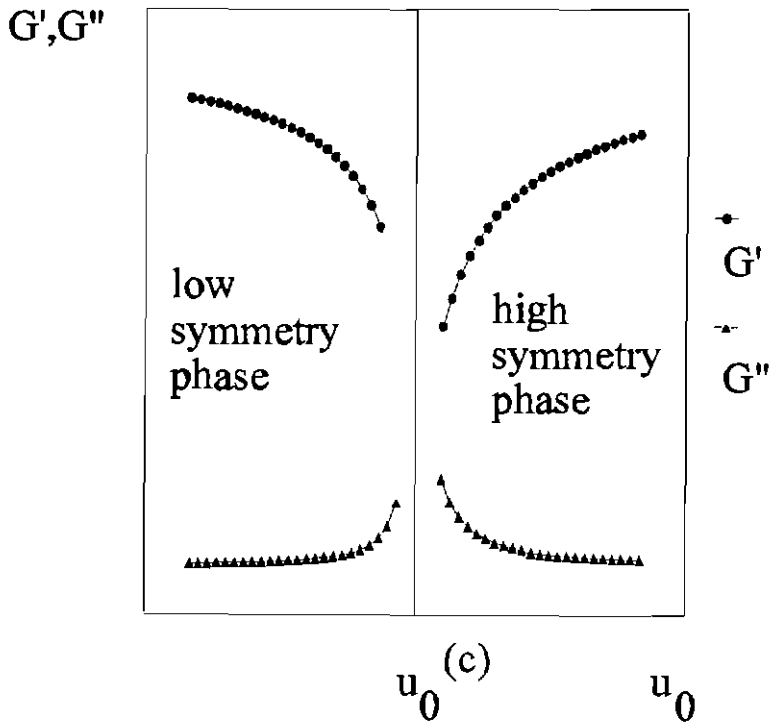


Figure 17 The storage modulus G' and the loss modulus G'' as a function of the applied shear strain u_0 in relative units.

The frequency dependence of $G'(\Omega)$ and $G''(\Omega)$ can be seen in the Figures 18 and 19. $G'(\Omega)$ increases with the frequency Ω . The loss modulus $G''(\Omega)$ depends on the applied strain u_0 . On increasing the strain the maximum in the loss modulus shifts to lower frequency values by approaching the transition.

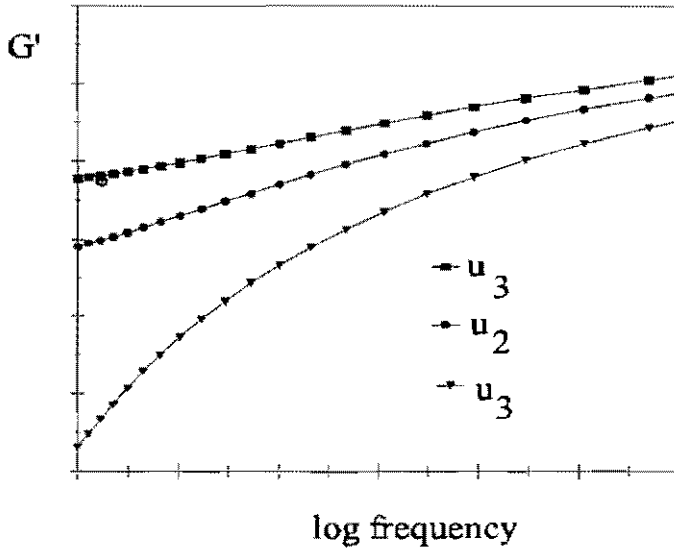


Figure 18 Frequency dependence of the storage modulus G' in relative units for applied shear strains u_0 , while approaching a transition with $|u_1| < |u_2| < |u_3|$.

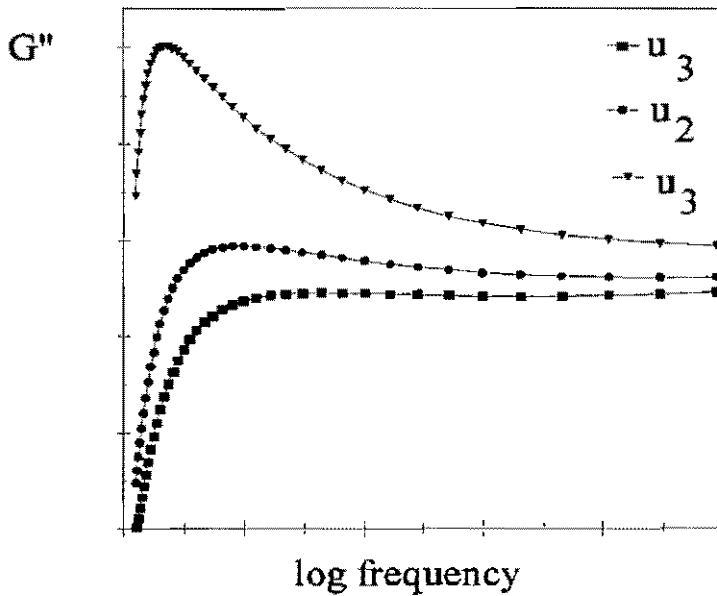


Figure 19 Frequency dependence of the loss modulus G'' in relative units for applied shear strains u_0 , while approaching a transition with $|u_1| < |u_2| < |u_3|$.

Applying a quasi-static ($\Omega_0 \rightarrow 0$) sinusoidal deformation with an amplitude U_0 the response of the suspension will be non-harmonic. This can be indicated by calculating the stress as a function of a strain u_0 , with the form:

$$u_0 = U_0 \cos(\Omega_0 t) \quad (119)$$

We applied the equations of G' (113) and G'' (114), while neglecting the coexistence region by setting $\zeta = 0$. Figure 20 displays the resulting stresses determined for a number of relative amplitudes; the latter are the strain amplitudes U_0 scaled by the critical strain $u_0^{(c)}$ with $\Omega_0 \rightarrow 0$. It indicates the occurrence of a nonlinear response (higher harmonics).

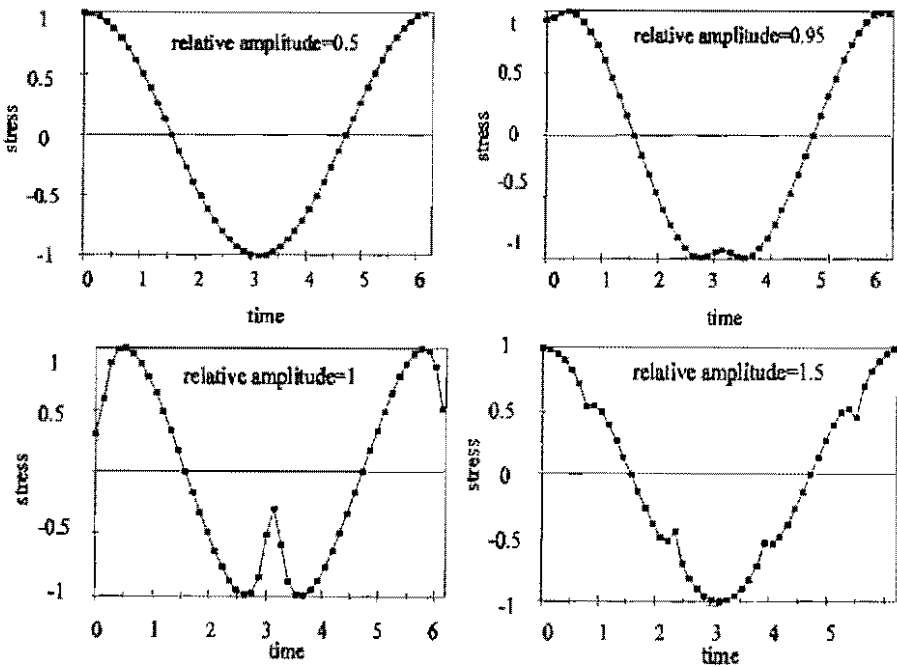


Figure 20 Stress response on a applied cosine shear strain ($\Omega \rightarrow 0$) for a number of relative amplitudes $U_0/u_0^{(c)}$ for one period in time.

5.3 Discussion

As expected from the theories of Bagchi & Thirumalai [2] and Ramaswamy & Renn [1] a shear strain perturbation can induce a symmetry breaking transition. The static shear melting transition in suspensions is accompanied by non-linearities in the transport properties, which can be detected easily in concentrated dispersions.

In order to analyze dynamic moduli of a strained colloidal crystal a very small oscillation with frequency Ω should be superimposed on a constant strain u_0 . However no such experimental data are available. A number of authors [9],[10] performed dynamic measurements on colloidal suspensions with varying amplitude but without a constant strain u_0 . On rising the amplitude first they found a constant elastic modulus. Beyond a critical strain they found an increase in G' . From the model we expect a decrease of the storage modulus due to the disappearance of the colloidal crystal at high volume fractions followed by an increase as the result of the transition into a disordered structure (Fig.17) that takes place at a critical strain $u_0^{(c)}$ (109).

Miller et. al. [9] studied solid propellants and observed a critical strain amplitude $U_0^{(c)}$ at the minimum of the elastic modulus of $U_0^{(c)} \approx 10\%$. This result is consistent with the generalized density functional theory of Bagchi & Thirumalai [2]. These authors calculated a maximal critical strain of $U_0^{(c)}(C) = 35\%$ above which any bcc-crystal disappears and a liquid-like structure occurs.

The dependence of the transport parameters on the strain provides a non-linear response on a sinusoidally applied strain (Fig. 20). In this figure a 'relative amplitudes', is employed defined as the strain amplitude U_0 scaled by the critical strain $u_0^{(c)}$. The appearance of these higher harmonics has been found by Miller et. al. [9] and Boersma et. al. [10] while performing dynamic testings. Under these conditions the linear response is lost and care has to be taken in the interpretation of the results. However in the range of small frequencies ($\Omega_0 \rightarrow 0$) the measurements are primarily given by G' . Therefore we consider here only the low frequency storage modulus.

Matsumoto & Okubo [11] investigated dilute polystyrene suspensions ($\Phi \approx 0.1$)

and estimated the decrease of the elastic modulus for small deformations and low frequencies to be $G' \sim (U_0)^{-1.56}$, where our model suggests $G' \sim (u_0)^{-0.5}$ in the hydrodynamic limit.

Using scattering techniques a characteristic transition from a crystal structure into a disordered structure can be expected at the static shear melting transition for small deformations, visible by a transition from Bragg-peaks of the colloidal crystal into a Debye-ring indicating a globally disordered structure for increasing strains. Static light scattering techniques have been applied by Ackerson [12] and Ackerson & Pusey [13] on nearly hard spheres of sterically stabilized PMMA-particles in tetralin/decalin mixtures. They found that a shear $U_0=1$ at $\Omega=1\text{Hz}$ orients the crystal structure of a dispersion with an absolute volume fraction $\Phi=0.48$ and transforms the system into oscillating fcc-twin structures, where the (1,1,1) planes are parallel to the cell walls. At a strain amplitude $U_0=4$ hexagonal planes were formed indicating a non-equilibrium structure.

Another light scattering investigation on soft sphere suspensions of silica particles in toluene/ethanol was performed by Yan et.al. [14]. Similar results as in the almost hard sphere case were obtained. After applying strain amplitudes ($U_0=1$) the initially poly-crystalline structure changes into fcc-twin structures; at larger amplitudes reorganization into a structure of close packed layers takes place. The transition from fcc-twins to sliding layers shifts to lower strain amplitudes at higher volume fractions.

Boersma et.al. [10] investigated concentrated silica suspensions in water/glycerol mixtures and found critical strain amplitudes for small frequencies of the order $U_0^{(c)} \approx 5\text{-}10\%$. At high frequencies the critical shear strain shifts to smaller values on increasing the frequency, while the product of $U_0^{(c)}\Omega$ is a constant. The latter result suggests that the increase of the modulus occurs at a constant shear rate if we assume that the typical shear rate in an oscillatory measurement can be approximated by $\dot{\gamma} \approx U_0\Omega$ [15].

We interpret the constant critical shear strain at low frequencies as reflecting the shear melting transition. The critical strain at higher frequencies is interpreted by the present authors as another instability denoted as dynamic shear melting, which is treated in Chapter 6. This instability is due to an acoustic resonance of the sheared

colloidal crystal and occurs at a constant critical shear rate. It is accompanied by an pronounced increase of the viscosity.

The experimental evidence of the static shear melting transition under continuous shear has already been found by using light scattering techniques by Pieranski [16] and Ackerson & Clark [17] on dilute colloidal crystals and in numerical simulations e.g. by Hess [18], for small shear rates. The accompanied rheological properties have been investigated first by Chen et. al. [19],[20] in a polystyrene latex suspension. Using small-angle neutron scattering they found the disappearance of the Bragg-peaks accompanied with a jump of the measured stress at very small shear rates. This jump is probably related to an increase in the elastic modulus during the transition into a disordered structure. Numerical simulations indicate a slight increase of the viscosity at this transition (Fig.7 of ref [21]).

In order to investigate the a shear induced transition, in Chapter 7, rheo-optical experiments are described. It will be reported that qualitatively the dependence of the viscoelastic properties has been obtained as predicted from this model, accompanied with the expected change of the structure as determined by static light scattering .

5.4 Conclusion

A model is presented predicting rheological parameters (G' and G''). It is based on a Landau theory of structural transitions, which predicts a shear induced symmetry breaking transition. The equilibrium colloidal crystal becomes unstable under an applied strain and is expected to change into a disordered colloidal glass structure. The model allows the qualitative evaluation of the transport parameters close to such a structural transition. The storage modulus is expected to have a minimum and the loss modulus a maximum at the critical strain. Experimental results presented in Chapter 8 qualitatively confirm the predicted dependence of the transport parameters.

Literature

[1]

Ramaswamy, S. and S.R. Renn, "Theory of Shear- Induced Melting of Colloidal Crystals" *Phys. Rev. Lett.* **56**, 945-948 (1986).

[2]

Bagchi, B. and D.Thirumalai, "Freezing of a colloidal liquid subjected to shear flow" *Phys. Rev. A* **37**, 2530-2538 (1988).

[3]

Stevens, M.J., M. O. Robbins and J.F. Belak, "Shear melting of colloids: a non-equilibrium phase diagram" *Phys. Rev. Lett.* **66** 3004-3007 (1991).

[4]

Landau, L.D. and E.M. Lifshitz, *Statistical Physics* (Pergamon Press, Oxford, 1980), Vol. 5, Part 1, Chapter 14.

[5]

Landau, L.D. and E.M. Lifshitz, *Theory of Elasticity* (Pergamon Press, Oxford, 1970), Vol. 7, Chapter 6.

[6]

Boersma, W., " Shear Thickening of Concentrated Dispersions", PhD-Thesis, (Eindhoven, 1991).

[7]

Ma, S.K. *Modern Theory of Critical Phenomena* (W.A. Benjamin, Inc. Massachusetts, 1976), Chapter 13.

[8]

Levanyuk,A.P. "Contribution to a Phenomenological Theory of Sound Absorbtion near Second-Order Phase Transition Points" *Soviet Physics JETP* **22** 901-906 (1966).

[9]

Miller, R.R., E.Lee, R.Powell, "Rheology of solid propellant dispersions" *J. Rheol.* **35**, 901-919 (1991).

[10]

Boersma,W.H., J. Laven and H.N. Stein, "Viscoelastic properties of concentrated shear-thickening dispersions" *J. Colloid Interface Sci.* **149**, 10-22 (1992).

[11]

Matsumoto, T. and T.Okubo, "Viscoelastic investigation of crystal-liquid transition in concentrated monodisperse latices" *J. Rheol.* **35**, 135-148 (1991).

[12]

Ackerson, B.J., " Shear induced order of hard sphere suspensions" *J. Phys. Condens. Matter* **2**, SA389-SA392 (1990).

[13]

B.J. Ackerson and P.N.Pusey,"Shear-Induced Order in Suspensions of Hard Spheres," *Phys. Rev. Lett.* **61**, 1033-1036.

[14]

Yan,Y.D. and J.K.G. Dhont, C.Smits, H.N.W. Lekkerkerker, "Oscillatory-shear induced order in non-aqueous dispersions of charged colloidal spheres" *Physica A* **202**, 68-80 (1994).

[15]

Xue, W. and G.S. Grest, "Shear-induced alignment of colloidal particles in the presence of a shear flow" *Phys. Rev. Lett.* **64**, 419-422 (1990).

[16]

Pieranski, P., "Colloidal Crystals" *Contemp. Phys.* **24**, 25-73 (1983).

[17]

Ackerson, B.J. and N.A. Clark, "Shear-induced melting" *Phys. Rev. Lett.* **46**, 123-126 (1981).

[18]

Hess,S., "Shear induced melting and reentrant positional ordering in a system of spherical particles" *Int. J. Thermophys.* **6**, 657-671 (1985).

[19]

Chen,L. B., M.K. Chow, B.J. Ackerson and C.F. Zukoski, "Rheological and microstructural transitions in colloidal crystals" *Langmuir* **10**, 2817-2829 (1990).

[20]

Chen,L.B., C.F. Zukoski, B.J. Ackerson, H.J.M. Hanlay, G.C. Straty, J.Barker and C.J.Glinka, "Structural changes and orientational order in a sheared colloidal suspension" *Phys. Rev. Lett.* **69**, 688-691 (1992).

[21]

Barnes, H.A., M.F. Edwards, L.V. Woodcock, "Applications of computer simulations to dense suspensions rheology" Chem. Eng. Sci. **42**, 591-608 (1987).

6. Shear Thickening as a Consequence of an Acoustic Resonance in Sheared Colloidal Crystals

6.1 Introduction

Under the application of a simple shear flow applied on a colloidal suspension the particles, having a soft interaction potential, may arrange themselves into a long ranged, crystalline structure of hexagonal layers sliding over each other. The existence of this non-equilibrium ordered state will be the starting point of our treatment. Experimental investigations [1],[2],[3],[4] indicate that this structure disappears with increasing shear rates. This disappearance is accompanied by a pronounced increase of the viscosity denoted as shear thickening. We will develop a model based on the assumption that this destruction of the periodic structure is due to the occurrence of an acoustic resonance within the sheared lattice.

Damped acoustic shear waves travel through a viscoelastic continuum as shown first by Joanny [5] and later by Pieranski [6]. A sheared crystal undergoes a periodic variation of the elastic modulus in the shear gradient direction. Harrowell & Fixman [7] demonstrated that this periodic variation amplifies long wave length transverse modes. By using an extension of the Lindemann criterion [8] they could predict an instability of the sheared colloidal crystal due to an acoustic resonance mechanism. Ronis & Kahn [9] improved the approach of Harrowell & Fixman. They analyzed the macroscopic equations of motion of a dilute colloidal crystal under shear and studied the dependence of the acoustic resonance on the system size.

In difference to the previous authors, we will apply a two 'medium' model, where both media are considered as infinite viscoelastic continua, which are coupled with each other. One medium is an elastic colloidal crystal, built up of monodisperse solid particles dispersed in the viscous solvent. The shear is applied on the viscous solvent and is transmitted to the particles. The other medium contains all viscous

contributions. Similar models have been used by other investigators in concentrated polymer solutions and gels [10] and in dilute colloidal crystals [11]. Taking into account the periodic variation of the elastic modulus in the sheared suspension, an acoustic resonance occur. This phenomenon is accompanied with shear thickening. The model presented here allows the calculation of the critical shear rate $\dot{\gamma}_C$, that will be compared with experimental results.

6.2 Theory

The Hydrodynamic Model

Starting point of our model is a two medium model, where one medium is treated as a Newtonian fluid with an effective viscosity η and density ρ_1 . The shear induced colloidal crystal is regarded as the other medium. It is an elastic continuum with a density ρ_2 , and an elastic modulus G . The effective viscosity η corresponds to the suspension with a volume fraction Φ of the dry colloidal particles. In our approach we thus suppose that all viscous effects are taken into account by the viscous medium with the viscosity η . This includes e.g. the viscous damping of movements of the colloidal crystal due to the hydrodynamic interaction between the colloidal particles. We will apply a phenomenological equation, that describes the viscosity increase of a suspension with the volume fraction, consisting of hard spheres dispersed in a solvent

with a viscosity η_0 .

Furthermore we assume that under the influence of a simple shear flow a spatial distribution of monodisperse particles in hexagonally close packed (hcp) layers occurs with the close packed array of particles pointed along e_x , the mean flow direction. The layers are orthogonal to and periodic in the e_z -direction (shear gradient direction). The applied simple shear flow

$$\underline{v}_0 = \begin{pmatrix} 0 & 0 & \dot{\gamma}_0 \\ 0 & 0 & 0 \\ 0 & 0 & 0 \end{pmatrix} \underline{r} \tag{120}$$

allows the hexagonal planes to slip freely over each other, as discussed e.g. in [1],[12]. The motion of the colloidal particles causes the elastic properties of the sheared colloidal crystal in the e_z -direction to vary periodically in time and space. The time-periodicity is determined by the externally applied (macroscopic) shear rate $\dot{\gamma}_0$. We define the shear modulus $\underline{G}(t)$ of the sheared colloidal crystal as the tensor:

$$\underline{G}(t) = G \begin{pmatrix} 1 & 0 & 0 \\ 0 & 1 & 0 \\ 0 & 0 & 1 - \epsilon \cos(\Gamma \dot{\gamma}_0 t) \end{pmatrix} \tag{121}$$

while G is the isotropic elastic modulus of the undisturbed two dimensional hcp-crystal and ϵ is a small valued parameter that describes the modulation of the elastic modulus. The parameter Γ depends on the direction of the shear and the structure of the lattice [9]. For a simple shear in a ortho-rhombic lattice the value of Γ is given by $\Gamma = 2\pi g_z / g_x$, with the lattice constants g_x and g_z in x and z -direction. The shear rate can be scaled by

$$\dot{\gamma} = \dot{\gamma}_0 \Gamma \tag{122}$$

In this work we are interested in the effects of deviations from a uniform shear field. As such, we introduce a displacement field $\underline{\delta u}$ for the colloidal particles and a velocity deviation field $\underline{\delta v}$ for the viscous medium:

$$\underline{u} = \underline{v}_0 + \delta \underline{u} \tag{123}$$

and

$$\underline{v} = \underline{v}_0 + \delta \underline{v} \tag{124}$$

The interaction between the elastic crystal and the viscous continuum is treated as an effective local friction force proportional to the difference between velocities of the particles of the colloidal crystal and the viscous medium.

Under these assumptions the linearized coupled equations of motion have the form

$$(1 - \Phi) \rho_1 \frac{\partial \delta \underline{v}}{\partial t} = \nabla \cdot \underline{\underline{\sigma}}^{(1)} - \underline{\underline{\Xi}}(\delta \underline{v}, \delta \underline{\dot{u}}) \tag{125}$$

$$\Phi \rho_2 \frac{\partial^2 \delta \underline{u}}{\partial t^2} = \nabla \cdot \underline{\underline{\sigma}}^{(2)} + \underline{\underline{\Xi}}(\delta \underline{v}, \delta \underline{\dot{u}}) \tag{126}$$

while $\underline{\underline{\sigma}}^{(1)}$ and $\underline{\underline{\sigma}}^{(2)}$ are the viscous medium and the crystal stress tensor, respectively. The medium-crystal coupling vector $\underline{\underline{\Xi}}$ takes the form:

$$\underline{\underline{\Xi}} \sim \xi(\Phi)(\delta \underline{\dot{u}} - \delta \underline{v}) \tag{127}$$

while $\xi(\Phi)$ is an increasing function of the volume fraction.

On hydrodynamic length and time scales, i.e. neglecting the diffusive motion of the colloidal particles, the coupling between the velocities of the colloidal crystal and the solvent is very strong. Following Lindsay & Chaikin [11] we confine our

investigation to the limit of strong coupling. The essential physics of the strong coupling is when the solvent velocity approaches the velocity of the colloidal crystal

$$\delta \dot{u} \approx \delta v \tag{128}$$

In this limit the coupled set of the equations of motion reduces to a single formula:

$$\rho \frac{\partial^2 \delta u}{\partial t^2} = \nabla \cdot \underline{\underline{\sigma}} \tag{129}$$

with

$$\begin{aligned} \rho &= (1 - \Phi)\rho_1 + \Phi\rho_2 \\ \underline{\underline{\sigma}} &= \underline{\underline{\sigma}}^{(1)} + \underline{\underline{\sigma}}^{(2)} \end{aligned} \tag{130}$$

The stress tensor term in Equation (129) becomes

$$\nabla \cdot \underline{\underline{\sigma}} = \underline{\underline{G}}(t) \nabla^2 \delta u + \eta \nabla^2 \delta \dot{u} \tag{131}$$

while η is the high shear viscosity of the suspension, corresponding to a layered hcp structure.

The Acoustic Resonance

To investigate Equation (129), we introduce a spatial Fourier transform of the deformation field:

$$\underline{\underline{A}}(\underline{k}, t) = \int \delta \underline{\underline{u}}(\underline{r}, t) e^{-i \underline{k} \cdot \underline{r}} d^3 r \tag{132}$$

where $\underline{\underline{A}}(\underline{k}, t)$ is the time and wave number dependent amplitude of local displacements of a volume element from its initial position. Inserting (132) in (129) we obtain

According to Equation (121) the modulus $\underline{\underline{G}}(t)$ is periodic in time. Therefore Equation (133) is a Mathieu equation [14]. Equation (133) can be solved for small

$$\rho \frac{\partial^2 \underline{A}(t)}{\partial t^2} + k^2 \eta \frac{\partial \underline{A}(t)}{\partial t} + k^2 \underline{G}(t) \underline{A}(t) = 0 \quad (133)$$

values of the parameter ϵ defined in Eq. (121) as a Taylor expansion of the amplitude in factors of ϵ :

$$\underline{A}(t) = \underline{A}^{(0)}(t) + \epsilon \underline{A}^{(1)}(t) + O(\epsilon^2) \quad (134)$$

Using this expansion in (133), the zeroth order in ϵ leads to a damped wave equation in the unsheared system:

$$\frac{\partial^2 \underline{A}^{(0)}(t)}{\partial t^2} + k^2 b \frac{\partial \underline{A}^{(0)}(t)}{\partial t} + k^2 c^2 \underline{A}^{(0)}(t) = 0 \quad (135)$$

where the coefficient b is given by

$$b = \frac{\eta}{\rho} \quad (136)$$

and the sound velocity c of the suspension is given by:

$$c^2 = \frac{G}{\rho} \quad (137)$$

Equation (135) can be solved by writing the zeroth-order amplitude as a damped wave

$$\underline{A}^{(0)}(t) = \underline{A}^{(0)} e^{-pt} \quad (138)$$

Substitution of Equation (138) in (135) gives a dispersion relation in p

$$p^2 - bk^2 p + c^2 k^2 = 0 \quad (139)$$

Here p is either real, describing an overdamped creeping motion

$$p_{1,2} = \frac{bk^2}{2} \pm \sqrt{\frac{b^2 k^4}{4} - c^2 k^2} \quad (140)$$

or complex, related to damped propagating waves, with

$$p_{1,2} = \delta \pm j\omega \tag{141}$$

while

$$\delta = \frac{bk^2}{2} \tag{142}$$

$$\omega = \sqrt{c^2k^2 - \frac{b^2k^4}{4}}$$

Now we will investigate contributions to $\underline{A}(\mathbf{k},t)$ originating from first order perturbations in ϵ . Because the G_x and G_y moduli are assumed to be constant, the transverse modes in e_x and e_y are always damped waves. However in Equation (133) we get a contribution in the z-direction from the first order in ϵ of the form

$$\frac{\partial^2 A_z^{(1)}(t)}{\partial t^2} + k^2 b \frac{\partial A_z^{(1)}(t)}{\partial t} + k^2 c^2 A_z^{(1)}(t) = c^2 k^2 A_z^{(0)}(e^{-p_1 t} + e^{-p_2 t}) \cos(\dot{\gamma} t) \tag{143}$$

where we have chosen a linear combination of (138) with the solutions (140) and (142). This formula can be solved by means of a Laplace transform as performed in the Appendix E.

For damped propagating waves with $p_{1,2}$ given by (141) the amplitude of the first order becomes infinite at a specific, externally applied shear rate. For this instability the amplitudes in the e_x -direction become

$$A_z^{(0)}(t, \omega) = 2A_z^{(0)} e^{-\delta t} \cos(\omega t)$$

$$A_z^{(1)}(t) = \frac{2A_z^{(0)} c^2 k^2 e^{-\delta t}}{(\delta^2 + \omega^2)(\dot{\gamma}^2 - 4\omega^2)} [2\omega \cos(\dot{\gamma} t)(\omega \cos(\omega t) + \delta \sin(\omega t)) - \dot{\gamma} \sin(\dot{\gamma} t)(\delta \cos(\omega t) - \omega \sin(\omega t))] \tag{144}$$

The first order amplitude has a singularity, as known from the theory of Mathieu equations [14], at a critical value of the shear rate equal to 2ω with

$$\Gamma \dot{\gamma}_c(k) = 2\omega(k) = 2\sqrt{c^2 k^2 - \frac{b^2 k^4}{4}} \tag{145}$$

for a wave with wave number k . The dependence of the scaled critical shear rate on k is displayed in Figure 21, for a PVC/DOP suspension with $\Gamma = 1$. For practical systems the range of possible values of wave numbers k is limited on the one hand by the system size and on the other hand by the root in Equation (145).

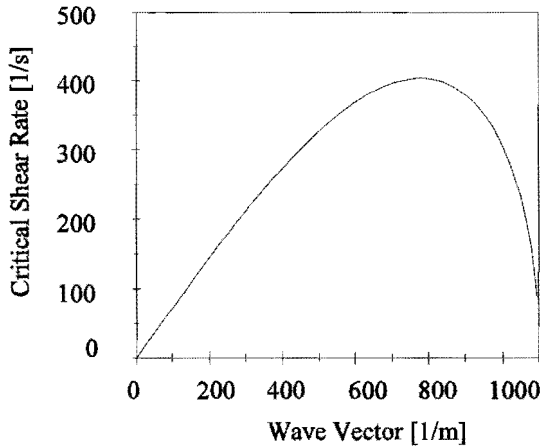


Figure 21 The critical shear rate as a function of the wave vector amplitude k for a PVC-DOP suspension ($\Phi = 0.45$).

The singularity of the amplitude $A_z(k,t)$ describing propagating acoustic shear waves is essentially a resonance effect. Unclear at the first sight is however, which wave number k_0 out from the range of possible wave number k dominates this instability. From dimension analysis of the argument under the root in (145) we know that the size of the wave vector can be written as

$$|k_0| = a_0 \frac{c}{b} \quad (146)$$

while we regard a_0 as a free dimensionless parameter. Below we will estimate the value of this unknown parameter from experiments.

Using (146) and (122) the critical shear rate Equation (145) turns into

$$\dot{\gamma}_c = \frac{a_0}{\Gamma} \sqrt{4 - a_0^2} \frac{1}{\tau} \quad (147)$$

where Γ and a_0 are dimensionless constants and the characteristic relaxation time τ is given by

$$\tau = \frac{b}{c^2} = \frac{\eta}{G} \quad (148)$$

Note that for a suspension with a constant elastic modulus the instability takes place at a constant critical shear stress:

$$\sigma^{(c)} = a_0 \sqrt{4 - a_0^2} \frac{G}{\Gamma} \quad (149)$$

Excess Dissipation

We will consider here the relative increase in dissipation due to an increase of the amplitude of the first order in ϵ . The average rate of energy dissipation of a wave with amplitude A_z in z-direction of angular frequency ω is given by [15]

$$E^{dis}(\omega) = \frac{\omega}{2\pi} \int_0^{2\pi} F^{dis}(t, \omega) \dot{A}_z(t, \omega) dt \quad (150)$$

with the dissipative force density component

$$F^{dis} = k^2 \eta \dot{A}_z(t, \omega) \quad (151)$$

given by the second term of equation (133).

The relative increase of the dissipation due to the contribution of the wave amplitude of the first order in ϵ can approximately be evaluated from

$$\Delta E_{rel}^{dis}(\dot{\gamma}, \omega) \sim \frac{\int_0^{2\pi} \dot{\omega} \dot{A}_z^{(1)}(t, \dot{\gamma}, \omega)^2 dt}{\int_0^{2\pi} \dot{\omega} \dot{A}_z^{(0)}(t, \dot{\gamma}, \omega)^2 dt} \quad (152)$$

The time derivatives of the amplitudes are

$$\begin{aligned} \dot{A}_z^{(0)}(t, \omega) &= -2A_z^{(0)} e^{-\delta t} (\sin(\omega t) \omega + \delta \cos(\omega t)) \\ \dot{A}_z^{(1)}(t, \omega, \dot{\gamma}) &= -\frac{2A_z^{(0)} k^2 c^2 e^{-\delta t}}{(\dot{\gamma}^2 - 4\omega^2)(\delta^2 + \omega^2)} (\cos(\dot{\gamma} t) (\delta \dot{\gamma}^2 \cos(\omega t) + \omega \sin(\omega t) (2\delta^2 - \dot{\gamma}^2 + 2\omega^2)) \\ &\quad - \dot{\gamma} \sin(\dot{\gamma} t) ((\delta^2 - \omega^2) \cos(\omega t) - 2\delta \omega \sin(\omega t))) \end{aligned} \quad (153)$$

Substituting the latter equations into (152) and using ω from (145) we arrive at:

$$\Delta E_{rel}^{dis}(\dot{\gamma}, \dot{\gamma}_c) \sim \frac{1}{\Gamma^4(\dot{\gamma}_0^2 - \dot{\gamma}^2)^2} \quad (154)$$

The extra dissipation leads to an increase of the viscosity of the sheared system, which therefore has a maximum when the external shear rate $\dot{\gamma}_0$ is equal to the critical shear rate $\dot{\gamma}_c$. This acoustic resonance instability is thus accompanied with an increase of the viscosity (dilatancy).

Note that the critical shear rate for shear thickening defined here differs from that generally employed in discussions of the shear rate dependence of the viscosity. The latter critical shear rate is determined from the point where the viscosity increases, whereas in the sense of a resonance the critical shear rate corresponds to the maximum of the viscosity.

Estimation of the Free Parameter

To estimate the free parameter a_0 of Equation (146) we will study two examples and predict the critical shear rates: (i) of a suspension of PVC-particles dispersed in DOP as investigated by Hoffman [16] and (ii) of a suspension of glass particles in glycerol/water as investigated by Boersma et al. [4].

In order to evaluate the critical shear rate using (147) we have to determine the elastic modulus and the viscosity of the sheared suspension. We neglect, as a first approximation, the shear rate dependence of G of the colloidal crystal, which leads to the assumption:

$$G(\dot{\gamma}) \approx G(\dot{\gamma} = 0) \quad (155)$$

For estimating the critical shear rate we assume an ordering of the particles as in a 2-dimensional hcp lattice. Two particles in successive layers have, on closest passage, in the direction of the shear gradient the same interparticle distance as two adjacent

particles within a layer. The volume fraction dependent elastic modulus of a 2-dimensional hcp crystal can now be approximated by [17]

$$G(\Phi) = \frac{1}{2} N n(\Phi) h(\Phi)^2 \frac{\partial^2 U(x, \kappa)}{\sigma_0^2 \partial x^2} \Big|_{x = \frac{h(\Phi)}{\sigma_0}} \quad (156)$$

where x is the interparticle centre to centre distance scaled by $\sigma_0 = 2a$, where a is the particle radius. Here the number N of next nearest neighbours per unit cell is taken as $N=8$. The number density n of the particles at volume fraction Φ obeys the formula

$$n(\Phi) = \frac{\Phi}{V_0} \quad (157)$$

while

$$V_0 = \frac{4}{3} \pi a^3 \quad (158)$$

is the volume of a particle. The distance h between the surfaces of two nearest neighbours in a hexagonally layered structure [18] is

$$h(\Phi) = \left(\frac{8\pi a^3}{3\sqrt{3}\Phi} \right)^{\frac{1}{3}} - 2a \quad (159)$$

The two particle interaction potential is assumed to be given by the Poisson-Boltzmann theory as a screened Coulomb potential in the linear superposition approximation [19],[20]:

$$U(x,\kappa) = \frac{16\pi\epsilon_0\epsilon_r\sigma_0}{e_0^2} \left[k_B T \tanh\left(\frac{e_0\Psi_0}{4k_B T}\right) \right]^2 \frac{\exp(-\kappa(x-1))}{x} \tag{160}$$

We define a scaled Debye reciprocal length κ through $\kappa = \kappa_D \sigma_0$, where

$$\kappa_D = \sqrt{\frac{2N_a C z^2 e_0^2}{\epsilon_0 \epsilon_r k_B T}} \tag{161}$$

The second spatial derivative of the interaction potential is given by

$$\frac{\partial^2 U(x,\kappa)}{\sigma_0^2 \partial x^2} = \frac{B \exp(-\kappa(x-1))(\kappa^2 x^2 + 2\kappa x + 2)}{\sigma_0^2 x^3} \tag{162}$$

We will use a phenomenological equation, that describes the viscosity increase of a hard sphere suspension with the volume fraction. The influence of the temporary formation of clusters of colloidal particles on the viscosity of the sheared colloidal suspension has been determined by Campbell and Forgacs [13], applying a percolation theory. They established an equation for the low shear suspension viscosity η_{low} :

$$\eta_{low}(\Phi) = \eta_0 \left[\exp\left(\frac{\Phi_{hcp} - \Phi_p}{\Phi_{hcp} - \Phi}\right) - 1 \right] \tag{163}$$

for volume fractions $\Phi > \Phi_p$. The parameter Φ_p is the percolation threshold, which is independent of the underlying structure ($\Phi_p = 0.16$), and $\Phi_{hcp} = \pi/3\sqrt{3} = 0.605$ is the maximum packing fraction of a hexagonally layered structure; η_0 is the viscosity of the solvent fluid.

In our analysis we need the viscosity η of the suspension in the high shear rate limit, undisturbed by the resonance. In order to obtain the viscosity η we introduce an unknown coefficient ξ_0 independent of the volume fraction by:

$$\eta(\Phi) = \eta_{low}(\Phi)\xi_0 \tag{164}$$

while η_{low} is given by Equation (163). We can write Equation (147) in the form

$$\dot{\gamma}_c = \xi \frac{G(\Phi)}{\eta(\Phi)} \tag{165}$$

while we have reduced the unknown parameters to a single fitting parameter ξ , which is given by Eq. (147)

$$\xi = \frac{a_0}{\Gamma \xi_0} \sqrt{4 - a_0^2} \tag{166}$$

With the equations above the critical shear rates can be evaluated as a function of the volume fraction. We use the following set of data [16], [4] summarized in Table 6.1:

Table 6.1.	(i) PVC in DOP	(ii) Glass in Glycerol/Water
relative dielectric constant of the solvent ϵ_r	5.2	48.65
radius of the particles a	$0.625 \cdot 10^{-6}$ m	$1.2 \cdot 10^{-6}$ m
surface voltage of the particles Ψ_0	$90 \cdot 10^{-3}$ V	$75 \cdot 10^{-3}$ V
temperature T	298 K	293 K
valency of the ions z	1	1
density of the solvent ρ_0	981 kg/m^3	1000 kg/m^3
density of the particles ρ_1	1400 kg/m^3	2530 kg/m^3
solvent viscosity η_0	0.054 Pa.s	0.14 Pa.s
salt concentration C	0.00167 mol/m^3	0.01 mol/m^3

The salt concentration of the PVC in DOP suspension is an estimation from Figure 9 of ref. [26] for the used surface potential.

(i) PVC in DOP

The shear rates at the maxima of the viscosity measurements ('critical shear rates') on a PVC latex by Hoffman [16] are summarized in Table 6.2:

volume fraction Φ	critical shear rate $\dot{\gamma}_c$ [1/s] theory	critical shear rate $\dot{\gamma}_c$ [1/s] experiment [16]
0.45	400	400
0.47	380	390
0.49	303	300
0.51	186	180
0.53	72	70
0.55	11	18
0.57	0.1	≈ 4

Table 6.2

By choosing the parameter $\xi=4$ we fitted our model to the experimental value of the critical shear rate of the lowest volume fraction (highest critical shear rate). For the other volume fractions we obtain a quite good agreement. Deviations occur for very high volume fractions. Here the critical shear rate is very small and the strong coupling limit is not valid. This is because the movement of the particles and the solvent can be different for small shear rates. The dependence of the critical

shear rate on the volume fraction is shown in Figure 21 for the used set of data. At small volume fractions the critical shear rate is small but it increases with increasing volume fraction. At small volume fractions the viscosity is almost constant, thus here the variation in the critical shear rate originates mainly from the increase of the elastic modulus according to (156). The critical shear rate reaches a maximum at Φ_m and thereafter decreases with increasing volume fraction, because in this region the viscosity increases faster than the elastic modulus does. The acoustic resonance can occur only for $\Phi < \Phi_{hcp}$, because the viscosity of the sheared hcp-layered structure becomes infinite at Φ_{hcp} .

With the same set of parameters the dependence of the critical shear rate has been determined as a function of the salt concentration at constant volume fraction $\Phi=0.45$ and is shown in Figure 21. The viscosity was assumed independent of the salt concentration and thus the critical shear rate is determined completely by the dependence of the elastic modulus on the salt concentration. The elastic modulus increases in the crystal phase with decreasing salt concentration and therefore the critical shear rate increases. The maximum in the critical shear rate with increasing salt concentration is due to the competition of the decreasing exponent factor with the increasing polynomial factor in the second derivative of the interaction potential (162).

Another characteristic dependence of the critical shear rate is on the particle diameter σ_0 . As can be seen from Figure 21 the critical shear rate increases dramatically for small particle sizes at constant volume fraction $\Phi=0.45$ and salt concentration $C=0.00167 \text{ mol/m}^3$.

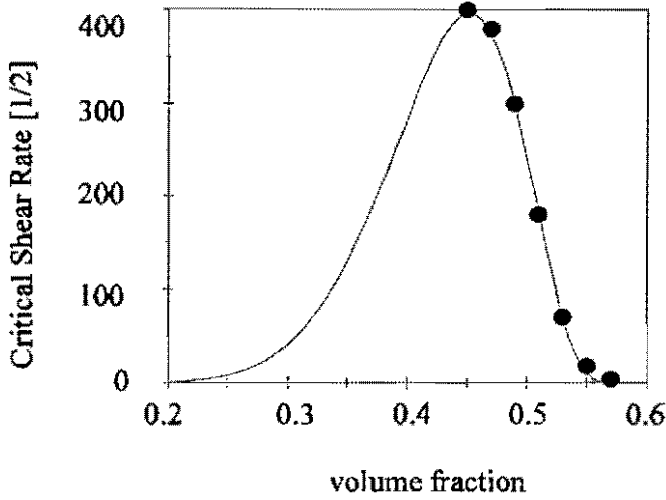


Figure 22 Comparison of the critical shear rate by theory and by experiment (PVC-DOP suspensions [16]).

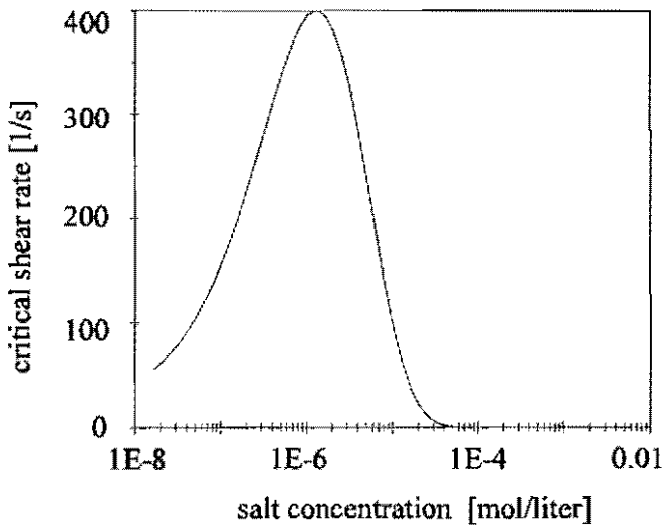


Figure 23 Model prediction of the dependence of the critical shear rate on the salt concentration ($\Phi=0.45$, $a=0.625 \mu\text{m}$).

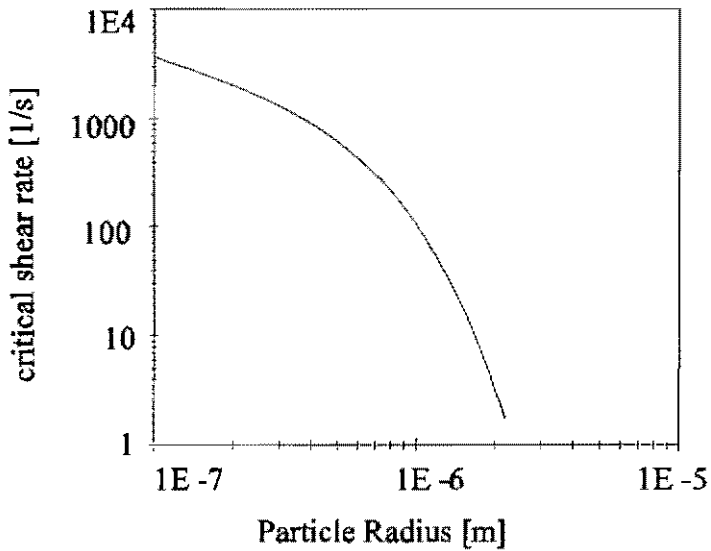


Figure 24 The model prediction of the critical shear rate of a $\Phi=0.45$ suspension is displayed as a function of the particle size.

With decreasing particle size at constant volume fraction and salt concentration the elastic modulus increases, because κ decreases in Equation (162).

(ii) *Glass in Glycerol/Water (86.1% w/w)*

Applying the same formalism developed above, the critical shear rate can be evaluated while we set the free parameter $\xi=4$. The experimental values of the critical shear rate have been obtained from the maximum of the viscosity in reference [4]. The results are summarized in Table 6.3.

volume fraction Φ	critical shear rate $\dot{\gamma}_c$ [1/s] theory	critical shear rate $\dot{\gamma}_c$ [1/s] experiment [4]
0.5	77	≈ 100
0.54	40	30
0.55	18	10
0.57	0.4	8
0.585	$0.4 \cdot 10^{-4}$	2

Table 6.3

The agreement between the experimental and theoretical data is reasonable. Note that the maximum of the lowest viscosity versus shear rate curve was difficult to determine because the variation in the viscosity is rather small. Also the range of volume fractions is smaller than with Hoffmans experiments. As with the PVC/DOP suspension the critical shear rates deviates from the expected value for high values of the volume fraction, presumably because the strong coupling assumption is not justified any more. That the agreement between experiment and theory is less than with the PVC/DOP system may also be due to the larger polydispersity of the glass particle size as compared with that of the PVC particles.

6.3 Discussion

Comparison with Experiments

The application of light, x-ray and neutron scattering techniques allows the simultaneous investigation of the microstructure and the transport properties, as first utilized by Hoffman [1] with a PVC latex in DOP. He established the connection

between an order-disorder transition and the variation of the transport properties. Ackerson found similar transitions in dilute dispersions [12]. Starting at high shear rates and going down to lower values he denoted the transition from a disordered structure into a sheared layer structure as transition I. Decreasing the shear rate further, a transition into a polycrystalline (disordered) structure occurs. Here the layered structure becomes unstable. He denoted this as transition II. In our interpretation the equilibrium state of a colloidal crystal is unstable against a shear perturbation and forms a disordered structure at a critical shear strain as discussed in Chapter 5. On increasing the shear rate, a shear induced order transition takes place (Chapter 6), which is similar to the transition II as denoted by Ackerson, but passed in the opposite direction. The transition I however is the instability, where the hexagonal planes disappear due to an acoustic resonance.

When the relaxation time of the suspension in the equilibrium colloidal crystal is large at high volume fractions and high Peclet numbers the non-equilibrium layered structure seems to be frozen when the perturbation starts with high shear rates as shown in an experiment carried out by Yan & Dhont [21].

The shear thickening as well as the shear melting transition in colloidal suspension has been the interest of a great number of authors. Before the work of Hoffman [1] shear thickening was considered as a rheological phenomenon and mainly treated in a phenomenological manner as summarized in the review article by Barnes [3].

Originally shear thickening was described as 'dilatancy', implying an increase of the volume under a continuous shear deformation. Note that although normal forces are neglected in the model presented here they are expected to occur, since the resonance appears in the shear gradient direction only.

Decreasing the absolute value of the surface charge and the concentration of the counter ions by varying the pH value, Laun [22] obtained the expected shift of the critical shear rate of dilatancy to lower values for decreasing repulsive forces (smaller elastic modulus) by investigating a concentrated polystyrene latex dispersion. In the same publication the temperature dependence of a suspension of polystyrene particles in diethyleneglycol/formamide has been studied. It was found that the critical shear

rate shifts to lower values for decreasing temperatures. A similar result has been obtained by Boersma et. al. [4] from a polystyrene in water/glycerol suspension. These results are in agreement with the model, since the increase of the viscosity with decreasing temperatures shifts according to equation (147) the critical shear rate to lower values. The critical shear stress is expected to be rather independent of the temperature according to Equation (149), because the elastic modulus varies only slightly with the temperature.

With the same argument we can understand the effect of solvents of different viscosity on shear thickening. Figure 11 of reference [3] and Figure 9 of [4] confirm Equation (149) that for equal elastic moduli the transition takes place at a constant stress.

The increase of the critical shear rate for decreasing particle sizes, as shown by Barnes [3], is partially due to the increase of the elastic modulus with decreasing particle diameter according to a decrease in the scaled Debye parameter κ in Equation (162). Also the liquid viscosities of the suspensions with larger particles are usually larger. Note that our model is developed under the assumption of monodisperse particles. A polydisperse distribution has been found experimentally to correspond with a less pronounced increase of the viscosity. In the approach here a possible explanation for this phenomenon is that the density variations become less well periodic in the sheared colloidal crystal and the resonance effects are reduced.

Chow & Zukoski [24] introduced a relation $\dot{\gamma}_C \sim G/\eta_0$ similar to (147). But they used the solvent viscosity η_0 instead of the suspension viscosity η . The latter assumption leads to a systematic deviation of the results for the critical shear rate from the volume fraction (see e.g. table IV of ref. [25]).

Experimental results on the system size dependence of the critical shear rate of shear thickening obtained by Chen & Zukoski [24] show that it is important especially at high volume fractions. They found that the critical shear rate decreases with decreasing system sizes. In our model the system size becomes limiting, when the corresponding wavelength k_{s,y_1} is greater than the wavelength k_0 of the dominant deformation wave of the sheared suspension. The experimentally found dependence can only occur when k_s is on the right side of the maximum of the $\dot{\gamma}_C(k)$ dependence

shown in Figure 21. However the experimental investigations by Chen & Zukoski [24] show that the critical shear rate is independent of the system size for practical systems ($> 1\text{mm}$).

Comparison with Other Models

Other explanations for shear thickening in colloidal suspensions have been given by Hoffman [26], Ackerson & Clark [2] and Boersma et. al. [18]. The basic idea of Hoffman is that a shear stress couple acting on a doublet of particles in a sheared crystal is the reason for the instability. Recall that when shear is applied to a suspension, shear induces a transition to a layered structure, which means that the flow field stabilizes this layered hcp structure [28]. Thus the shear stress stabilizes the ordered structure and from considering particles in one hcp-layer only, an instability cannot be derived. In the model presented here the reason for the instability comes from the periodic modulation of the modulus in the flow gradient direction, leading to a resonance between the modulation frequency and the eigen frequency of propagating acoustic shear waves.

An increase of the local oscillations coming from the acoustic resonance can lead to a structural transition with a formation of clusters (flow blockage), when the forces acting on a colloidal particle are of the order of the repulsive stabilization as assumed by Boersma et. al. In this case the critical shear rate of shear thickening is ruled by Boersma's equation [4],[29] with the critical shear rate

$$\dot{\gamma}_c = \frac{2\pi\epsilon_0\epsilon_r\Psi_0^2\kappa h}{6\pi\eta_0 a^2} \quad (167)$$

Note that the acoustic resonance can be expected to cause an instability even in very dilute suspensions accompanied by a global disordering and an alteration of the dynamic properties. Such phenomena have been observed by Lindsay & Chaikin [11]. The attempt by Chow & Zukoski [25] to expand Boersma's approach to dilute suspensions, by creating a maximum of the critical shear rates at a specific volume

fraction Φ_{\max} , evolves in the model presented here in a natural way (Fig. 22).

6.4 Conclusions

The model presented here explains shear thickening of sheared colloidal suspensions as the occurrence of an acoustic resonance. The resonance is the result of the periodic modulation of the elastic modulus in a shear colloidal crystal structure. Applying the hydrodynamic equation of the colloidal suspension the critical shear rate, where a maximum in the viscosity occurs, can be derived. A good agreement with experimental results for high critical shear rates could be found. For low critical shear rates the used approximations have to be improved.

Appendix E

In order to solve Equation (143) we introduce the standard Laplace transform $A(s) = L(A)$:

$$A(s) = \int_0^{\infty} A(t) e^{-st} dt \quad (\text{E.1})$$

and the reverse transform

$$A(t) = \frac{1}{2\pi j} \int_{\delta s - j\infty}^{\delta s + j\infty} A(s) e^{st} ds \quad (\text{E.2})$$

where δs is a positive constant.

Choosing the initial conditions as

$$A^{(1)}(t=0) = \dot{A}^{(1)}(t=0) = 0 \quad (\text{E.3})$$

the Laplace transform of Equation (143) becomes

$$A^{(1)}(s) = \frac{c^2 k^2 A^{(0)}}{s^2 - bk^2 s + c^2 k^2} \left[\frac{s + p_1}{(s + p_1)^2 + \dot{\gamma}^2} + \frac{s + p_2}{(s + p_2)^2 + \dot{\gamma}^2} \right] \quad (\text{E.4})$$

where we used the relation

$$L(e^{-pt}\cos(\omega t)) = \frac{s+p}{(s+p)^2 + \omega^2} \tag{E.5}$$

The reverse Laplace transform of (E.4) contains the sum of all residua s_i of $A^{(1)}(s_i)$ with $\text{Re}(s_i) < 0$. The poles s_i of $A^{(1)}(s_i)$ are at

$$\begin{aligned} s_1 &= -p_1 - j\dot{\gamma} \\ s_2 &= -p_1 + j\dot{\gamma} \\ s_3 &= -p_2 - j\dot{\gamma} \\ s_4 &= -p_2 + j\dot{\gamma} \end{aligned} \tag{E.6}$$

The reverse Laplace transform of (E.4) has thus the form

$$A^{(1)}(t) = c^2 k^2 A^{(0)} \sum_{i=1}^4 [A^{(1)}(s_i)(s+s_i)e^{st}]_{s=s_i} \tag{E.7}$$

Using (E.4) and (E.6) in (E.7) we obtain the time dependent first order amplitude

$$A^{(1)}(t) = c^2 k^2 A^{(0)} \left[\frac{e^{-p_1 t}((p_1 - p_2)\cos(\dot{\gamma}t) - \dot{\gamma}\sin(\dot{\gamma}t))}{p_1(\dot{\gamma}^2 + (p_1 - p_2)^2)} - \frac{e^{-p_2 t}((p_1 - p_2)\cos(\dot{\gamma}t) + \dot{\gamma}\sin(\dot{\gamma}t))}{p_2(\dot{\gamma}^2 + (p_1 - p_2)^2)} \right] \tag{E.8}$$

In the case of damped propagating waves p_1 and p_2 are given by (141) and the amplitude turns into

$$A^{(1)}(t) = \frac{2A^{(0)}c^2k^2e^{-\delta t}}{(\delta^2 + \omega^2)(\dot{\gamma}^2 - 4\omega^2)} [2\omega\cos(\dot{\gamma}t)(\omega\cos(\omega t) + \delta\sin(\omega t)) - \dot{\gamma}\sin(\dot{\gamma}t)(\delta\cos(\omega t) - \omega\sin(\omega t))] \tag{E.9}$$

Literature

- [1]
Hoffman, R. L." Discontinuous and dilatant viscosity behaviour in concentrated suspensions" *Trans. Soc. Rheol.* **16**, 155-173 (1972).
- [2]
Ackerson, B.J. and Clark, N.A." Shear-induced melting" *Phys. Rev. Lett.* **46**, 123-126 (1981).
- [3]
Barnes, H.A., " Shear-thickening ('dilatancy') in suspensions of nonaggregating solid particles dispersed in newtonian liquids" *J. Rheol.* **33**, 329-366 (1989).
- [4]
Boersma, W. H., J. Laven and H.N. Stein, " Shear thickening (dilatancy) in concentrated dispersions" *AIChE J.* **36**, 321-332 (1990).
- [5]
Joanny, J.F., " Acoustic shear waves in colloidal crystals," *J. Colloid Interface Sci.* **71** 622-623 (1979).
- [6]
Pieranski, P.," Colloidal Crystals," *Contemp. Phys.* **24**, 25-73 (1983).
- [7]
Harrowell, P. and M. Fixman, "The shear melting of colloidal crystals: a long wavelength driven transition," *J. Chem. Phys.* **87**, 4154-4161 (1987).
- [8]
Lindeman F. A., "Über die Berechnung Molecularer Eigenfrequenzen, " *Z. Phys.* **11**, 609-612 (1910).
- [9]
Ronis, D. and S. Khan, "Stability and fluctuations in sheared colloidal crystals," *Phys. Rev. A* **41**, 6813- 6829 (1990).
- [10]
Harden, J.L., H.Pleiner and P.A. Pincus, "Hydrodynamic surface modes in concentrated polymer solutions and gels," *J. Chem. Phys.* **94**, 5208-5221 (1991).

[11]

Lindsay, H.M. and P.M. Chaikin, "Shear elasticity and viscosity in colloidal crystals and liquids," *J. de Physique C3*, 269-280 (1985).

[12]

Ackerson, B.J. and N.A. Clark, "Sheared colloidal suspensions," *Physica 118 A* 221-249 (1983).

[13]

Campbell, G.A. and G. Forgacs, "Viscosity of concentrated suspensions: an approach based on percolation theory," *Phys. Rev. A* 41 4570-4573 (1990).

[14]

Mc Lachlan, N.W., *Theory and Application of Mathieu Functions* (Dover, New York, 1964).

[15]

Landau, L.D. and E.M Lifshitz., *Mechanics* (Pergamon Press, Oxford, 1964) Vol.1.

[16]

Hoffman, R.L., "Discontinuous and dilatant viscosity behaviour in concentrated suspensions III," *Adv. Colloid Interface Sci.* 17, 161- 184 (1982).

[17]

Buscall, R., J.W. Goodwin, M.W. Hawkins and R.H. Ottewill, "Viscoelastic properties of concentrated latices," *J. Chem. Soc. Faraday Trans. 1* 78, 2873-2887 (1982).

[18]

Boersma, W.H., " Shear Thickening of Concentrated Dispersions," Ph.D. Thesis, Eindhoven University of Technology, 1990.

[19]

Verwey, E.J.W. and T.Th. Overbeek, *Theory of Lyophobic Colloids* (Elsevier, Amsterdam 1948).

[20]

W.B. Russel, D.A. Saville and W.R. Schowalter, *Colloidal dispersions* (Cambridge University, Cambridge, 1989) Equation 4.10.13.

[21]

Yan Y.D. and K.G. Dhont, "Shear-induced structure distortion in non-aqueous dispersions of charged colloidal spheres via light scattering," *Physica A* **198** 78-107 (1993).

[22]

Laun, H.M., "Rheology and particle structures of concentrated polymer dispersions," in *Xth International Congress on Rheology Sydney 1988*, edited by P.H.T.Uhlkerr (Academic, New York, 1988), pp. 37-42

[23]

Barnes, H.A., J.F. Hutton and K. Walters, *An Introduction to Rheology* (Elsevier Science Publishers B.V. 1989).

[24]

Chow, M.K. and C.F. Zukoski, "Gap size and shear history dependencies in shear thickening of a suspension ordered at rest," *J. Rheol.* **39**, 15-32 (1995).

[25]

Chow, M.K. and C.F. Zukoski, "Non-equilibrium behaviour of dense suspensions of uniform particles: volume fraction and size dependence of rheology and microstructure," *J. Rheol.* **39**, 33-59 (1995).

[26]

Hoffman, R.L. "Discontinuous and dilatant viscosity behavior in concentrated suspensions II," *J. Colloid Interface Sci.* **46**, 491-506 (1974).

[27]

Boersma, W. H., P.J.M. Baets, J. Laven and H.N. Stein, "Time-dependent behavior and wall slip in concentrated shear thickening dispersions," *J. Rheol.* **35**, 1093-1120 (1991).

[28]

Loose, W., and S. Hess, "Rheology of dense model fluids via nonequilibrium molecular dynamics: shear thinning and ordering transition" *Rheol. Acta* **28**, 91-101 (1989).

[29]

Boersma W. H., J. Laven, H.N. Stein, "Computer Simulations of Shear Thickening of Concentrated Dispersions" *J. Rheol.* **39**, 841-860 (1995).

CHAPTER III.

EXPERIMENT

7. Rheology and Rheo-optics of Concentrated Colloidal Suspensions

7.1 Introduction

In order to facilitate the interpretation of experimental data, this paper starts with summarizing a number of theoretical findings. Colloidal suspensions have, depending on the inter-particle interaction and the volume fraction of the dispersed particles, a colloidal crystal, fluid or liquid (flocculated) structure (Chapter 3). In chapter 4 we discussed the mutual influence of structural phase transitions and rheological properties of colloidal suspensions. The model presented there concerns the stability of colloidal crystals formed as an equilibrium phase in concentrated soft sphere colloidal suspensions. The underlying assumption is that a colloidal crystal may become unstable under the action of a static shear strain. This assumption is also based on theoretical [1] and experimental [2],[3] evidence. This effect has been interpreted (Chapter 5) as a shear induced phase transition and the qualitative behaviour of the dynamic rheological properties was derived.

To test the applicability of that model dynamic shear measurements were performed on three different systems of colloidal suspensions. Additionally rheo-optical investigations on one of the suspensions were made to confirm the idea that a shear strain can destroy a colloidal crystal. Therefore static light scattering was applied to determine the microscopic structure of a strained concentrated suspension.

The model in Chapter 5 is not applicable under steady shear conditions. Therefore another theoretical model has been developed in Chapter 6, that predicts the occurrence of shear thickening under steady shear. The latter model is based on the idea that a sheared colloidal suspension forms a layered structure, in which the periodic modulation of the elastic modulus induces an acoustic resonance. This effect will lead to an increase of the

dissipation and therefore to a viscosity increase (shear thickening). The model predicts the shear rate, at which the maximum of the viscosity can be found, denoted in this paper as the critical shear rate (which is not related to critical effects close to a phase transition). Steady-state shear measurements were performed on concentrated colloidal suspensions to compare the model predictions of the critical shear rate with the experiments.

7.2. Experimental

Materials

Rheological measurements were performed on suspensions of

- Polymethylmethacrylate (PMMA) particles in silicon oil
- Polyvinylchloride (PVC) particles in dioctylphthalate (DOP)
- Glass particles in a glycerol/water (86.1/13.9 m/m) mixture

The silicon oil was obtained from Aldrich Chemical Co. Ltd. with a density $\rho = 1050 \text{ kg/m}^3$ and a viscosity $\eta = 0.15 \text{ Pa.s}$. Dioctylphthalate (DOP) (Fluka AG) was used as supplied. The density is $\rho = 985 \text{ kg/m}^3$ and the viscosity is $\eta = 0.054 \text{ Pa.s}$. Glycerol (Merk, reinst) was used as supplied. It was mixed with twice-distilled water yielding a 86.1/13.9 mass/mass mixture with a density of 1224 kg/m^3 and a viscosity of 0.14 Pa.s . All values are obtained at constant temperature $T = 293 \text{ K}$.

Dispersion samples were prepared by mixing by hand while adding the particles to the liquid until the correct volume fraction Φ was reached. Then the samples were stirred mechanically until no separate aggregates could be seen by eye. The characteristic properties of the suspensions are summarized in Table 7.1.

Table 7.1 Characteristics of the suspensions.

	particle density in kg/m^3	particle diameter in μm	ζ -potential in mV	salt concentration in mol/m^3
PMMA/ Silicon Oil	1190	0.16 ± 0.06	-35 ± 10	
PVC/DOP	1390	1.25 ± 0.08	-90 ± 10	0.01
Glass/Glycero l/Water	2530	2.4 ± 1.2	-75 ± 10	0.05

The particle sizes were determined with a Coulter Counter ZM 256, ζ -potentials were measured with a Malvern Zetasizer 3, all densities were measured with a pycnometer and the conductivities were measured with a Philips PW 9505 conductivity tester. The concentration of electrolyte in the liquid was estimated by comparison of the conductivity of the supernatant of a suspension with conductivities of solutions of KCl with known concentrations.

The PMMA particles were obtained from Röhm GmbH as an aqueous dispersion. They were dried and redispersed in silicon oil. The PVC particles were supplied by Hoffman [4],[6] (prepared by standard emulsion polymerization procedures and dried). We dispersed them in DOP. Note that experimental investigations by Görnitz & Zecha [7] indicate that the stabilization of the particles in PVC/DOP suspensions are not only determined by electrostatic forces but by steric interactions as well. In addition they found that the PVC particles can change their size due to the DOP.

Glass particles were obtained from Potters Ballotini (soda lime glass). They were washed twice with concentrated nitric acid and then washed with twice distilled water until the pH became constant at 8.3. Washing was performed by centrifugation, decanting the

liquid and resuspending the solid in a fresh liquid. After washing, the particles were dried in a vacuum oven at 423 K.

The PVC/DOP suspension employed here ($\Phi=0.57$) has been chosen for the rheo-optical study, because the rheological measurements indicate the presence of a colloidal crystal at small strains. Additionally the refractive index of the PVC particles ($n=1.54$) and of the DOP ($n=1.486$) are close to each other and the size of the particles are of the order of the wavelength of the light employed.

Equipment

Rheological Equipment

Rheological measurements were carried out with a Weissenberg Rheogoniometer (TA Instruments) and a Rheometrics RFS 130. Cone and plate geometries (4°) were applied with a diameter of 2 cm and 4 cm respectively. After the measuring system was filled the gap was set, while applying a small oscillation (0.01 rad, 0.1 rad/s) on the plate for about 5 min. With this standard procedure the equilibration of the suspension is expected to be accelerated (see below)-leading to a reproducible starting point of all measurements. The measurements were performed at room temperature (295 K). The rheometer was able to automatically carry out dynamic as well as steady state measurement procedures. The dynamic procedures are frequency sweeps (varying frequency at constant strain) and amplitude sweeps (varying strain amplitudes at constant frequency) while the time dependence of the input and output signal could be monitored (time dependence). The strain amplitude could be increased or decreased in steps, denoted as 'up' and 'down' measurements respectively.

Dynamic and steady state experiments were carried out on three quite different systems of colloidal suspensions.

Rheo-optical Setup

The geometries for studying the rheology of high volume fraction dispersions are plate-plate,

cone-plate, concentric cylinder (Couette) and a tapered Couette geometry [5]. A cone-plate geometry has the disadvantage that a slight mismatch of the refractive indices between the suspension and the cone leads to the occurrence of a second beam. In a coaxial cylinder geometry the path length of the light beam through the sample is fixed but we preferred an adjustable path length. Although a tapered Couette geometry may fulfil this condition, we have chosen the design of a plate-plate geometry because the construction was more simple, despite the occurrence of a radius dependent deformation.

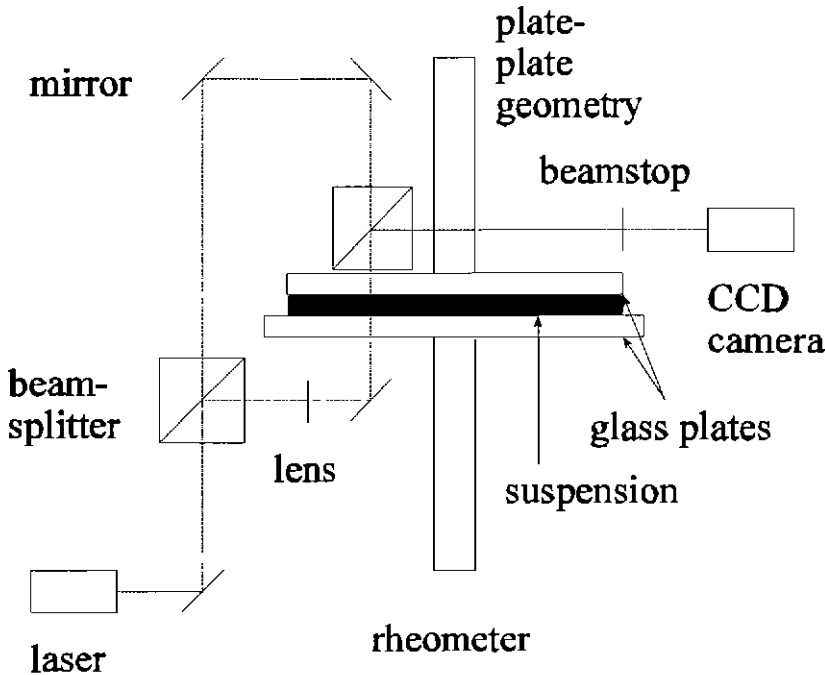


Figure 25 Plate-plate rheo-optical setup.

In order to prevent shear force driven diffusion of particles that may lead to changes in local volume fractions [9], we only applied a few droplets of suspension. The gap was only filled near the optical beam, so as to assure that the strain amplitude variation over the sample did not vary by more than 15% and the rest of the gap was empty. The simultaneously obtained rheological signal is not quantitatively correct any more, but only indicative [10]. We used the Weissenberg (TA Instruments) rheometer to obtain rheological data of quantitative

accuracy.

An experimental setup was built and mounted on a Sangamo R18 Weissenberg Rheogoniometer R18, to determine simultaneously the rheological properties and the diffraction pattern of a colloidal suspension. The setup is shown in Figure 25. A colloidal suspension was introduced between two glass plates ($n = 1.5168$) mounted on a Sangamo Weissenberg Rheogoniometer. The light source was a 10 mW He-Ne-laser (Lambda Physics) with a wave length of 632.8 nm. The laser beam has its focus between the two glass plates and is adjusted by a system of mirrors and beam splitters on a suitable position between the glass plates. Note that it is possible to operate in forward as well as in back scattering. A diffraction pattern appears at the air-glass interface, which acts as a screen. This pattern has been observed by means of a beam splitter and a CCD-camera (HCS Vision MX5 with 630×490 pixel). The incident beam was directed perpendicular to the glass plates, adjusted by aligning the reflections of all parts of the optical system. The incident beam was dimmed by a beam stop in front of the camera. A digital picture obtained by the camera was sent to a frame grabber (Datacube Maxvision AT-1), working with a frequency of 25 Hz per frame and having 3 image stores with $512 \times 512 \times 8$ bit. It was possible to apply real time transformations on the picture (e.g. convolution). The chosen standard measurement procedure was to average over 12 pictures (temporal filter).

After the rheometer was filled the gap was adjusted while a small periodic oscillation was applied (0.1 rad, 0.252 rad/s, 5 min), with a gap of $10 \mu\text{m}$. During this procedure Bragg peaks appeared indicating a colloidal crystal with a preferential orientation.

7.4. Results

Rheological Measurements

(i) glass in glycerol/water

We will first consider a glass/glycerol/water suspension ($\Phi = 0.58$). In Figure 26 the dependence of the storage modulus G' and the phase angle on the applied shear strain

as obtained with the RFS 130 is shown. The colloidal suspension is rather viscous for small strains showing a high phase angle, and a relatively small elastic modulus. The phase angle decreases with increasing shear strains, while the elastic modulus increases, indicating a progressively elastic character.

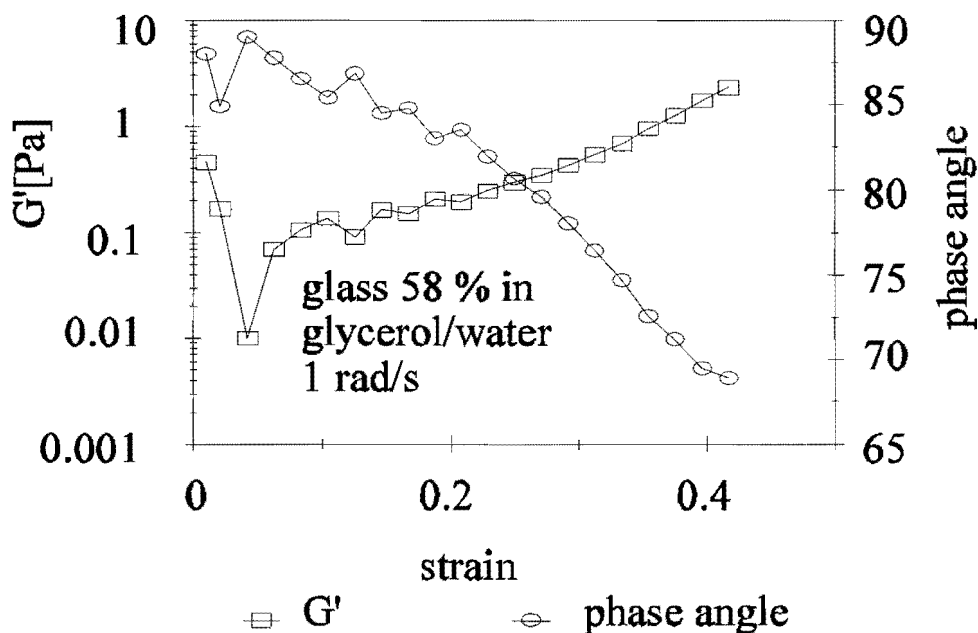


Figure 26 The storage modulus and the phase angle for increasing strains of a glass/glycerol/water suspension ($\Phi=0.58$) at 1 rad/s.

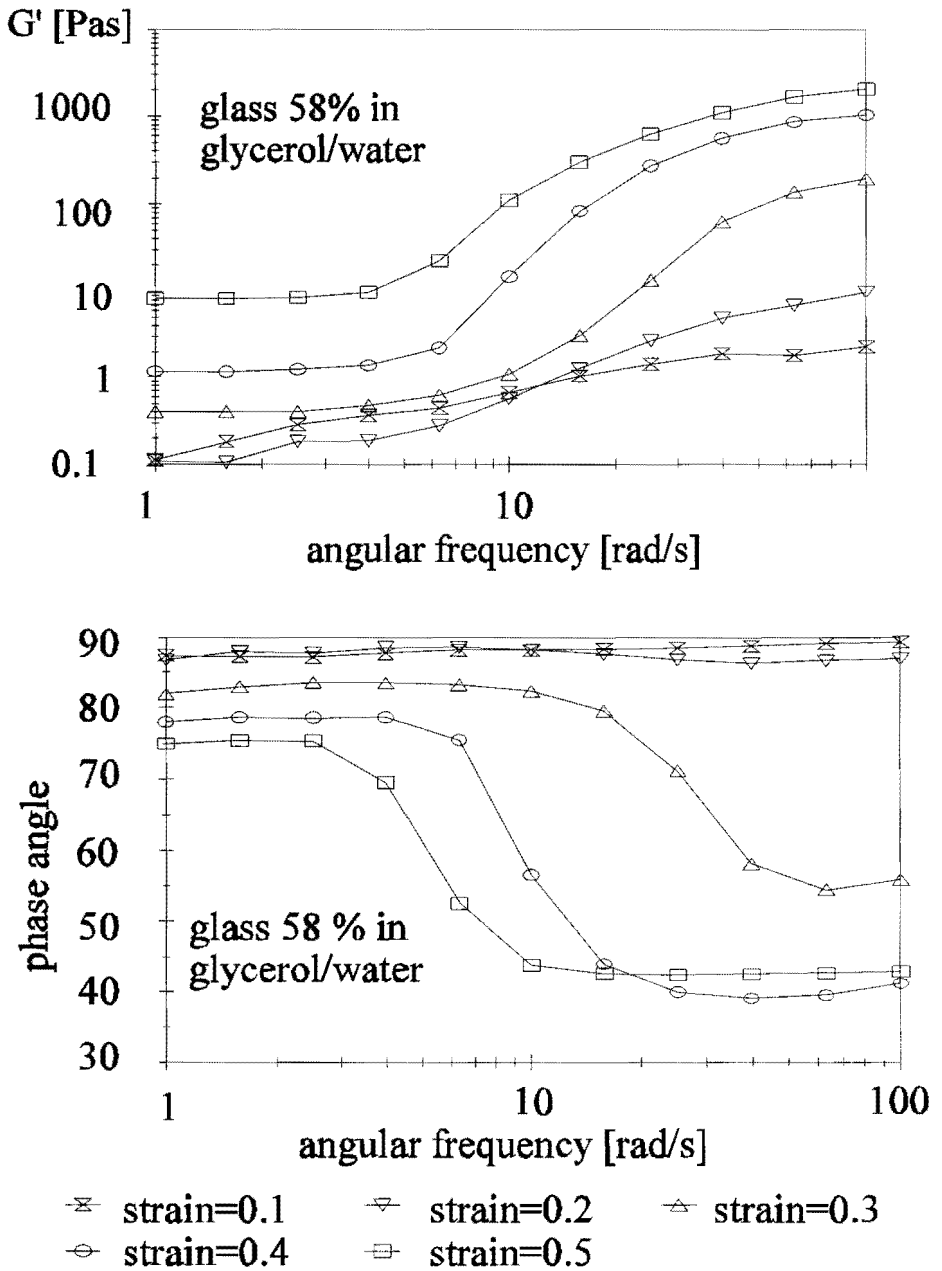


Figure 27 The storage modulus and the phase angle as a function of the frequency for varying values of the strain amplitude of a glass/glycerol/water suspension ($\Phi = 0.58$).

The frequency dependence of the rheological properties for various values as a function of the applied strain was investigated and summarized in Figure 27. The storage modulus and the phase angle are displayed, while the oscillatory strain amplitude was varied from 0.1 to 0.5. For shortness sake the oscillatory strain amplitude will be indicated as strain. The experimental results indicate that for small frequencies the suspension has viscous properties with a high phase angle and a low elastic modulus. At increasing frequencies the suspension behaves more elastically, with an increasing elastic modulus and a decreasing phase angle. The elastic properties are more pronounced for higher shear strains, as expected from the strain dependence.

The dependence of the viscosity on the shear rate is shown in Figure 28. After a slight decrease in the viscosity for small shear rates the suspension shows a pronounced shear thickening behaviour and reaches a maximum in the viscosity at about 10 s^{-1} .

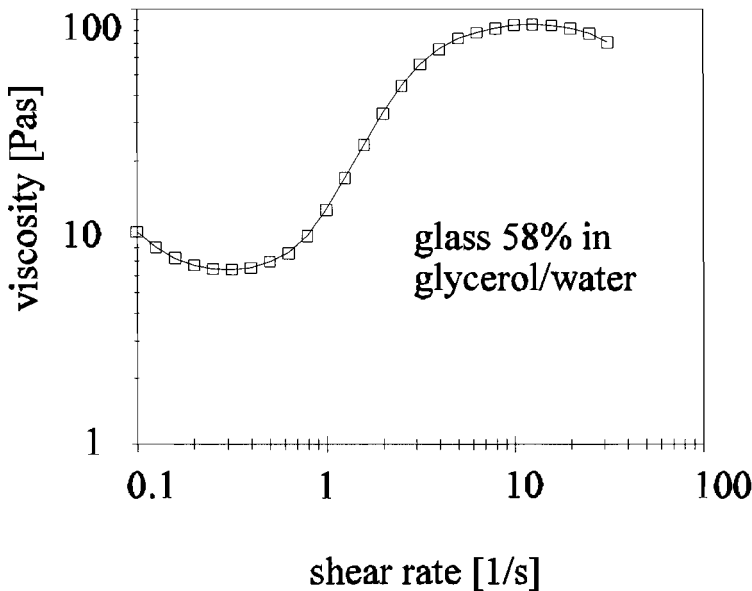


Figure 28 The steady state viscosity of a glass/glycerol/water suspension ($\Phi=0.58$) as a function of the shear rate.

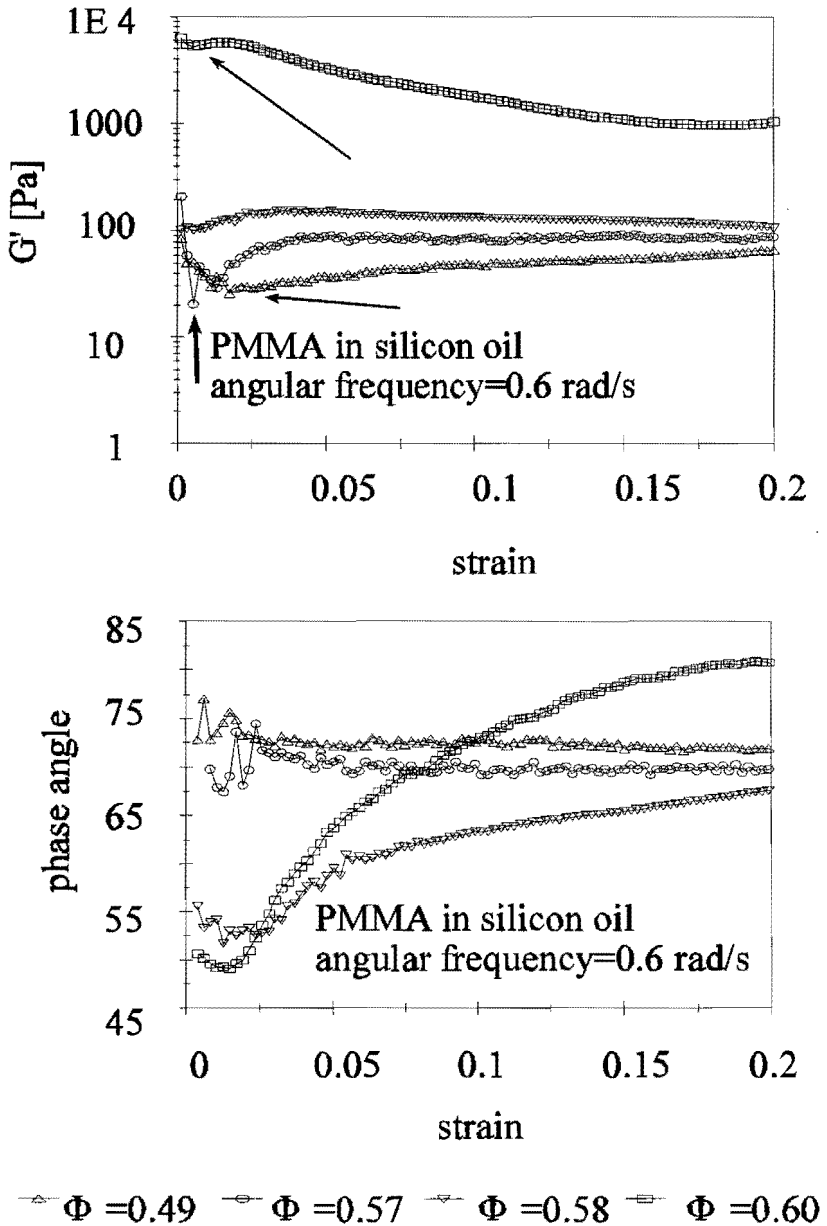


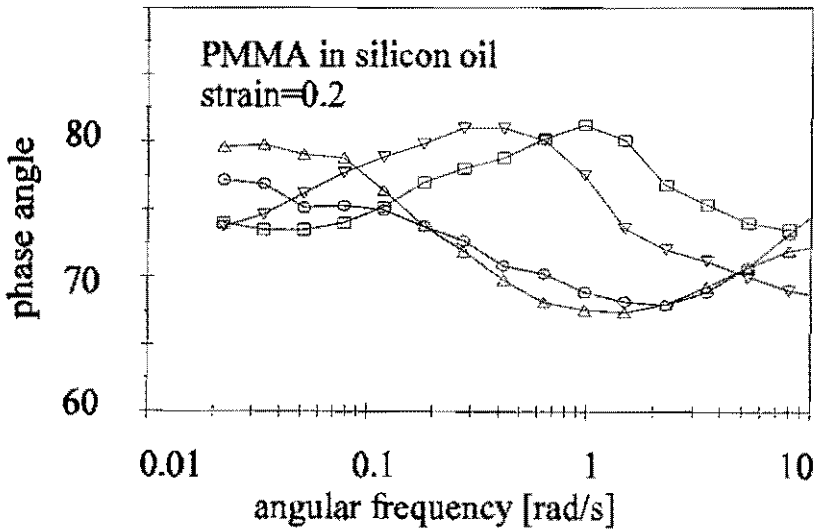
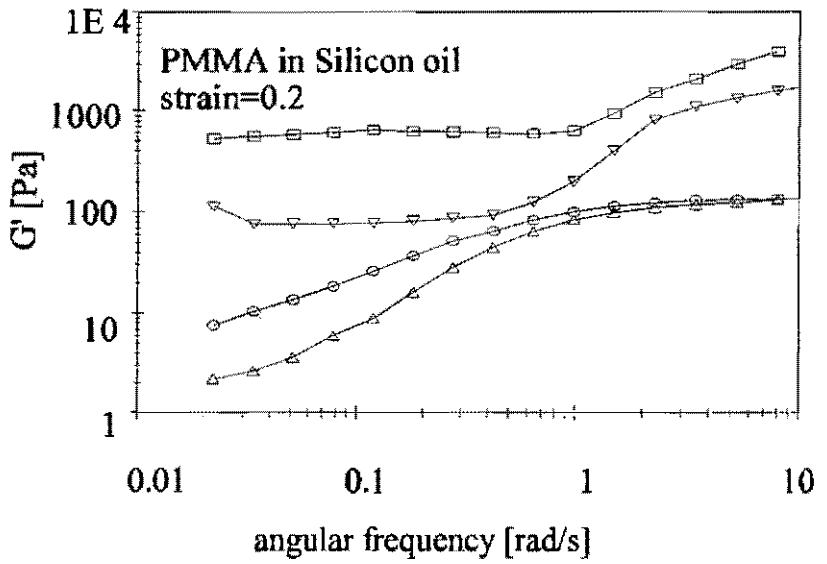
Figure 29 The storage modulus and the phase angle as a function of the strain at a constant angular frequency of 0.1 Hz for PMMA/Silicon Oil suspensions at four volume fractions. The arrows indicate the position of the minima.

(ii) PMMA in silicon oil

The dependence of the storage modulus G' and the phase angle δ on the applied shear strain has been investigated with PMMA/silicon oil suspensions for a number of different volume fractions (Figure 29). The dynamic shear properties were measured while decreasing the amplitude starting at a strain = 0.2, using a constant angular frequency of 0.1 rad/s.

The value of the storage modulus decreases with decreasing volume fraction. On varying the applied strain a minimum in the storage modulus has been found, that is indicated by arrows in Figure 29. It shifts to higher strain values and seems to broaden with decreasing volume fraction. The $\Phi = 0.60$ system also has a second minimum at a much larger strain. The phase angle decreases with increasing volume fraction at small strain values. However with increasing strain this trend becomes less pronounced. After a slight decrease, the phase angle increases with the strain at high volume fractions.

In Figure 30 the frequency dependencies of the PMMA/silicon oil suspensions at four volume fractions are shown for a strain of 0.2. The elastic moduli increase with increasing angular frequency and volume fraction. A maximum of the phase angle has been detected, which shifts to values of higher frequencies for increasing volume fractions.



$\Phi = 0.49$
 $\Phi = 0.57$
 $\Phi = 0.58$
 $\Phi = 0.60$

Figure 30 The storage modulus and the phase angle as a function of the angular frequency for various PMMA/silicon oil suspensions at a constant strain.

(iii) PVC in DOP

The evolution of the stress response to a sinusoidal strain was investigated for the PVC in DOP suspension with a volume fraction of 57%. The result is displayed in Figure 31 for four different values of the relative shear amplitude, which is defined as the ratio of the actual amplitude U_0 and the critical amplitude $U_0^{(c)}$ ($U_0^{(c)}=0.8$ with this sample, as assessed from Fig.32). At a relative amplitude > 1 the output signal becomes very complex, but shows a qualitatively similar dependence as the calculated inharmonic signal in Figure 20.

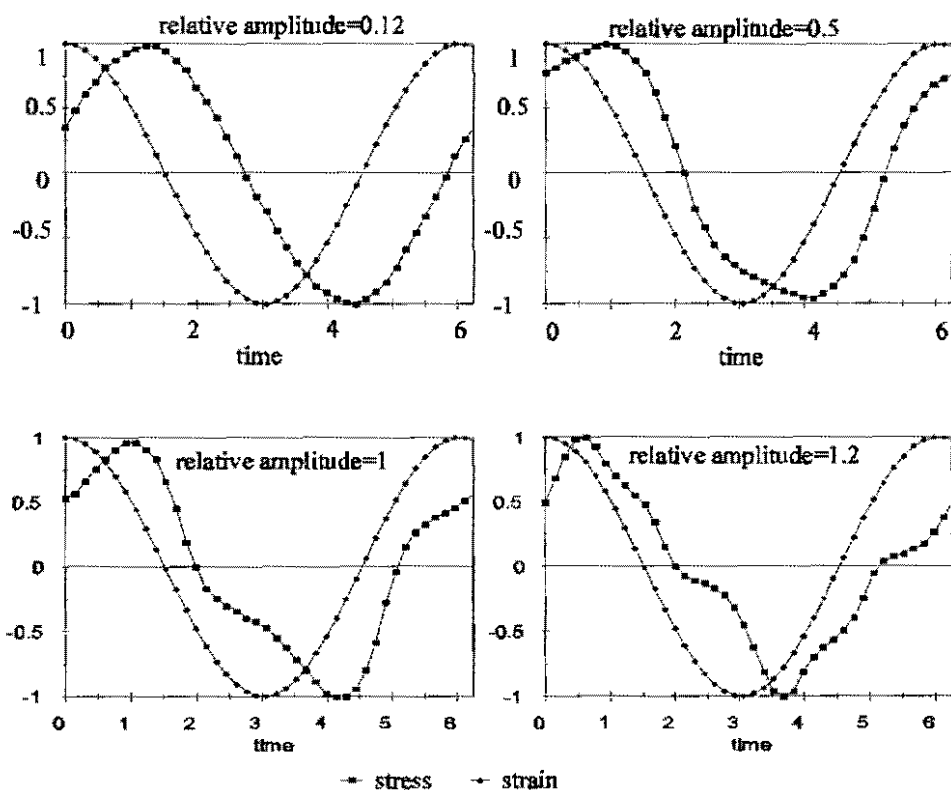


Figure 31 The stress response (squares) of a PVC/DOP suspension on a harmonic strain (circles) for four different relative amplitudes.

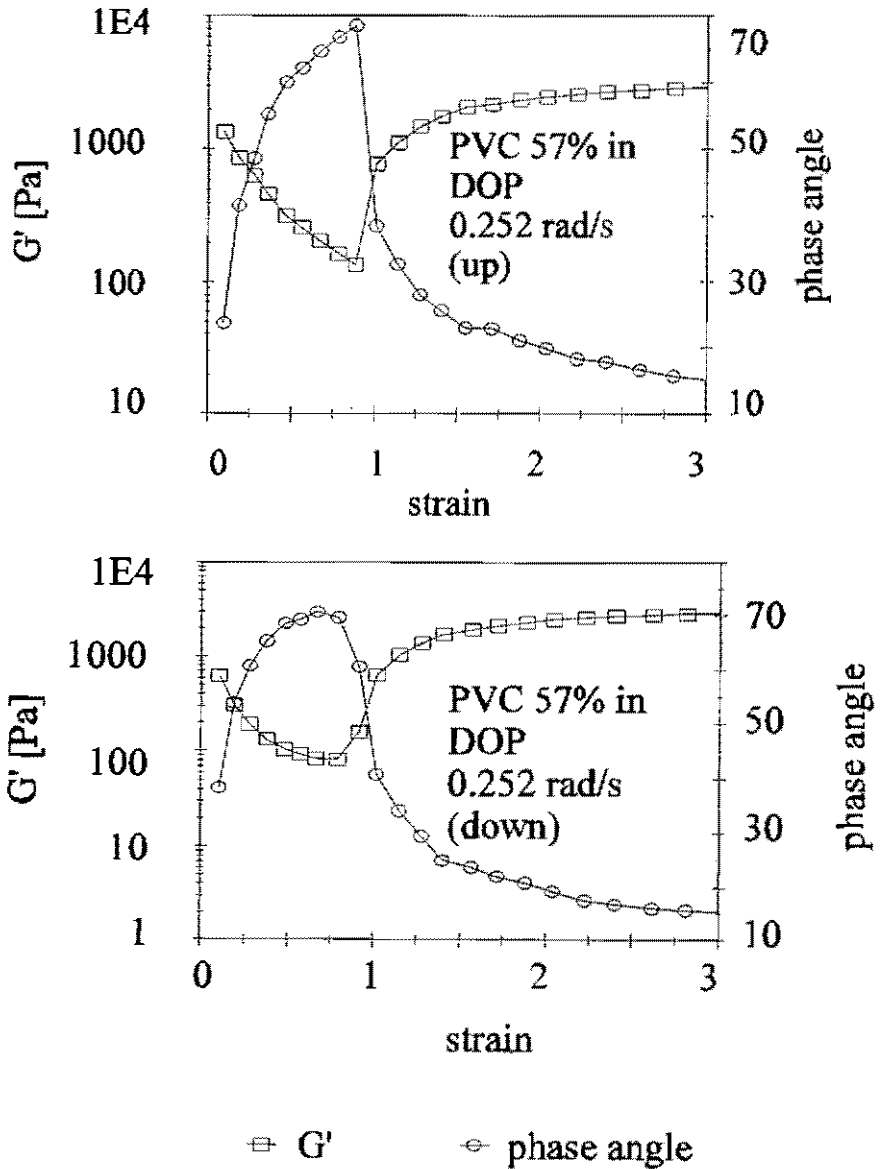


Figure 32 The elastic modulus and the phase angle for increasing (up) and decreasing (down) strains of an PVC/DOP suspension ($\Phi=0.57$).

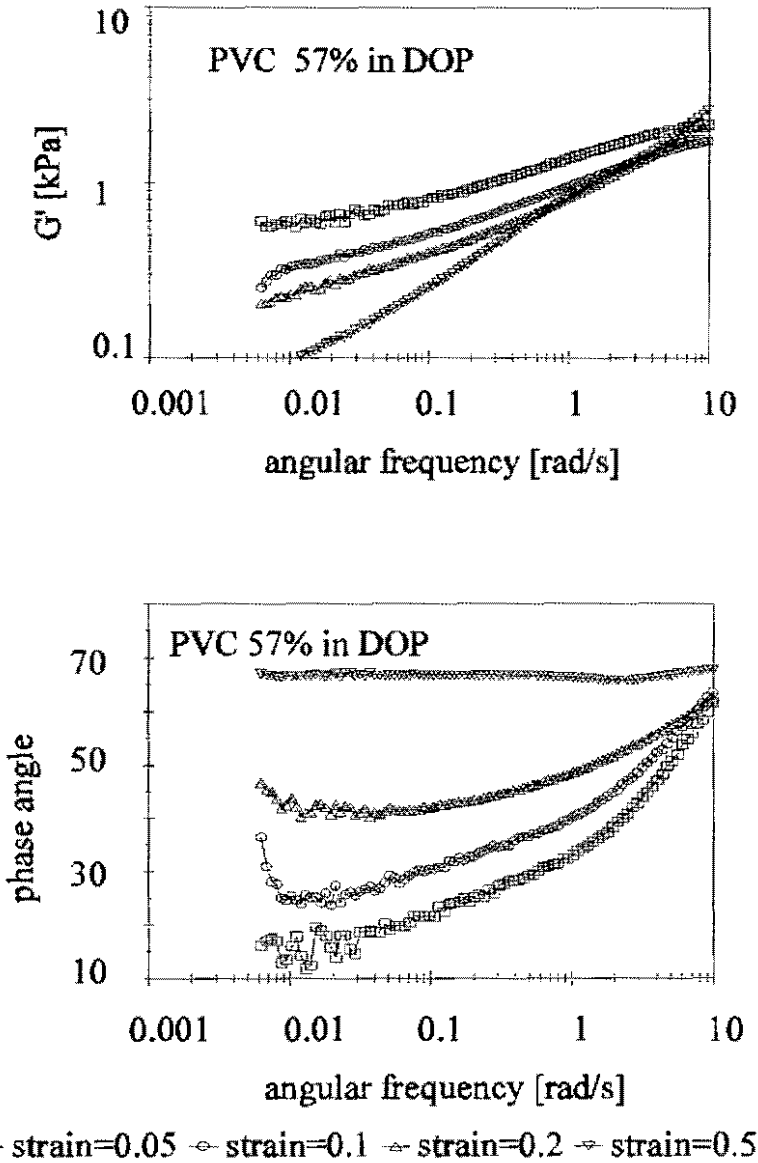


Figure 33 The storage modulus and the phase angle of a PVC/DOP suspension as a function of the frequency for different values of the strain amplitude.

The dynamic rheological behaviour of a PVC/DOP suspension ($\Phi=0.57$) is shown in Figure 32 for increasing (up) and decreasing (down) strains. A very pronounced minimum in the storage modulus and a maximum in the phase angle were found. The minimum in G' is slightly broader for decreasing strains as compared to increasing strains.

In Figure 33 the frequency dependence of the dynamic properties of the PVC/DOP suspension is presented for the lower strains ($U_0 < 0.5$). The storage modulus G' decreases with increasing strain, and increases with increasing angular frequency. The phase angle behaves differently in that it increase with increasing strain. The differences due to strain seem to disappear at high frequencies.

The dependence of the viscosity on the shear rate is given in Figure 34. After a gradual decrease for small shear rates the viscosity shows a pronounced increase with increasing shear rate. The viscosity has a maximum at a shear rate of 6 s^{-1} .

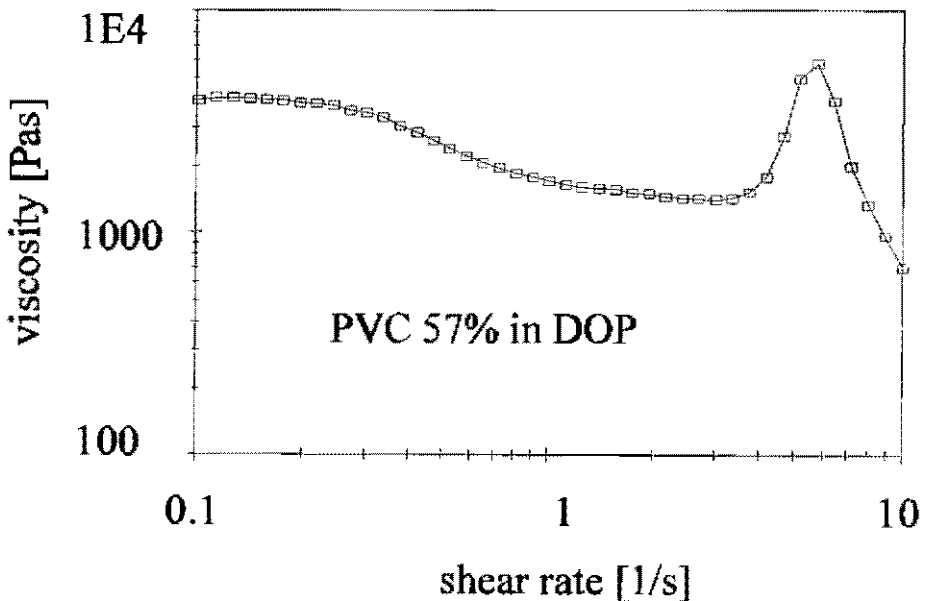


Figure 34 The shear rate dependent viscosity of a PVC/DOP suspension ($\Phi = 0.57$).

Rheo-optical Measurements

From the rheological measurements we expected a pronounced shear induced transition in the PVC/DOP suspension ($\Phi = 0.57$). This suspension was analyzed in more detail using the rheo-optical setup. Both the rheological parameters and the optical diffraction patterns were analyzed, while applying various constant strains going from small to large deformations ("up") and back again ("down").

A number of representative diffraction patterns for the various applied shear strains are presented in Figure 34. On increasing the strain essentially the same sequence of pictures was found in the reverse order. The patterns F-A were taken while stepwise decreasing the strain amplitude. The corresponding rheological properties are shown in Figure 35. The patterns were taken perpendicular to the glass plates in the shear gradient direction, while the shear oscillation movements were from left to right and vice versa. Note that these pictures are integrations of the whole oscillation period, thus an average of all deformations.

The diffraction patterns A, B and C are taken at small applied shear strains. They consist of Bragg peaks arranged in two circles around the central beam that is dimmed by a beam stop. The first order Bragg peaks form a hexagonal arrangement with a background Debye ring, indicating an imperfect periodic lattice formed by the colloidal particles. The Bragg peaks of the second order ring are partially smeared out and it is therefore difficult to pinpoint their location.

The experimental results indicate that an oriented colloidal crystal was formed during the filling procedure. On increasing the strain the Bragg peaks and thus the colloidal crystal disappear as can be seen on the pattern D, E and F. In the transition region however (pattern D and E) the colloidal particles form an intermediate structure which suggests the arrangement of chains of colloidal particles that form an optical grid in the flow direction [3]. This is reflected in two bright Bragg peaks in the upper and lower part of the scattering pattern.

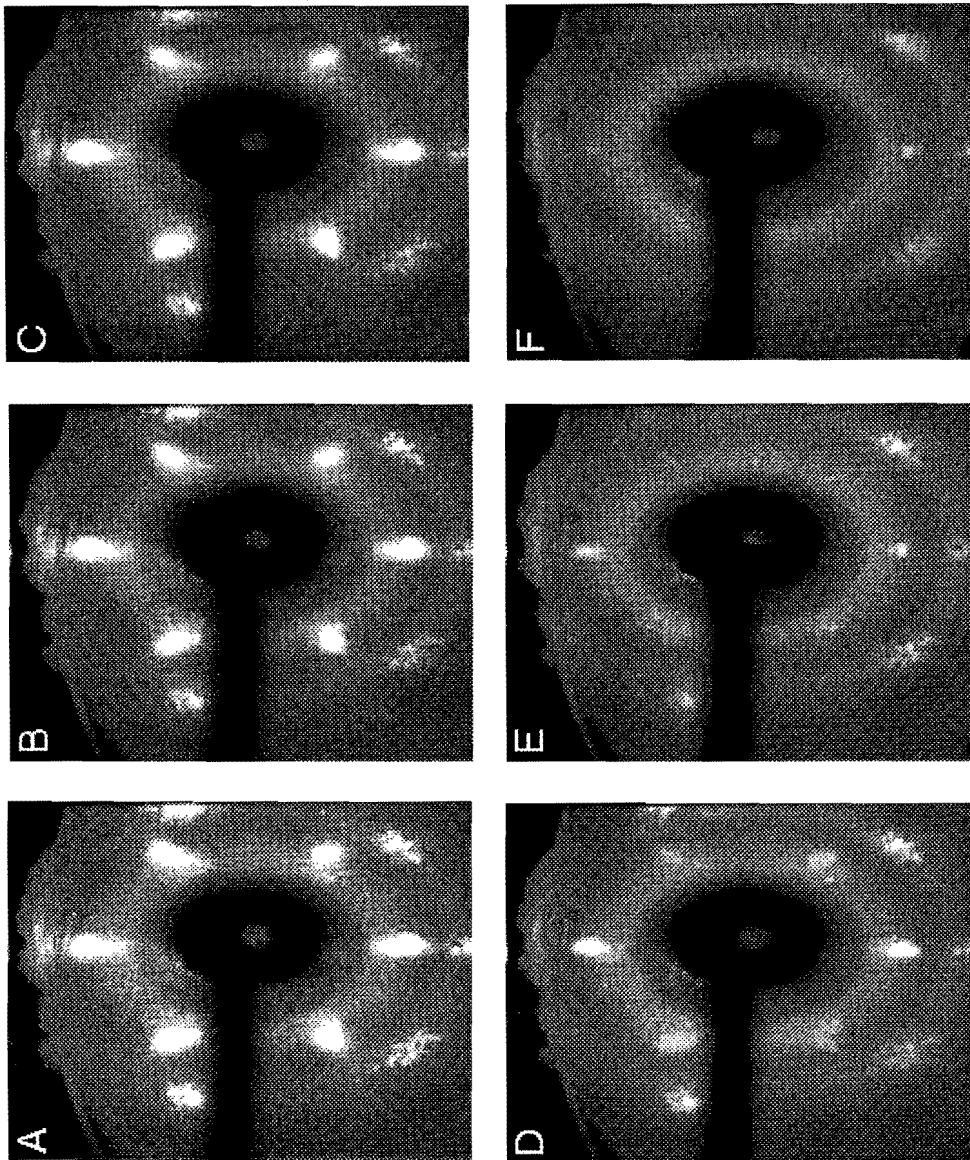


Figure 35 Rheo-optical scattered patterns for a number of different strains as indicated by the capitals in Figure 36.

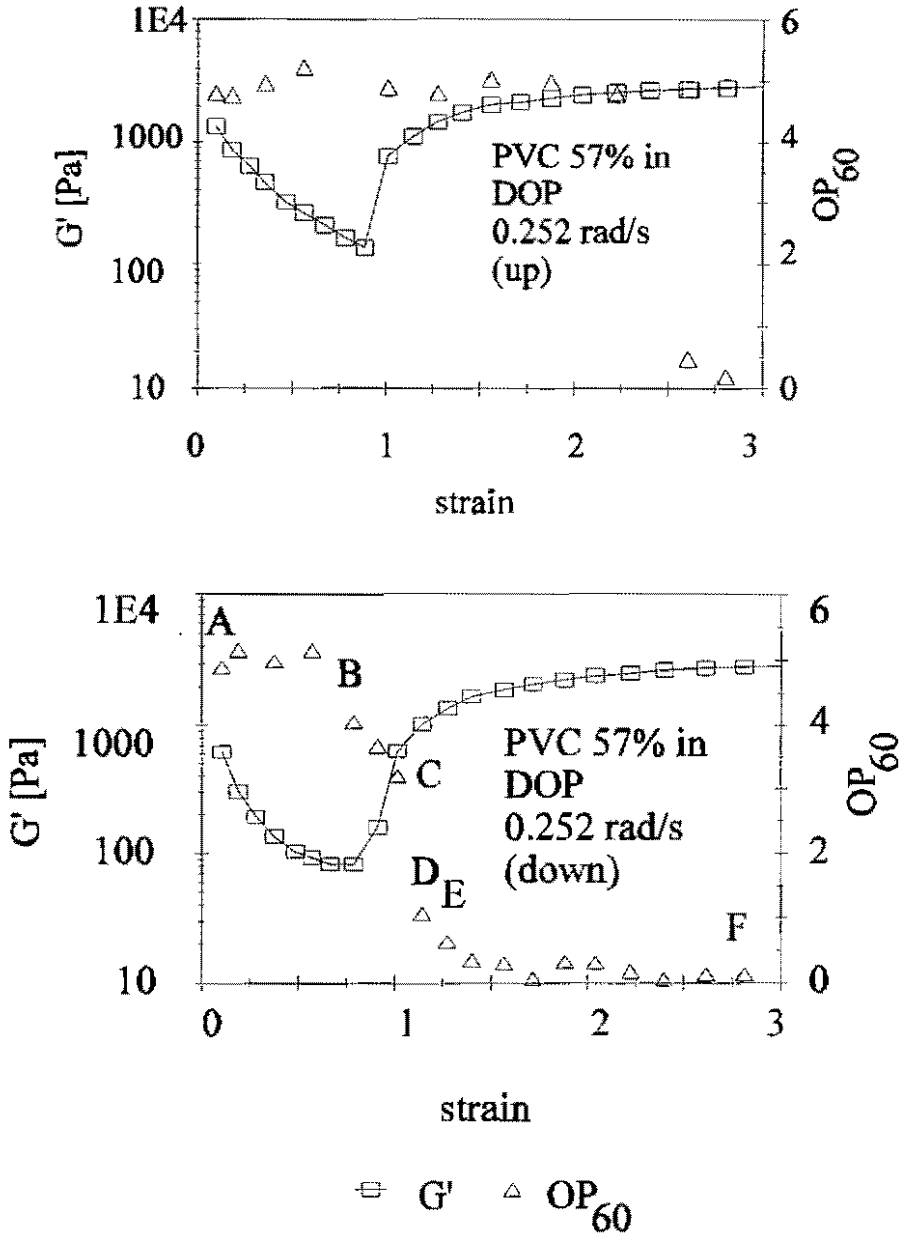


Figure 36 Dependence of the elastic modulus and the order parameter OP_{60} on the strain for increasing (up) and decreasing (down) strains in a PVC/DOP suspension.

In the presence of crystalline structures, colloidal suspensions are expected to exhibit Bragg scattering, provided there is an appropriate opacity of the sample. Several researchers [4],[5] have published rheo-optical static light scattering results of suspensions, usually under steady-shear rate conditions. In order to characterize the degree of long-range orientational order in a sheared suspension Chow & Zukoski [5] introduced an order parameter OP_{60} by writing for the scattered intensity $I(\theta_k)$ of the first order scattering ring (in the velocity/vorticity plane):

$$OP_{60} = \sum_{k=1}^N \frac{(I(\theta_k)I(\theta_k + \frac{\pi}{3}) - \bar{I}^2)}{I_{\max}^2} \quad (168)$$

where the θ_k is the angle measured from the velocity axis. The average intensity is given by $1/N [\sum_k I(\theta_k)]$ and I_{\max} is the maximum intensity of all $I(\theta_k)$ measured. We will take this parameter to discuss the connections between the theoretical model and the experimental results.

In Figure 36 are displayed the elastic modulus of the suspension together with the value of the order parameter OP_{60} both for increasing and decreasing strains. The experimental investigations show that close to the minimum in G' the Bragg peaks disappear as indicated by a decreasing OP_{60} value. While in the measurement with a decreasing amplitude (down) the minimum in G' shows a coincidence with the disappearance of the Bragg peaks. In the "up" measurement there is a difference between the position of the minimum in G' and that of the decrease of OP_{60} .

7.5. Discussion

We have chosen three different systems of colloidal suspensions, with quite different rheological properties. We expect therefore different structures to be responsible for their

rheology. Here we will compare the experimental results with the theoretical model of the in Chapters 3-6.

The glass/glycerol/water suspension with $\Phi = 58\%$ as shown in Figure 26 has a rather constant and small elastic modulus for small strains that gradually increases with increasing strains. The phase angle is however very high. From this result the theoretically expected strain dependence, with a minimum in G' , cannot be confirmed. At first sight one would expect that the equilibrium phase is a colloidal crystal. It is however known, that such a crystal phase cannot occur for polydisperse colloidal systems. The rheological properties for small strains indicate a highly viscous concentrated glass-like structure.

The dependence of the viscosity on the shear rate is shown in Figure 28. From this the critical shear rate of this suspension at the maximum viscosity can be determined to be $\dot{\gamma}_c \approx 10 \text{ s}^{-1}$. The minimum in the viscosity of the glass/glycerol/water suspension can be obtained from Figure 28 to be $\eta \approx 8 \text{ Pa}\cdot\text{s}$. The elastic modulus of the colloidal crystal in equilibrium as derived from Figure 28 in the high frequency limit for small strains is $G_0 \approx 2 \text{ Pa}$. The theoretical prediction of the critical shear rate, according to $\dot{\gamma}_c = 4 G_0/\eta$, is therefore $\dot{\gamma}_c \approx 1 \text{ s}^{-1}$, while the experimental maximum is at $\dot{\gamma}_c \approx 10 \text{ s}^{-1}$. This discrepancy is though not to be serious since the model in chapter 6 was derived on the basis of monodisperse particles but the glass particles have a relatively broad size distribution leading to deviations from the expected theoretical result.

The storage modulus of the PMMA/silicon oil suspension in Fig. 29 shows a minimum for low volume fractions. The storage moduli in these suspensions are significantly higher than in the glass/glycerol/water suspension, while the phase angles are lower. Our interpretation is therefore that a colloidal crystal is present at small strains for the volume fractions $\Phi = 0.49$ and $\Phi = 0.57$. On increasing the strain the structure changes into a colloidal glass (Chapter 5), a disordered structure of colloidal particles with a non-zero elastic modulus. The minimum disappears for the higher volume fractions $\Phi = 0.58$ and $\Phi = 0.6$. Apparently these highly concentrated suspensions form a colloidal glass structure during preparation and are not able to form a colloidal crystal within an experimentally accessible timescale.

Fig. 29 suggests that the transitional strain, at the minimum in G' , decreases with increasing volume fractions. On the other hand the model in Chapter 5 predicts that the distance to the transition into a colloidal fluid increases with increasing volume fraction. Thus an increase of the critical strain could be expected to be accompanied by a decrease

of the internal relaxation time on increasing volume fraction. The occurrence of the colloidal glass not taken into account in the model in Chapter 5 may be responsible for the qualitative difference. The frequency dependence of G' (Fig.30) at the higher volume fractions ($\Phi = 0.58$, $\Phi = 0.6$) differ from that at the lower volume fractions ($\Phi = 0.49$, $\Phi = 0.57$). The latter show the expected increase of the elastic modulus for increasing frequencies, approaching the value of a modulus independent of the frequency. The phase angle indicates that the relaxation time at the lower volume fractions is relatively high compared to the values found at high volume fractions.

Continuous shear experiments have been carried out indicating a yield stress of the samples. However no shear thickening of these suspensions could be detected within the measuring range of the rheometers employed.

A very pronounced transition could be found in the measurements for PVC/DOP with $\Phi = 0.57$ (Fig. 32) with a minimum in G' and a maximum in the phase angle as qualitatively expected from the model in Chapter 4. Note however that this experiment is not exactly conforming to the theoretical requirements, in which a very small oscillating amplitude is superimposed on a static deformation. The critical shear strain found from the minimum in G' in Fig. 32 is at $U_0^{(C)} = 0.8$. A similar result has been found for slightly flocculated ferric-oxide suspensions by Kanai & Amari [11], but with critical strains between 0.1 and 1. The reason for this 'strain-thickening' in a flocculated suspension is at present not clearly understood. However the results by Kanai & Amari can be interpreted by means of a shear induced transition, when we assume that their preshear procedure has led to a stable colloidal crystal-like structure, which is being broken up by increasing strains.

The fact that the minimum in G' for the "down" measurement is different compared to the "up" measurement indicates the existence of metastable states. This is supporting evidence for the existence of a first order character of the transition.

In Fig. 31 on approaching the transition in the stress signal a contribution twice the frequency of the strain signal is shown to be theoretically expected. This effect is not pronounced in the experimental results. However the minimum of G' is not a very sharp at the transition. This is in difference to the assumptions in the theoretical calculations.

The frequency dependence of Fig. 33 indicates, that on increasing the frequency a frequency independent storage modulus is approached as expected from the model in Chapter 5.

Figure 34 presents a continuous shear measurement of the PVC/DOP suspension. After a shear thinning region, shear thickening occurs with its maximum at $\dot{\gamma}_c \approx 6 \text{ s}^{-1}$. A calculation of the critical shear rate can be performed. When we estimate the elastic modulus from Figure 32 to be $G_0 \approx 2000 \text{ Pa}$ and estimate the viscosity from its minimum in Figure 34 to be $\eta \approx 1400 \text{ Pa}\cdot\text{s}$, we obtain to $\dot{\gamma}_c \approx 5.7 \text{ s}^{-1}$ which is in good agreement with the experimental value.

It is evident, that the size and the size distribution of the dispersed particles determine the structural and rheological properties of a suspension. The PVC particles have a narrow size distribution, allowing the formation of a long range colloidal crystal. Increasing the spread of the size distribution inhibits the crystal formation. The size distribution of the PMMA particles is comparable with that of the glass particles, leading to a similar rheological behaviour for high volume fractions. The PMMA particles are small compared to the PVC or glass particles leading to a relatively high elastic modulus for small strains.

The fact that for the suspension with small particles no shear thickening could be found can, in the sense of the model in Chapter 6, be explained by the absence of a periodically layered structure. This can either be due to an increased Brownian motion of the particles (condition of the strong coupling is lost), or to the fact that the high elastic modulus prevents the particles from forming a layered structure.

The rheo-optical investigations allow the simultaneous determination of the integral rheological properties and the local microscopical structure. For small strains the Bragg peaks indicate a colloidal crystal for the case of a PVC/DOP suspension. This colloidal crystal is stable against small oscillations. From the equilibrium phase diagram a colloidal fcc-crystal can be expected (Chapter 3). According to the model in Chapter 5 the colloidal crystal is expected to melt under the influence of an applied shear strain. The colloidal crystal changes into a disordered glass structure. The results of Fig. 35 and Fig. 36 are in agreement with this idea.

The order parameter OP_{60} , indicating the presence of a long range periodic order, decreases close to the critical strain, and the Bragg peaks disappear. The transitional strain values indicating the microstructural changes, can also be obtained from the point of a rapid increase of the value of OP_{60} . The transitional values as obtained from the measurement with increasing and decreasing strain (up and down), derived from the order parameter OP_{60} can be interpreted as a hysteresis effect. The glass structure can be metastable in

the transition region in accordance with the first order character of this structural transition.

Additionally, in the transition region two pronounced Bragg peaks remain visible, indicating the occurrence of a string-like structure. This string structure is not present in the equilibrium phase diagram and will therefore be interpreted as a shear induced non-equilibrium structure. It is not included in the simple thermodynamic model in Chapter 6. The occurrence of this structure can be understood from the formation of a non-equilibrium structure by oscillations with a frequency which is of the order of the relaxation time of the critical fluctuations. A similar structure has been obtained e.g. by Yan and Dhont [3]. The occurrence of this structure will lead to deviations of the expected rheological properties near the transition from the theoretical model.

7.6. Conclusions

The dynamic shear properties of glass in glycerol/water, PMMA in silicon oil and PVC in DOP suspensions has been investigated at volume fractions $0.48 < \Phi < 0.6$. The broad size distributions of the glass and PMMA particles prevents the occurrence of a colloidal crystal at high volume fractions; instead a colloidal disordered glass structure is formed. While the suspension with a crystalline structure shows a minimum in the elastic modulus with increasing strain, this dependence is absent in the colloidal glass structure. The experimental investigations suggest that the statistical model (Chapter 5) of a shear induced transition indeed allows the interpretation of the obtained results. This model is based on the assumption that a colloidal crystal becomes unstable under an externally applied shear strain. This instability is accompanied by the occurrence of a minimum in G' at the critical strain, where the global structure changes. The narrow size distribution of the PVC particles allows the investigation of the colloidal crystal by rheo-optical techniques and the simultaneous determination of the storage and the loss moduli. Rheo-optical investigations confirm the idea that a shear strain can induce a structural transition in concentrated colloidal suspensions. On increasing the applied shear strain the initially existing Bragg peaks disappear and a Debye ring appears indicating a globally disordered structure at the critical strain. At the transition however deviations are found which indicate a string-like structure.

At continuous shear only the suspensions with large colloidal particles show shear thickening. The model of an acoustic resonance instability in sheared colloidal suspensions

(Chapter 6) provides a critical shear rate. A good agreement between the calculated and measured critical shear rate has been found.

Literature

[1]

Boersma, W. H., J. Laven and H.N. Stein " Computer Simulations of Shear Thickening of Concentrated Dispersions" *J. Rheol.* **39**,841-860 (1995).

[2]

Ackerson, B.J., " Shear induced order of hard sphere suspensions" *J. Phys. Condens. Matter* **2**, SA389-SA392 (1990).

[3]

Yan, Y.D. and J.K.G. Dhont, "Shear-induced structure distortion in non-aqueous dispersions of charged colloidal spheres via light scattering" *Physica A* **198** 78-107 (1993).

[4]

Hoffman, R. L. " Discontinuous and dilatant viscosity behavior in concentrated suspensions" *Trans. Soc. Rheol.* **16**, 155-173 (1972).

[5]

Chow, M.K. and C.F. Zukoski, "Gap size and shear history dependencies in shear thickening of a suspension ordered at rest," *J. Rheol.* **39**, 15-32 (1995).

[6]

Hoffman, R.L. "Discontinuous and dilatant viscosity behaviour in concentrated suspensions II," *J. Colloid Interface Sci.* **46**, 491-506 (1974).

[7]

Görnitz, E. and H. Zecha, "Interactions in PVC-Plasticizer Dispersions" *Langmuir* **3** 738-741 (1987).

[8]

Buscall, R., J.W. Goodwin, M.W. Hawkins and R.H. Ottewill, "Viscoelastic properties of concentrated latices," *J. Chem. Soc. Faraday Trans. 1* **78**, 2873-2887 (1982).

[9]

Acrivos, A., " Bingham Award Lecture-1994: Shear induced particle diffusion in concentrated suspensions of noncolloidal particles," *J. Rheol.* **39**, 813-827 (1995).

[10]

Laven, J. W., W.H. Boersma, J.Kaldasch and H.N. Stein, " Flow-Induced Structural Phenomena in Highly Concentrated Dispersions", in *Advances in Structured and Heterogeneous Continua* (Allerton Press, London, 1993) edit. by D.A. Siginer and Y.G. Yanovsky pp. 479-492.

[11]

Kanai, H. and T. Amari, "Strain-thickening in Ferric-oxide Suspensions under Oscillatory Shear," *Rheol. Acta* **32**, 539-549 (1993).

CHAPTER IV.

CONCLUSIONS

A number of theoretical and experimental investigations have been carried out in this thesis on colloidal suspensions. The work was focused however on the rheology of electrically stabilized concentrated suspensions. The equilibrium structure determines the rheological properties under small shear perturbations. In order to determine the equilibrium structure the phase diagram of electrically stabilized suspensions has been calculated, by means of a statistical theory. Based on this perturbation theory the stability regions of a colloidal fluid, crystal and a liquid phase have been obtained in the volume fraction-Debye parameter phase diagram. The liquid phase corresponds to a flocculated structure. The shift of the coexistence lines for various interaction potentials shows, that the liquid phase is not present for small attractive forces. On increasing the attraction, a critical and a triple point occur accompanied with a liquid phase. Increasing the repulsive force leads to a shift of the critical and triple points and also to a shift of the coexistence lines to lower values due to an increased effective diameter.

Whereas the transport properties of equilibrium phases is given by the corresponding structures, close to the coexistence lines critical fluctuations may play an essential role. This is because critical fluctuations rule the transport processes near phase transitions. We are interested in the rheology of structures close to structural phase transitions. Therefore a model was derived based on the Landau theory of phase transitions. It is based on the idea that close to a structural transition the free energy can be determined by studying the change of the symmetry properties at the transition. This thermodynamic model allows the calculation of the dynamic shear properties near a transition by applying a mode coupling theory.

According to this model a decrease of the storage modulus and an increase of the loss modulus are expected on approaching the phase transition, while the modulus of both phases is non-zero (e.g. crystal-liquid transition). The model does not allow a quantitative determination of the storage and the loss moduli. However in the

hydrodynamic limit close to the transition a characteristic increase of the viscosity of the form $\eta \sim (\Phi - \Phi_c)^{-1.5}$ and of the elastic modulus $G \sim (\Phi - \Phi_c)^{-0.5}$ as a function of the volume fraction has been derived. Comparing this theoretical findings with experimental results from the literature indicate that the transitional effects influence the rheological properties. A qualitative and sometimes semi-quantitative agreement between the model and the experimental data could be found.

From a thermodynamic point of view the transition lines of the equilibrium phase diagram are unstable against external perturbations. This has been shown e.g. by numerical simulations under an applied shear strain. A generalization of the model describing the rheology near a phase structural transition derived in this thesis allows the interpretation of this shift of the phase lines as a shear induced transition. According to this idea a static shear strain can break up a colloidal crystal accompanied by a similar variation of the rheological properties as in the case of a undisturbed transition. A minimum of the elastic modulus and a maximum of the phase angle at the critical shear strain is expected.

Concerning this static shear induced transition various experimental investigations have been carried out on three different types of suspensions, a glass in glycerol/water suspension, PMMA in Silicon oil suspensions and a PVC in DOP suspension. While the first two suspensions were characterized by a rather broad size distribution, the latter was monodisperse. For the polydisperse glass in glycerol/water suspension no colloidal crystal phase is expected and no indication of a shear induced transition could be found. However a very pronounced transition in the rheological properties could be observed for the PVC in DOP suspension with a minimum in G' and a maximum in the phase angle at the transition. On this sample rheo-optical investigations were performed.

For investigating changes in the structure of a suspensions, a rheo-optical setup was built. It consists of a transparent plate-plate geometry mounted on a Sangamo R18 Weissenberg Rheogoniometer. Static light scattering was performed on the PVC in DOP sample perpendicular to the flow direction. For small strains Bragg peaks were obtained, indicating the presence of a colloidal crystal structure. This crystal structure disappears on increasing the strain, and a Debye-ring occurred. The vanishing of the Bragg peaks was accompanied by a decrease of the elastic modulus and an

increase of the phase angle. This experimental result agrees with the model assumptions, that on increasing the strain on a colloidal crystal, the latter changes into a disordered structure accompanied by critical fluctuations.

Another model was developed concerning a continuous shear experiment. A continuous shear can induce a non-equilibrium ordered structure, as known from numerical simulations. This continuous sheared structure consists of hexagonally close packed layers in the shear gradient direction slipping over each other. This process causes a periodic variation of the elastic modulus perpendicular to the flow direction. Studying the corresponding hydrodynamic equations, an acoustic resonance effect has been established. A maximum of the viscosity occurs (shear thickening) at a critical shear rate given by $\dot{\gamma}_c = \xi G/\eta$, where ξ is a constant, G the elastic modulus of the sheared two-dimensional hexagonal crystal and η the viscosity of the suspension. The comparison with experiments indicates that $\xi \approx 4$. Although the glass in glycerol/water suspension deviate from the predicted value, for the PVC/DOP suspension a good agreement between the theoretical and the experimental results could be obtained.

SUMMARY

Structural Transitions and the Rheology of Soft Sphere Suspensions

In this thesis theoretical and experimental investigations are presented devoted to the rheological properties of concentrated colloidal suspensions. The theoretical approach is based on three basic ideas:

1. The rheology of colloidal suspensions at equilibrium close to a phase transition is changed by the presence of critical fluctuations.

2. The equilibrium structure of a colloidal crystal is unstable against perturbations by shear. This instability can be viewed as a shear induced structural transition.

3. A continuously sheared suspension forms a non-equilibrium periodic structure with a periodic variation of the shear modulus in the shear gradient direction. This modulation leads to a flow instability which can be described as an acoustic resonance accompanied by an increase of the viscosity (shear thickening).

First a perturbation approach was developed to calculate the equilibrium phase diagram of electrically stabilized colloidal suspensions.

Applying a Landau theory with a suitable expression for the free energy together with a mode-coupling dynamics to the structural transition, the shear properties of concentrated suspensions were determined in a qualitative sense. A comparison between the predicted rheological behaviour and the experimental investigations indicates a good agreement.

This concept has been developed further to the region of high shear deformations. With the model of a shear induced structural transition, established in this thesis, the strain dependent rheological properties of a colloidal crystal have been given qualitatively.

Based on the assumption that a continuous shear induces a periodic modulation of the elastic modulus, a hydrodynamic model for the rheology has been developed. This model predicts an acoustic resonance leading to an increase of the viscosity of

the sheared suspension when resonance conditions are approached. This increase corresponds to shear thickening in concentrated suspensions. Good agreement between the calculated critical shear rate and the experimental data has been found.

The experimental part of this thesis focuses mainly on the shear induced structural transition. A rheo-optical setup has been developed to simultaneously determine the rheological and the microstructural properties of a sheared suspension. The shear induced structural transition and its influence on the rheological properties has been confirmed by experiments.

SAMENVATTING

Structurele Overgangen en de Reologie van Zacht Bol Suspensies

In dit proefschrift worden theoretische en experimentele gegevens gepresenteerd op het gebied van de reologische eigenschappen van geconcentreerde colloïdale suspensies. De theoretische aanpak is gebaseerd op de volgende basisgedachten:

1) In de buurt van een fasenovergang verandert de reologie van een colloïdale suspensie in evenwicht sterk ten gevolge van kritische fluctuaties.

2) De evenwichtsstructuur van een colloïdaal kristal is niet stabiel onder kleine afschuifstromingen. Deze instabiliteit kan beschouwd worden als een door afschuifstroming geïnduceerde, structurele overgang.

3) Een suspensie onder continue afschuiving vormt een niet-evenwichtsstructuur, met periodieke veranderingen van de shear modulus in de richting van de afschuifsnelheidsgradient. Deze modulaties leiden tot een instabiliteit van de stroming die het best beschreven kan worden als een akoestische resonantie die leidt tot een toename van de viscositeit ('shear thickening').

Het wordt het evenwichtsfasendiagram voor een electrostatisch gestabiliseerde colloïdale suspensie berekend. Door de Landau theory, met een geschikt gekozen uitdrukking voor de vrije energie, te combineren met 'mode-coupling dynamics' voor de structurele overgangen konden de afschuifeigenschappen van geconcentreerde suspensies kwalitatief bepaald worden. Er bestond redelijke overeenstemming tussen het voorspelde reologische gedrag en experimentele gegevens. Met het model van door afschuifstroming geïnduceerde fasenovergangen, ontwikkeld in dit proefschrift, konden de snelheidsafhankelijke reologische eigenschappen kwalitatief bepaald worden.

Uitgaande van de aanname dat een continue afschuifstroming gepaard kan gaan met periodieke modulaties van de elasticiteitsmodulus werd een

hydrodynamische model voor de reologie opgesteld. Dit model voorspelt akoestische resonantie, die tot een toename van de viscositeit leidt als de resonantieomstandigheden bereikt worden. Deze toename komt overeen met 'shear thickening' in geconcentreerde suspensies. Er is goede overeenstemming gevonden tussen de berekende, kritische afschuifsnelheid en de experimentele gegevens.

Het experimentele gedeelte van dit proefschrift is vooral gericht op de door afschuifstroming geïnduceerde structurele overgangen. Een reo-optische opstelling is ontwikkeld om gelijktijdig zowel de reologie als de microstructuur van een suspensie onder afschuifcondities te kunnen bestuderen. De experimenten bevestigen de door afschuifstroming geïnduceerde structurele overgang en zijn invloed op de reologische eigenschappen.

SYMBOLS

Roman symbols

A	Hamaker's constant
\underline{A}	deformation amplitude vector
$\underline{A}^{(0)}$	zero order amplitude vector
$\underline{A}^{(1)}$	first order amplitude vector
a	particle radius
a_0	free dimensionless parameter
B	coefficient
b	damping coefficient
C	salt concentration
C_{tr}	transitional salt concentration
c	sound velocity
D	dimension of the system
De	Deborah number
D_c	critical dimension
d	centre to centre distance between particles
dA	surface element
dV	volume element
E^{dis}	dissipated energy
e	Eulers number
\underline{e}	unit vector in x,y,z-direction
e_0	electron charge
F	free energy
F_{tr}	free energy at the transition
F_{HS}	hard sphere free energy
F^{dis}	dissipative force
f	free energy density
f_0, f_0'	free energy density independent of the order parameter
G	Gibbs free energy
$\underline{\underline{G}}$	elastic shear modulus tensor
G_0	isotropic elastic shear modulus
G'	storage modulus
G'_H	high symmetry storage modulus
G''	loss modulus
G''_H	high symmetry loss modulus
G_{H0}	elastic modulus of the high symmetry phase
G_{L0}	elastic modulus of the low symmetry phase
g_{HS}	hard sphere correlation function
g_0	group of high symmetry operations
g_1	group of low symmetry operations
$g(r_i, t)$	fluctuating term
$H(t)$	Green function
h	distance between the surfaces of the particles

h_1	Green function
I	constant
$J(\mathbf{k}, \Omega)$	perturbation integral
J_{H1}	correction of the high symmetry storage modulus
J_{H2}	correction of the high symmetry loss modulus
J_{L1}	correction of the low symmetry storage modulus
J_{L2}	correction of the low symmetry loss modulus
j	complex number
\underline{K}	wave vector
$\underline{k}, \underline{k}'$	wave vector
k_B	Boltzmann constant
\underline{k}_0	specific wave vector
L	Operator
M	constant
N	number of particles
N_n	number of next nearest neighbors
N_a	Avogadro number
n	number density
OP_{60}	order parameter
p	pressure
Pe	Peclet number
p_1, p_2	solutions of a dispersion relation
\underline{Q}	phase wave vector
Q_0	surface charge
q	order parameter; i.e. amplitude of the reciprocal lattice density wave
\underline{q}	displacement vector as the order parameter in Appendix A
q_0	equilibrium value of the order parameter (2. order)
q_{00}, q_{01}, q_{02}	equilibrium value of the order parameter (1. order)
R	constant
$\underline{r}, \underline{r}'$	distance vector
S	Barker Henderson parameter
\underline{s}	symmetry transformation matrix
T	temperature
T_A	temperature parameter
T_R	temperature parameter
T_{tr}	transitional temperature
t, t'	time
U	interaction energy
\underline{U}	amplitude vector
U_{HS}	two particle hard sphere interaction energy
U_p	two particle attractive perturbation energy
U_0	amplitude of a periodic deformation
$U_0^{(C)}$	critical shear strain amplitude
\underline{u}	strain tensor
$u_0^{(C)}$	critical shear strain
u_0	external shear strain
\underline{v}	velocity vector
v_0	simple shear flow velocity

W_0	repulsive potential
W_1	attractive potential
\underline{w}	deformation tensor
\underline{X}	displacement vector
x	reduced center to center distance
x_M	distance to the maximum of the interaction potential
x_m	distance to the secondary minimum of the interaction potential
Z_{HS}	hard sphere function of state
z	valency of the ions

Greek symbols

α	distance to the transition
α^*	free parameter
$\alpha_{0T}, \alpha_C, \alpha_\Phi$	free parameter
α_{tr}	transitional value of α
$\alpha_{00}, \alpha_{01}, \alpha_{02}$	transitional values of α of a first order transition
β^*	constant
Γ	parameter
γ	coupling constant
$\dot{\gamma}$	shear rate (scaled)
$\dot{\gamma}_0$	shear rate (macroscopic)
$\dot{\gamma}_C$	critical shear rate
δ	phase angle
$\delta_x, \delta_y, \delta_z$	reflections about the x, y, z planes
δ_{ik}	Kronecker symbol $\{\delta_{ik} = 1 \text{ if } i=k \text{ else } \delta_{ik} = 0\}$
$\delta(t)$	Dirac δ -function
δs	small parameter
δv	velocity variation
$\delta h(\underline{k})$	wave vector dependent perturbation
$\delta h(\underline{r})$	space dependent perturbation
$\langle \delta q(\underline{k})^2 \rangle$	wave vector dependent order parameter correlation function
$\delta q(\underline{r}, t)$	space and time dependent order parameter perturbation
δq^0	undisturbed order parameter
δq^1	disturbed order parameter up to the first order
$\delta \rho$	density increment
ϵ	small parameter
ϵ_r	relative dielectric constant
ϵ_0	dielectric constant of vacuum
ζ	positive free parameter in the free energy
η	viscosity of the suspension
η_c	parameter in Casson's equation
η_{HO}	low shear viscosity of the high symmetry phase
η_{LO}	low shear viscosity of the low symmetry phase
η_l	low shear viscosity
η_s	viscosity of the solvent
η_0	isotropic shear viscosity

$[\eta]$	intrinsic viscosity
θ_k	angle between Bragg peaks
κ	reduced Debye reciprocal length
κ_D	Debye reciprocal screening length
κ_0	Debye reciprocal screening length of a dilute sample
λ	free parameter
λ_k	components of the irreducible set
ν	free parameter in the free energy
Ξ	coupling term
ξ	free parameter
ξ_s	Stokes factor
ξ_0	correction parameter for the high shear viscosity
π	3.1415...
ρ	density of the suspension
ρ_1	density of the viscous medium
ρ_2	density of the elastic medium
ρ_{tr}	density at the transition
σ	effective particle diameter
$\underline{\underline{\sigma}}$	stress tensor
$\underline{\underline{\sigma}}^1$	viscous medium stress tensor
$\underline{\underline{\sigma}}^2$	elastic medium stress tensor
σ_c	parameter in Casson's equation
$\sigma^{(C)}$	critical shear stress
σ_0	particle diameter
τ	relaxation time
τ_e	time scale of the experiment
τ_r	internal relaxation time
ν	free parameter
Φ	absolute volume fraction
Φ^0	relative volume fraction
Φ_{tr}	transitional volume fraction
Φ_g	maximal random packing fraction
Φ_{hcp}	maximal volume fraction of hexagonal closed packed layers
Φ_m	maximal volume fraction
Φ_p	percolation threshold volume fraction
χ	damping coefficient
Ψ_k	irreducible set element
Ψ_0	surface potential
ψ_0	dimensionless parameter
Ω	frequency
Ω_0	externally applied frequency
ω	frequency

Subscripts

i,k,l	pertains vector index
ik	pertains to matrix

CURRICULUM VITAE

Joachim Kaldasch werd 3 mei 1963 geboren te Nauen (Duitsland). Na de Oberschule Senzke bezocht te hebben begon hij in 1979 een opleiding voor electrotechnicus. In 1984 haalde hij het Abitur examen aan de Bergakademie te Freiberg (Sachsen)

Hij koos in 1984 voor de studierichting Natuurkunde aan de Humboldt Universität Berlin. Het afstudeeronderzoek werd verricht bij prof.dr. R. Hermann en omvatte een studie naar het geleidingsgedrag van $\text{Hg}_x\text{Cd}_{1-x}\text{Te}$ bij lage temperaturen en hoge drukken. In 1989 behaalde hij het Physik-Diplom, waarna hij een baan als ontwikkelaar aan het Zentralinstitut für Wissenschaftlichen Gerätebau vond.

In juli 1990 begon hij het promotieonderzoek bij de vakgroep Colloidchemie onder leiding van prof.dr. H.N. Stein aan de Technische Universiteit Eindhoven, waarvan de resultaten beschreven worden in dit proefschrift.

DANKWOORD

Bij een promotieonderzoek zijn velen betrokken. Al deze mensen wil ik op deze plaats danken. Een aantal van hen wil ik echter met name noemen.

Allereerst dank ik mijn promotor, prof.dr. H.N. Stein voor de mogelijkheid van het uitvoeren van mijn promotieonderzoek in de vakgroep Colloidchemie en voor de waardevolle adviezen. Bijzondere dank ben ik dr. Jos Laven verschuldigd, die mij altijd ter zijde stond bij welk probleem dan ook. Zijn kennis heeft de basis gelegd voor dit proefschrift en zijn zienswijze heeft bijgedragen tot een nieuw inzicht in de reologie van geconcentreerde suspensies.

Verder dank ik mijn tweede promotor prof.dr. D. Bedeaux voor zijn kritische discussies en opmerkingen. De leden van de vakgroep wil ik danken voor hun assistentie en ondersteuning, in het bijzonder Wies van Diemen en Stan Holten.

Paul Venema en Gert Tuin, mijn kamergenoten, dank ik voor de opbouwende discussies en voor de vriendschap in goede en in slechte tijden. Veel steun heb ik gekregen van Peter Baets, Jacques van der Donck, Jan Vaessen, Peter Krutzen en Rudy Folkersma.

Altijd een verrijking waren de discussies, die ik met Marcel Visschers heb gevoerd en zijn steun met boeken. Soyen Wu wil ik bedanken voor de getoonde inzet tijdens haar research-stage.

Zeer gewaardeerd heb ik de steun die ik van Sylke Woelk en Irene Bach-
Huber heb ontvangen op een aantal momenten tijdens mijn opleiding. Mede dank zij de familie Berger voelde ik mij in Nederland op mijn gemak. Ook Jennifer Müller de la Llana Saveedra y Montisinos ben ik erkentelijk voor haar vormende invloed op mijn persoonlijkheid.

Tenslotte wil ik mijn ouders en mijn familie bedanken, die dit proefschrift mede mogelijk hebben gemaakt.

Stellingen
behorende bij de proefschrift van
J. Kaldasch

1. *Shear thickening* kan beschouwd worden als een *Poincaré-catastrofe*; zodra interactie tussen de deeltjes optreedt, wordt de ongestoorde beweging van de colloïdale deeltjes verhinderd door resonantie.
2. Sturing van *shear thickening* van geconcentreerde dispersies is mogelijk door aanleggen van een magnetisch veld op 'zachte' deeltjes met een klein magnetisch moment. Het biedt interessante, technische mogelijkheden voor de toepassing in mechanische dempings- en koppelingssystemen.
3. Omdat *shear thickening* een verschijnsel is dat het kollektief gedrag van een groot aantal deeltjes beschrijft, is de golf-beschrijving zoals in dit proefschrift voor het eerst gepleegd is beter van toepassing dan de deeltjes-beschrijving.
4. De enige voorwaarde voor een akoestische resonantie zijn het bestaan van monodisperse deeltjes die tijdens afschuiving een periodiek rooster vormen. Dit verschijnsel zou zich dus ook voor kunnen doen in vloeibare kristallen en zelf in molekulere materialen zoals water.
5. Het *fluctuatie-dissipatie theorem* eist dat stationaire processen constante transport eigenschappen bezitten. De studie van de reologie van geconcentreerd suspensies met shear afhankelijke transport parameters is daarom eigenlijk een studie van de overgangen in zo'n systeem.
6. The shear induced order transition in colloidal suspensions can be viewed as a non-equilibrium structural transition.
7. Wissenschaftliche Arbeit is ein schöpferischer Prozeß, der in der Suche nach neuen Kombinationen von Relationen im Zusammenhang mit einem Problem besteht. Es dauert seine Zeit bis man den Sinn oder Unsinn dieser neuen Beziehungen erkennt.
8. *Kritische fluctuaties* in de samenleving van mensen leiden tot een intensief gewaarworden van hun leven.
9. Het is eigenlijk al te laat, als zich in de samenleving een meerderheid voor een verandering aftekent.
10. Een van de meest fundamentele bronnen van onrecht in onze maatschappij, de werkloosheid, kan niet overwonnen worden zolang men arbeid fiscaal belast. Alleen indien men zich van deze koppeling ontdoet en in plaats daarvan belastingvoordelen verbindt aan ecologisch verantwoorde productiekringlopen, kan zich een maatschappij in harmonie van mens en natuur ontwikkelen.

11. **Het feit dat de Nederlandse politie niet optreedt tegen fietsendieven, is, één van de belangrijkste redenen achter de mislukte terugdringing van het aantal fietsendiefstallen.**